EXAMINING THE ROLES OF SUCROSE SYNTHASE ISOFORMS IN ARABIDOPSIS GROWTH AND DEVELOPMENT

by

Danyu Yao

BSc, The Northwest Agriculture and Forestry University, 2012

A THESIS SUBMITTED IN PARTIAL FULFILLMENT OF

THE REQUIREMENTS FOR THE DEGREE OF

DOCTOR OF PHILOSOPHY

in

THE FACULTY OF GRADUATE AND POSTDOCTORAL STUDIES

(Forestry)

THE UNIVERSITY OF BRITISH COLUMBIA

(Vancouver)

March 2019

The following individuals certify that they have read, and recommend to the Faculty of Graduate and Postdoctoral Studies for acceptance, the dissertation entitled:

Examining the roles of sucrose synthase isoforms in *Arabidopsis* growth and development

submitted by Danyu Yao in partial fulfillment of the requirements for

the degree of Doctor of Philosophy

in Forestry

Examining Committee:

Shawn Mansfield, Forestry
Supervisor

Lacey Samuels, Botany
Supervisory Committee Member

Robert D Guy, Forestry
Supervisory Committee Member

George Haughn, Botany
University Examiner

Patrick Ted Martone, Botany
University Examiner

Abstract

Sucrose synthase (SuSy) is one of the two enzyme families catalyzing the first step of sucrose utilization. It has been reported to serve different functional roles during plant growth and development, including supplying carbon for plant respiration, modulating sink strength and phloem loading, and facilitating the biosynthesis of starch and cell wall polymers. In a widely accepted model of cellulose biosynthesis, sucrose synthase is proposed to be tightly associated with the plasma membrane-localized cellulose synthase (CesA) complex and serves to channel carbon from photoassimilate (sucrose) directly to cellulose biosynthesis. Although many studies support this model, direct evidence of true interaction between SuSy and CesA is still lacking. As such, the primary objective of this thesis was to investigate the proposed model of cellulose biosynthesis using *Arabidopsis thaliana* as a model. The spatiotemporal localization of each of the six *Arabidopsis* SuSy proteins was investigated via live-cell imaging in a series of tissues including stems, roots, petioles, and siliques. Surprisingly, no single isoform of SuSy was detected in xylem, the major site of cellulose deposition in *Arabidopsis* plants. In contrast, SuSy1 and SuSy4 were expressed exclusively in phloem companion cells, SuSy5 and SuSy6 were confined to sieve elements, while SuSy2 and SuSy3 showed elevated expression in developing seeds. Thus, a new *sus1/sus4/sus5/sus6* quadruple mutant was generated and examined for a putative cellulose/cell wall phenotype, however, the plants showed no obvious growth defect. This can be explained by the activity of invertase (INV) which may compensate for the lack of SuSy activity in phloem tissue. Furthermore, the effect of phosphorylation on SuSy4 activity and membrane association was examined. Results showed that both phosphomimetic and phosphoresistant SuSy4 were largely localized to the cytoplasm of companion cells, similar to that of the native SuSy4. When subjected to flooding, only SuSy4 phosphomimetic transgenic lines exhibited obvious reductions

in soluble sugar and starch content. Collectively, these findings suggest a need to reconsider the established and largely accepted model of cellulose biosynthesis in *Arabidopsis*, and implicate SuSy in biological events related to phloem loading and carbon allocation.

Lay Summary

As the most abundant biopolymer synthesized on earth, cellulose is ubiquitous and has several uses that impact the daily lives of society, including wood and paper, fiber and cloth, bioenergy and biomaterials. In higher plants, cellulose is synthesized by the cellulose synthase complex at the plasma membrane, and sucrose synthase is proposed to have a major role in channelling UDP-glucose derived from sucrose directly to cellulose. This work provides evidence showing that the predominant role of SuSy in *Arabidopsis* is to supply energy for phloem loading and unloading, not direct cellulose synthesis. Moreover, our findings suggest that SuSy could be manipulated to modulate carbon allocation and modify sink strength.

Preface

This thesis contains four chapters written with the intent of publishing in a peer-reviewed journal.

Chapter 2 and Chapter 3: Danyu Yao was responsible for proposal development, experimental design and performance, data analysis, and manuscript preparation. Lacey Samuels helped on experimental design and data interpretation. Eliana Gonzales-Vigil assisted with manuscript editing. Prof. William Plaxton (Queen's University) and Prof. Raymond Chollet (University of Nebraska) kindly provided the anti-soybean root nodule SuSy immune serum. A plant line containing *35S$_{pro}$::VND7::VP16::GR* was generated and kindly provided by the Taku Demura's lab at Nara Institute of Science and Technology (NAIST). Shawn Mansfield was involved in the identification and design of the research project, providing research opportunity, data interpretation, and manuscript preparation. A version of Chapter 2 and Chapter 3 will be submitted for publication: DY Yao, E Gonzales-Vigil, and SD Mansfield. 2018. Live-cell imaging implicates *Arabidopsis* sucrose synthase in phloem transport, not cellulose biosynthesis.

Chapter 4: Danyu Yao was responsible for proposal development, experimental design and performance, data analysis, and manuscript preparation. Yuxin Wang assisted in experimental performance and data analysis. Prof. Alison Smith kindly provided the *Arabidopsis sus5/sus6* homozygous line. Shawn Mansfield was involved in the identification and design of the research project, providing research opportunity, data interpretation, and manuscript preparation. A version of Chapter 4 will be submitted for publication: DY Yao, YX Wang, and SD Mansfield. Sucrose synthase is dispensable for normal growth and development in *Arabidopsis*.

Chapter 5: Danyu Yao was responsible for proposal development, experimental design and performance, data analysis, and manuscript preparation. Melissa Roach assisted in experimental design. Shawn Mansfield was involved in the identification and design of the research project, providing research opportunity, data interpretation, and manuscript preparation. A version of Chapter 5 will be submitted for publication: DY Yao, SD Mansfield. Effect of phosphorylation on intracellular distribution and functional properties of sucrose synthase protein in *Arabidopsis*.

Figure 1.3 has been reprinted with the permission of Elsevier from the publication, "Roitsch, T., and Gonzalez, M.C. (2004). Function and regulation of plant invertases: sweet sensations. Trends in plant science. 9, 606-613."

Figure 1.5 has been reprinted with the permission of Elsevier from the publication, "Koch, K. (2004). Sucrose metabolism: regulatory mechanisms and pivotal roles in sugar sensing and plant development. Current opinion in plant biology. 7, 235-246."

Table of Contents

List of Tables

List of Figures

List of Supplementary Movies

List of Abbreviations

A	alanine
CesA	cellulose synthase
CSCs	cellulose synthase complexes
CSI	cellulose synthase interactive protein
CTL	chitinase-like protein
CCs	companion cells
CWINs	cell wall invertases
CINs	neutral and alkaline invertases
CDPKs	calcium-dependent protein kinases
DP	degree of polymerization
DEX	dexamethasone
DAF	days after flowering
DPA	days post anthesis
D	aspartic acid
E	glutamic acid
GR	glucocorticoid receptor
HPLC	high-performance liquid chromatography
INVs	invertases
LED	light emitting diode
MS	Murashige and Skoog
NFDM	nonfat dry milk
PI	propidium iodide

P-SuSy	plasma membrane associated SuSy
SuSy	sucrose synthase
SE-CC	sieve element-companion cell
SEs	sieve elements
SUT	sucrose transporter
SPS	sucrose phosphate synthase
S-SuSy	soluble SuSy
TE	tracheary element
UGPase	UDP-glucose phyrophosphorylase
UBQ5	ubiquitin5
VINs	vacuolar invertases
VND7	vascular-related NAC domain 7
VP16	viral protein 16
WT	wild-type
YFP	Yellow Fluorescent Protein

Acknowledgements

I would like to first thank my supervisor Dr. Shawn Mansfield, for giving me the opportunity to join his lab. Thank you for all your invaluable guidance, constant support, patience and kindness during these years. I really enjoyed doing research in this great environment. I would also like to thank my committee members, Drs. Rob Guy and Lacey Samuels for your helpful advice and assistance on my project. Thanks to Dr. William Plaxton for the gift of anti-SuSy immune serum. I appreciate his kindness and helpful advice.

I am really grateful to the members of Mansfield's lab and Samuels's lab, it has been impossible for me to finish my PhD program without your help. Big thanks to Drs. Faride Unda, Letitia Da Ros, and Eliana Gonzales-Vigil for all the stimulating discussions, encouragement and technical support. Special thanks to Yoshi Watanabe, Sam Livingston, and Miranda Meents for sharing their microscopy expertise with me. I also thank UBC bio-imaging facility, for training and technical support in microscopy. I would like to thank the Chinese Scholarship Council (CSC) and UBC international award for providing financial support for my PhD program.

Finally, the biggest thanks to my family for understanding and unconditional support throughout my years of PhD.

Chapter 1: Introduction

1.1 Overview

Cell walls are important features of plant cells that perform several essential functions, including defining cell shape, conferring mechanical support, and acting as a barrier to macromolecules and pathogen attack (Cosgrove and Jarvis, 2012). Plant cell walls are usually divided into the primary and secondary cell walls based on morphological and chemical properties. The primary cell walls form during cell division and expansion, while the secondary cell walls deposit between the primary cell walls and plasma membrane after anisotropic growth of the primary cell walls has ceased. The primary cell walls are thin and flexible layers ranging in width from 50 to 200nm, and function to resist the internal turgor generated by cell expansion (Cosgrove, 2005). In contrast, the secondary cell walls are typically much thicker and can be lignified, which significantly increases the mechanical resistance of the walls (Cosgrove and Jarvis, 2012). Cell walls are a complex matrix composed mainly of cellulose, hemicellulose, pectin, and lignin, as well as a small amount of protein. Cellulose is the principal structural component of cell walls and is composed of long chains of β-1,4-linked glucose that can interact with one another via hydrogen bonds to form a crystalline microfibril (Somerville, 2006). Sucrose synthase (SuSy) is one of two enzymes that can catalyze sucrose cleavage, and has been proposed to be integral in providing substrate, UDP-glucose derived from sucrose, directly to cellulose biosynthesis (Amor et al., 1995).

1.2 Plant cell wall

1.2.1 Primary cell wall

Primary and secondary cell walls have distinct chemical compositions and structural organizations, which ultimately confer different functionality during plant development. Primary cell walls are deposited during rapid cell growth, and their flexibility and extensibility enable cell expansion. Primary cell walls are composed of four major components, namely cellulose, hemicellulose, pectin and protein. In the wall, cellulose microfibrils are interconnected by cross-linking hemicellulose chains that are hydrogen-bonded to their surface, while pectin is assembled into the cellulose-hemicellulose network through calcium cross-bridges or borate diester linkages (Cosgrove, 2005; Frankova and Fry, 2013). Compared to secondary cell walls, primary cell walls contain less cellulose (comprising between 20 to 30%), and cellulose that displays a lower crystallinity and shorter degree of polymerization (DP; Fry, 2011; Cosgrove and Jarvis, 2012). The DP of cellulose microfibrils is estimated to range from hundreds to thousands of glucose units in primary cell walls, and up to 15,000 glucose units in the secondary cell walls of plants such as cotton (Fry, 2011). Xyloglucan is the major hemicellulose in primary cell walls of eudicot species, while the dominant hemicelluloses found in secondary cell walls vary between cell type as well as species (Cosgrove, 2005; Eklof and Brumer, 2010). In addition, primary cell walls contain a large amount of pectin (comprising between 30 to 35%), while lignin is absent (Cosgrove and Jarvis, 2012; Zhong and Ye, 2015). The overarching belief is that primary cell walls play an important role in regulating cell expansion and resisting internal turgor pressure (Hamant and Traas, 2010).

1.2.2 Secondary cell wall

Once cell expansion has ceased, secondary cell walls are deposited in specialized cells such as vessel elements and fiber cells (Keegstra, 2010). The majority of xylem (*i.e.* wood) is composed of secondary cell walls. Cellulose is the most abundant polysaccharide in secondary cell walls, and consistently displays crystallinities ranging from 40-65%, and DPs between 7,000 to 15,000 (Fry, 2011; Zhong and Ye, 2015). Secondary cell walls also contain a large amount of lignin which provides mechanical support and a water-impermeable surface to the walls (Schuetz et al., 2013). These two components together account for over 60% of the secondary cell walls, and the bulk of the renewable biomass occupying the globe (Zeng et al., 2014). During lignification, the hydrophobic polyphenolic polymers are deposited to surround cellulose microfibrils and provide rigidity and compressive strength to the cross-linked network of polysaccharides (Salmen, 2004; Fernandes et al., 2011). Secondary cell walls also contain additional hemicelluloses (in a species-specific manner) while pectin may be absent (Cosgrove and Jarvis, 2012). Morphologically, secondary cell walls in xylem are much thicker than primary cell walls and are generally defined by three distinct layers, namely S1, S2 and S3 (Preston, 1974). The three layers are largely defined by the changes in the orientation of the cellulose microfibrils, where the S1 and S3 are typically thin and house cellulose microfibrils with a relatively large angle (perpendicular to the long axis of growth), and a thick S2 layer that has much smaller microfibril angles (in normal grown cells) which largely determines the mechanical strength of wood fibers (Barnett and Bonham, 2004; Cosgrove and Jarvis, 2012).

1.3 Cellulose and cellulose synthase complexes

Cellulose is a polymer composed of linear, unbranched chains of β-1,4-D-glucose polymerized from a UDP-glucose precursor. In a polymeric chain, each glucose molecule is rotated by 180˚ in relation to its neighboring molecule, forming the repeating disaccharide cellobiose (Cosgrove, 2005). Intramolecular and intermolecular hydrogen bonds promote aggregation of parallel glucan chains to form crystalline cellulose microfibrils that are thought to be synthesized by the cellulose synthase complexes (CSCs) on the plasma membrane (Haigler and Brown, 1986; Somerville, 2006). CSCs are large multi-protein structures composed of individual cellulose synthase proteins (CesAs), which contain both transmembrane helices and a cytosolic component (Carpita, 2011). CesAs are assembled into hexameric arrays called particle rosettes, and the smallest subunit is made of three types of CesA proteins (Delmer, 1999). In *Arabidopsis thaliana* the CesA family contains ten genes that are expressed in a spatiotemporal fashion in different tissue and cell types (Endler and Persson, 2011). Through various tissue-specific expression analyses and mutant characterization experiments, it has been shown that three different CesA isoforms non-redundantly function in a complex to synthesize 18 to 36 glucan chains during cell wall formation (Taylor, 2008; Lei et al., 2012). For the synthesis of primary cell walls, CesA1, CesA3, CesA6 and CesA6-like proteins (CesA2, CesA5 and CesA9) are required, whereas the complexes specific to the secondary cell wall are composed strictly of CesA4, CesA7 and CesA8 (Taylor et al., 2000; Taylor et al., 2003; Desprez et al., 2007; Persson et al., 2007). The delivery of CesA proteins from the Golgi to the plasma membrane where they form the CSCs is facilitated via vesicle-mediated transport, and once assembled, the cortical microtubules guide the deposition of cellulose into the apoplast (Haigler and Brown, 1986; Paredez et al., 2006; Watanabe et al., 2015). Many non-CesA

proteins have also been identified to be involved in cellulose synthesis including COBRA, cellulose synthase interactive protein (CSI), KORRIGAN, KOBITO and chitinase-like protein (CTL; Pagant et al., 2002; Zhong et al., 2002; Takahashi et al., 2009; Lei et al., 2013; Sorek et al., 2014). In addition, sucrose synthase has also been proposed to be part of CSCs, where it has been hypothesized to channel UDP-glucose, the precursor for CesAs, directly from sucrose to cellulose synthesis according to studies of Amor et al. (1995). SuSy has been shown to be tightly associated with plasma membrane in developing cotton fiber and distributed in a pattern similar to the oriented cellulose microfibrils.

1.4 Phloem structure and sugar translocation

Xylem tissue is known to be important for water and mineral conduction, while phloem tissue is responsible for the translocation of sugars from mature leaves (source tissue) to sink organs for growth and storage (Kuhn et al., 1999; Schuetz et al., 2013). Phloem tissues in angiosperms consist of sieve elements (SEs), companion cells (CCs), phloem parenchyma cells, and phloem fibers. SEs are directly involved in long-distance translocation and at maturity lose most of their cellular compartments (Cronshaw, 1981; Oparka and Turgeon, 1999). However, they still contain modified mitochondria, smooth endoplasmic reticulum, P-protein and sieve element plastids (Knoblauch and van Bel, 1998). Individual SEs are connected together via sieve plates to form the longitudinal sieve tube. Callose is deposited around the sieve pores of sieve plates and functions to efficiently seal off SEs in response to damage (Evert and Derr, 1964; Eschrich, 1975). CCs are derived from the same mother cell as SEs, and are closely associated with SEs via numerous plasmodesmata to form the sieve element-companion cell (SE-CC) complex (Esau, 1969; Oparka and Turgeon,

1999). CCs are always characterized by a dense cytoplasm and abundant mitochondria (Cayla et al., 2015). They also display a highly active metabolism and supply energy and macromolecules to adjacent SEs (Williams et al., 2000).

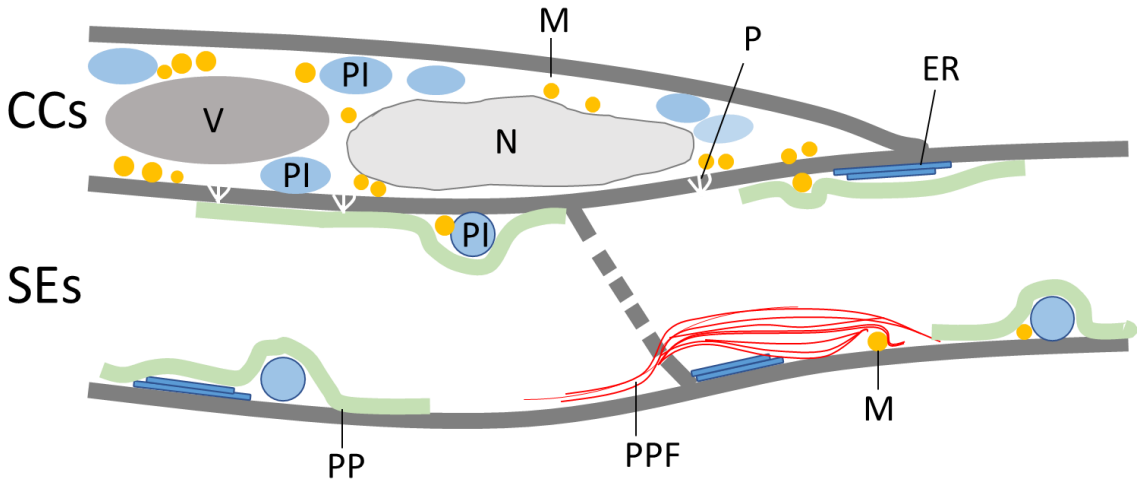

Figure 1.1 Structure of sieve elements (SEs) and companion cells (CCs). In SEs, the plastids (Pl), mitochondria (M) and endoplasmic reticulum (ER) are parietally positioned and evenly distributed. P-protein filaments (PPF) cluster closely to the sieve plates. In contrast, CCs contain a dense cytoplasm that consists of a vacuole (V), nucleus (N), plastids (Pl), and numerous mitochondria. SEs and CCs are connected via numerous plasmodesma (P). PP, parietal protein.

Sucrose can be loaded into the SE-CC complex apoplastically or symplastically, depending on the species (Braun et al., 2014). In many plants, phloem loading occurs from the apoplast via a sucrose transporter (SUT) localized on the plasma membrane of the SE-CC complex (Williams et al., 2000). In these cases, sucrose is actively transported against the chemical-potential gradient and ATP is required to complete the process (Carpaneto et al., 2005). In *Arabidopsis* nine SUT genes

have been identified (Sivitz et al., 2007). For example, the AtSUC2 H^+ symporter is specifically expressed in the companion cells and is essential for phloem loading (Stadler and Sauer, 1996). Mutants lacking AtSUC2 has been shown to have limited sugar transport to sink tissues, and the plants displayed severe phenotypes such as stunted growth, retarded development, and sterility (Gottwald et al., 2000). Several of the other SUTs have been widely detected in sink tissues: AtSUC1 in pollen (Stadler et al., 1999), AtSUC5 in seeds (Baud et al., 2005), and AtSUC8 and AtSUC9 in flowers (Sivitz et al., 2007). In contrast, AtSUC3 was found in the phloem sieve elements and has also been observed in numerous sink tissues, including guard cells, trichomes, pollens, root tips, and the developing seed coats (Meyer et al., 2004).

On the other hand, sucrose can be loaded into the SE-CC complex via the symplastic pathway, through the plasmodesmata. In this case, the sugars are retained in the SEs via the polymer trapping model where sucrose synthesized in mesophyll cells diffuses into intermediary companion cells via abundant plasmodesmata and then is converted to raffinose and stachyose (Haritatos et al., 2000; Turgeon and Medville, 2004). Given these trimeric and tetrameric sugars are larger in size than their sucrose precursors, they cannot diffuse back into the mesophyll cells, and are trapped in the SE-CC complex. It should be noted that although plants using the symplastic route do not employ a transporter, energy is still required to facilitate the synthesis of raffinose and stachyose to maintain the concentration gradient between mesophyll and intermediary cells. Similarly, phloem unloading can occur through either a symplastic or apoplastic pathway (Braun et al., 2014).

1.5 Sucrose metabolism in non-photosynthetic tissues

Sucrose is the primary transport sugar derived from photosynthesis and is crucial for plant growth and development. It serves an integral role as both a source of carbon and energy for non-photosynthetic tissues. When imported into sink tissue, sucrose is critical for maintenance of cellular metabolism including respiration, carbon skeleton synthesis, cell wall production, and can be converted to starch for storage (Koch, 2004; Lunn, 2016; Verbancic et al., 2018). During the day, sucrose is synthesized primarily in the mature leaves from photosynthesis, while at night sucrose can be released as products from starch remobilization and degradation (Lunn, 2016). Sucrose itself can be utilized by two pathways: sucrose synthase reversibly catalyzes the formation of fructose and UDP-glucose from sucrose and UDP, while invertase (INV) irreversibly cleaves sucrose into fructose and glucose (Koch, 2004). The released hexoses can subsequently be converted into glucose-6-phosphate and fructose-6-phosphate via hexokinase (Lunn, 2016). Fructose-6-phosphate is further converted by phosphoglucoisomerase into glucose-6-phosphate which is then transferred into glucose-1-phosphate by phosphoglucomutase (Verbancic et al., 2018). Next, UDP-glucose is produced by UDP-glucose pyrophosphorylase (UGPase) from the reaction consisting of glucose-1-phosphate and UTP (Kleczkowski et al., 2004; Kleczkowski et al., 2010). On the other hand, UDP-glucose is directly derived from the cleavage of sucrose via SuSy, and has been proposed to serve as the precursor for cellulose and callose biosynthesis (Amor et al., 1995). However, Barratt et al. (2009) provided evidence showing that SuSy is not necessary for cellulose production in *Arabidopsis*. In addition, hexose phosphates can be converted into triose phosphates that are further transformed into pyruvate to initiate plant respiration (Krook et al., 2000). In non-photosynthetic tissues, sucrose can be resynthesized either via SuSy or by sucrose

phosphate synthase (SPS; Lunn, 2016). SPS catalyzes the formation of sucrose-6-phosphate from fructose-6-phosphate and UDP-glucose, followed by the formation of sucrose from sucrose-6-phosphate via sucrose phosphate phosphatase (Winter and Huber, 2000).

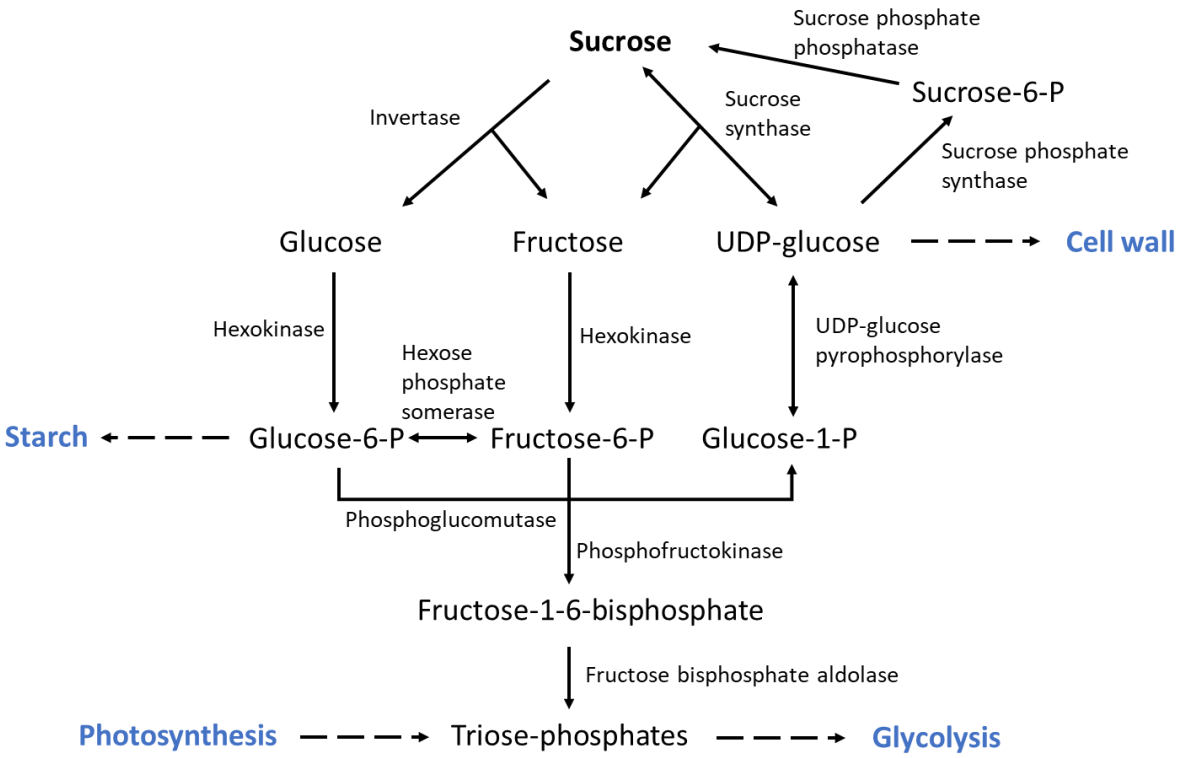

Figure 1.2 Sucrose metabolism in the plant cell. Sucrose synthase (SuSy) catalyzes the reversible conversion of sucrose and UDP into UDP-glucose and fructose, while invertase (INV) irreversibly cleaves sucrose into fructose and glucose. UDP-glucose, the precursor of cellulose and callose synthesis, can be produced either from sucrose hydrolysis via SuSy or by UDP-glucose pyrophosphorylase from the incorporation of glucose-1-phosphate (P) with UTP. The solid arrows indicate single-step chemical reactions while the dashed arrows indicate multiple-step reactions.

1.6 Invertase

Invertases are a group of β-fructosidases that can be classified by their solubility, localization, and optimal pH, and have been generally grouped as vacuolar, cell wall, and cytoplasmic invertases (Sturm, 1999; Roitsch and Gonzalez, 2004; Ruan et al., 2010). Vacuolar invertases (VINs) and cell wall invertases (CWINs) are acidic invertases, as they cleave sucrose most efficiently between pH 4.5 and 5 (Wan et al., 2018). These acid INVs cleave disaccharides containing fructose residues, thus they can also hydrolyze other β-fructose-containing oligosaccharides including raffinose and stachyose (Sturm, 1999; Lammens et al., 2009; Ruan et al., 2010). In contrast, neutral and alkaline invertases (CINs) are found in the cytosol and have optimal pH between 7-7.8 (Sturm, 1999; Wan et al., 2018). They specifically cleave sucrose, but are less well characterized.

CWINs (also known as insoluble acid invertases) are typically associated with cell wall matrix and believed to play an important role during phloem unloading (Eschrich, 1980; Ruan et al., 2010; Braun et al., 2014). When unloaded into the apoplast, sucrose could be hydrolyzed by CWINs into fructose and glucose, which are then transported into the symplast by hexose transporters located on the plasma membrane (Roitsch and Gonzalez, 2004; Hayes et al., 2007). CWINs have been shown to play a crucial role in modulating carbon partitioning and sink strength. During early seed development, high CWIN activity has been observed at the photoassimilate-unloading site in the seed coat of fava bean (*Vicia faba*; Weber et al., 1995). Repression of CWIN activity in tomato plants resulted in an increased rate of abortion and reduced fruit size (Zanor et al., 2009). In maize, loss of function of an endosperm-specific CWIN led to a reduction of seed size (Cheng et al., 1996). Similarly, a cell wall invertase gene *GIF1* has been shown to control carbon partitioning

and grain filling in rice (Wang et al., 2008). Overexpression of *GIF1* driven by its native promoter resulted in increased grain size (Wang et al., 2008). In addition, carrot plants with suppressed CWIN activity displayed smaller roots containing fewer carbohydrates (Tang et al., 1999). When an anther-specific CWIN was repressed, pollen development was blocked, which led to male sterility (Goetz et al., 2001). Furthermore, when subjected to wounding, pathogen attack, and other biotic stress, induction of CWIN expression has been reported in several plant species (Sturm and Chrispeels, 1990; Zhang et al., 1996; Berger et al., 2004; Swarbrick et al., 2006; Liu et al., 2016). In *Arabidopsis*, CWINs are encoded by a small multigene family containing six isoforms which show distinct levels and spatial patterns of expression (Sherson et al., 2003).

VINs (also known as soluble acid invertases) facilitate sucrose breakdown into hexoses in the vacuole, and have been reported to regulate sugar accumulation in fruits and storage organs (Ruan, 2014; Wan et al., 2018). Suppression of VIN activity resulted in the accumulation of sucrose content in tomato fruit (Klann et al., 1996), grape berry (Davies and Robinson, 1996), carrots (Yau and Simon, 2003) and potato tuber (Greiner et al., 1999). In addition, it is generally believed that VINs are important in determining sink strength and regulate cell expansion. Two isoforms of VINs have been identified in *Arabidopsis* and shown to modulate the elongation of roots and hypocotyls, probably through osmolality (Sergeeva et al., 2006). Rice mutants lacking one important VIN isoform displayed shorter panicles with smaller grains (Morey et al., 2018).

CINs have traditionally been thought to be cytosolic. However, several lines of evidence showed that CINs could be localized to multiple plant organelles (Ruan, 2014). Chloroplast localized CINs

have been identified in *Arabidopsis* and spinach, and shown to be involved in starch synthesis (Vargas et al., 2008). Two rice CINs were found to be localized in mitochondria and plastids respectively (Murayama and Handa, 2007). In *Arabidopsis*, a mitochondria-associated CIN has been suggested to supply substrate for hexokinase, maintaining homeostasis of reactive oxygen species (Xiang et al., 2011a). However, the functionality of CINs remains poorly studied. Mutants lacking individual isoform of CINs showed defects in root and shoot elongation in rice and *Lotus japonicus* (Jia et al., 2008; Welham et al., 2009). Loss of one CIN isoform in *Arabidopsis* also resulted in the reduced expansion of primary root, leaf and silique (Lou et al., 2007; Qi et al., 2007). In addition, *Arabidopsis* mutants deficient in two closely related CIN isoforms exhibited severe growth defects (Barratt et al., 2009). Anderson et al. (2018) recently showed that this growth defect is actually due to the inhibited cellulose production, as the *cinv1/cinve2* double mutant displayed abnormal cellulose biosynthesis and organization, and significantly reduced crystalline cellulose and free UDP-glucose. Consequently, the CIN and UGPase pathway has been suggested to be the dominant route of UDP-glucose production in *Arabidopsis*. Similarly, suppression of CINs in hybrid aspen (*Populus tremula* x *tremuloides*) resulted in the reduction of crystalline cellulose content in woody tissues and CIN has been proposed to facilitate cellulose biosynthesis in developing wood (Rende et al., 2017).

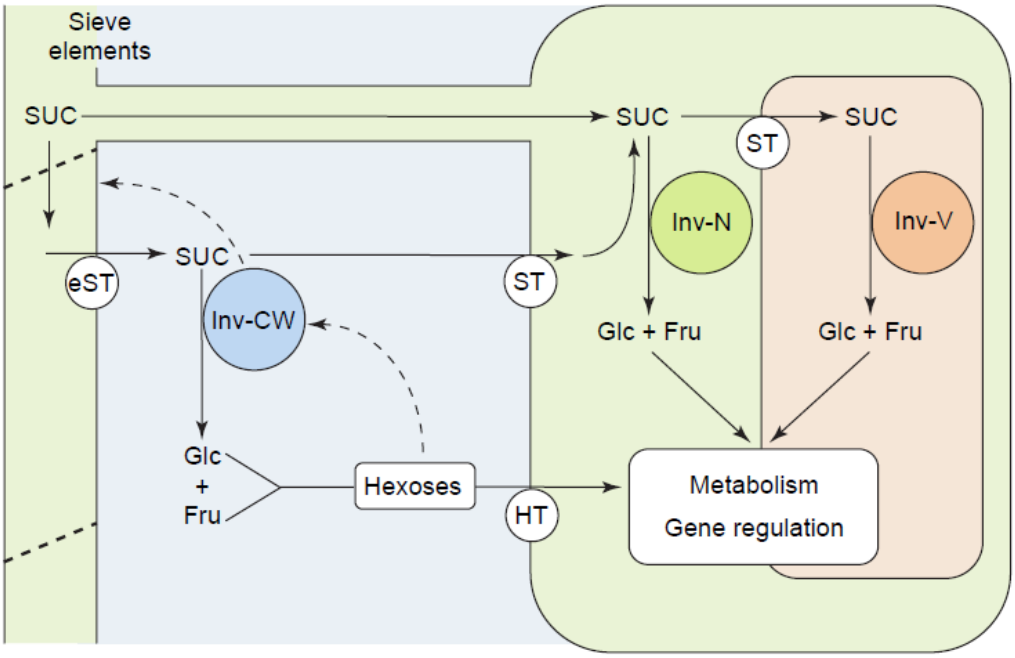

Figure 1.3 Subcellular localization of invertase and phloem unloading pathways (Roitsch and Gonzalez, 2004). Sucrose (SUC) unloaded from phloem to sinks can occur either apoplastically into cell wall or symplastically through plasmodesmata. When sucrose is unloaded into the apoplast, it can be hydrolyzed into glucose (Glc) and fructose (Fru) by cell wall invertases (Inv-CW). The resulting hexoses can then be transported into sink cells via a plasma-membrane-bounded hexose transporter (HT). Sucrose could also be imported into sink cells through the plasmodesmata or via sucrose transporters (ST). Moreover, it can be hydrolyzed in the cytosol by cytosol invertase (Inv-N) or in the vacuole by vacuolar invertase (Inv-V). Reprinted with permission from Elsevier.

1.7 Sucrose synthase in higher plants

Sucrose synthase is the enzyme able to catalyze the catabolism of sucrose, reversibly converting sucrose into fructose and UDP-glucose (sucrose + UDP ⟷ fructose + UDP-glucose). SuSys are characterized by the conserved sucrose synthase and glucosyl-transferase domains, and are

encoded by a multigene family in different plant species. Six isoforms of SuSy have been reported in *Arabidopsis* and rice plants (Baud et al., 2004; Hirose et al., 2008), while cotton and tobacco contain a SuSy multigene family with seven members (Chen et al., 2012; Wang et al., 2015). Similarly, seven SuSy genes have been identified in poplar, where three isoforms were shown to be predominantly expressed in developing and mature xylem (Zhang et al., 2011). The presence of three SuSy has been reported in maize, while five have been identified in castor bean plants (Carlson et al., 2002; Fedosejevs et al., 2014).

1.8 Sucrose synthase in *Arabidopsis*

The six *Arabidopsis* SuSy isoforms can be divided into three classes according to their amino acid similarity (Baud et al., 2004). *SuSy1* and *SuSy4* are the most highly related isoforms, showing 89% amino acid identity, and less than 68% identity to the other four isoforms. *SuSy2* and *SuSy3* are 74% identical to each other, and again display less than 67% identity to other isoforms. The final pair of SuSy isoforms, *SuSy5* and *SuSy6* are only 58% identical to one another, and share less than 48% identity to other isoforms. In addition, compared to other isoforms, *SuSy5* and *SuSy6* have a C-terminal extension of 3 and 14 kDa, respectively. Phylogenetic analyses show that AtSuSy1 and AtSuSy4 fall into the dicot group and are closely related to the pair of isoforms from poplar, which has been shown to be in abundance in xylem tissue (Zhang et al., 2011).

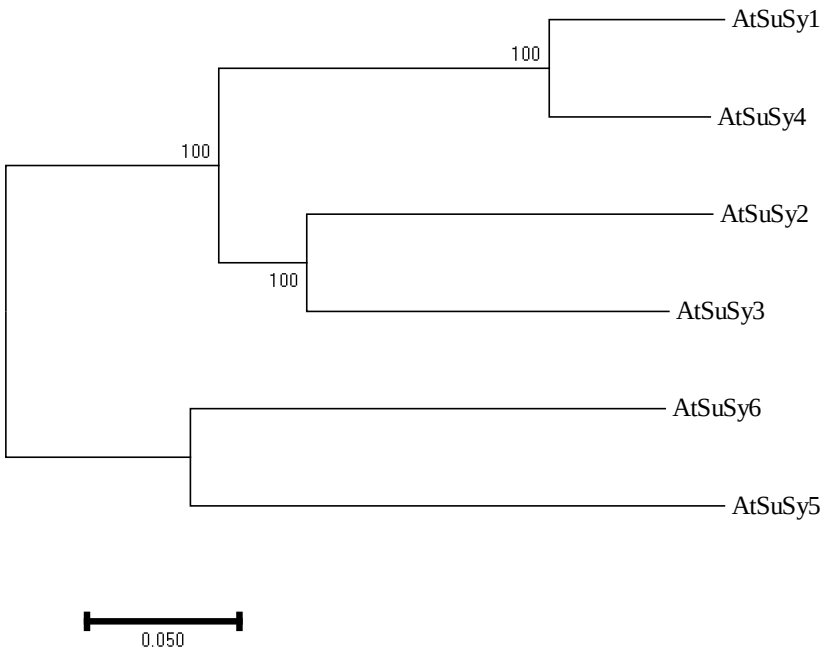

Figure 1.4 Phylogenetic relationship of the six SuSy isoforms in *Arabidopsis thaliana,* according to the Neighbor-joining method (Saitou and Nei, 1987). Bootstrap values are indicated at the branch junctions. Full-length amino acid sequences were employed for alignment and the generation of the phylogenetic tree in MEGA7 (Kumar et al., 2016).

In *Arabidopsis,* each SuSy isoform displays a tissue-specific expression profile (Baud et al., 2004; Bieniawska et al., 2007). *SuSy1* is constitutively expressed in all organs, while *SuSy4* is predominantly expressed in roots, stems and siliques. In addition, SuSy1 was clearly shown to be confined to the vasculature of cotyledons, rosette leaves and silique walls by GUS staining (Bieniawska et al., 2007). Consistently, histochemical GUS analyses of *Arabidopsis* and tobacco plants showed that AtSuSy1 was exclusively expressed in the phloem of leaves and roots (Martin et al., 1993). In contrast, *SuSy2* transcript is barely detectable in tissues other than seeds during

development (Bieniawska et al., 2007; Fallahi et al., 2008). Similarly, *SuSy3* transcript abundance is detected in mature seeds as well as in root vasculatures and stomatal guard cells (Bieniawska et al., 2007; Angeles-Nunez and Tiessen, 2010). *SuSy5* and *SuSy6* are more widely expressed in whole plants, and have been reported to be confined to phloem sieve elements (Baud et al., 2004; Bieniawska et al., 2007; Barratt et al., 2009). Expression analyses of AtSuSy in response to stress have shown that *SuSy1* and *SuSy4* transcript levels are significantly induced by the deprivation of oxygen (Klok et al., 2002; Baud et al., 2004). Similar phenomena were also widely observed in other species, including rice (Ricard et al., 1991), wheat (Marana et al., 1990; Albrecht and Mustroph, 2003), maize (Ricard et al., 1998; Zeng et al., 1999), and pea (Rolletschek et al., 2002). Compared to invertases, SuSy is often considered as the more energy conservative enzyme, as only half as much ATP is consumed for sucrose hydrolysis via the SuSy pathway. Therefore, under hypoxic conditions, when energy levels are limited by low oxygen, SuSy is more effective in sucrose catabolism (Guglielminetti et al., 1995; Zeng et al., 1999). Furthermore, an increase of both *SuSy1* and *SuSy3* transcript levels has been observed under dehydration conditions (Baud et al., 2004). In addition, *SuSy1* expression has been shown to be induced in response to cold treatment (Fowler and Thomashow, 2002; Baud et al., 2004; Hannah et al., 2005).

Arabidopsis mutants lacking individual isoforms of SuSy1, SuSy4, SuSy5, and SuSy6 exhibit no obvious phenotype (Bieniawska et al., 2007). Single knockouts of SuSy2 and SuSy3 are also not different from wild-type (WT) plants in final seed size and composition, but show different metabolic profiles at specific stages of seed development (Angeles-Nunez and Tiessen, 2010). Double mutants lacking similar isoform pairs (*sus1/sus4, sus2/sus3, sus5/sus6*) also display normal

growth, starch and cellulose content, seed weight and composition when grown under normal conditions (Bieniawska et al., 2007). Only double knockouts of SuSy1 and SuSy4 show a growth retardation and sugar accumulation under hypoxic conditions (Bieniawska et al., 2007). In addition, mutant plants lacking both SuSy5 and SuSy6 activity have sieve plates deficient in callose lining (Barratt et al., 2009). Furthermore, Barratt et al. (2009) have demonstrated that the *sus1/sus2/sus3/sus4* quadruple mutant lacking SuSy activity in all cell types except phloem is morphologically and metabolically indistinguishable from WT plants. Therefore, the functional role of SuSy in *Arabidopsis* has been questioned.

1.9 Subcellular localization and functionality of SuSy

The SuSy pathway has been generally considered as the dominant route of sucrose catabolism in many plants. It has been suggested that SuSy exists in two forms: a soluble enzyme (S-SuSy) and a particulate enzyme bound to the plasma membrane (P-SuSy; Amor et al., 1995; Salnikov et al., 2001; Subbaiah and Sachs, 2001; Duncan et al., 2006; Barrero-Sicilia et al., 2011). Most SuSy isoforms don't have predicted targeting signals. Consistent with this, within a cell, SuSy has been shown to be predominantly localized to the cytoplasm, although SuSy has been observed to bind to different subcellular structures (Winter et al., 1998; Etxeberria and Gonzalez, 2003; Barrero-Sicilia et al., 2011). In the cytoplasm, SuSy supports extensive metabolic networks including synthesis of building blocks and storage materials, such as starch (Munoz et al., 2005; Baroja-Fernandez et al., 2009; Li et al., 2013). In addition, sucrose breakdown via SuSy could supply carbon for plant respiration and produce energy for normal plant growth and development (Biemelt et al., 1999; Bologa et al., 2003). Western blot analysis and immunohistochemistry studies

demonstrated that SuSy could be associated with the plasma membrane or cell walls (Amor et al., 1995; Salnikov et al., 2003; Duncan et al., 2006; Persia et al., 2008; Brill et al., 2011). Thus, SuSy is proposed to directly facilitate cellulose or callose biosynthesis (Amor et al., 1995). Moreover, SuSy has also been observed to bind to actin filaments (Winter et al., 1998; Azama et al., 2003; Duncan and Huber, 2007; Cai et al., 2011), and be localized to endoplasmic reticulum (Barrero-Sicilia et al., 2011). In maize and barley plants, an isoform of SuSy has been shown to be localized inside mitochondria, and a putative mitochondrial targeting peptide was predicted by the TargetP and Predotar programs (Subbaiah et al., 2006; Barrero-Sicilia et al., 2011). However, unlike these two isoforms, most SuSy isoforms do not have a predicted mitochondrial targeting peptide. Furthermore, tonoplast-associated SuSy has been identified and suggested to be potentially involved in sucrose mobilization between vacuole and cytosol (Etxeberria and Gonzalez, 2003).

SuSy has been identified in different cell types, and as such has been implicated in different biological roles. For instance, SuSy3 was detected specifically in the guard cells of leaf stomata in *Arabidopsis*, and overexpression of AtSuSy3 in tobacco plants led to enhanced stomatal aperture and conductance, transpiration rate, net photosynthesis rate and plant growth (Bieniawska et al., 2007; Daloso et al., 2016). In addition, SuSy was found in the sieve elements of castor bean tumor and has been shown to be colocalized with the plasma-membrane-localized H^+-ATPases through double immunofluorescence labeling (Wächter et al., 2003). Similarly, sieve-element-specific localization of SuSy5 and SuSy6 was also visualized in *Arabidopsis* roots and stems using the technique of in situ RNA hybridization and tissue printing (Barratt et al., 2009). Thus, SuSy has been proposed to function in callose biosynthesis as well as sucrose transportation in sieve

elements (Wächter et al., 2003; Koch, 2004; Barratt et al., 2009). Furthermore, companion-cell-specific localization of SuSy has been shown through immunohistochemistry studies in various plant organs including citrus fruits and petioles (Nolte and Koch, 1993), rice and maize leaf petioles (Yang and Russell, 1990; Regmi et al., 2016), and *Arabidopsi*s petioles and silique walls (Fallahi et al., 2008; Regmi et al., 2016). In addition, maize *SuSy1* promoter has been shown to drive expression of GUS activity specifically in phloem cells (Yang and Russell, 1990). Therefore, SuSy has been suggested to supply reduced carbon for plant respiration and facilitate phloem loading and unloading.

Starch is the main form of storage carbohydrate in plants, and it accumulates in large amounts in organs such as seeds and tubers (Zeeman et al., 2010). SuSy is thought to be important for starch biosynthesis (Chourey et al., 1998; Munoz et al., 2005; Baroja-Fernandez et al., 2009; Li et al., 2013). Leaf starch synthesis is generally believed to take place in the chloroplast without SuSy. However, a study has proposed that SuSy is involved in an "alternative" pathway for starch biosynthesis, where ADP-glucose is produced from sucrose via SuSy in the cytosol and then transported into the chloroplast for starch biosynthesis (Munoz et al., 2005). In potato, SuSy-antisense transgenic leaves exhibited reduced ADP-glucose and starch content, whereas the amount of both ADP-glucose and starch was dramatically elevated in the leaves overexpressing SuSy (Munoz et al., 2005). Tubers of transgenic potato expressing antisense SuSy also accumulated less starch compared to WT plants (Zrenner et al., 1995). In addition, it has been shown that mutants lacking individual SuSy isoform exhibited defects in starch synthesis. For instance, pea plants exhibiting a mutation in the *rug4* locus and maize *Sh1/Sus1* double mutants

showed reduced starch content in embryos during seed development (Chourey et al., 1998; Craig et al., 1999).

It is believed that SuSy activity could determine sink strength in some crop plants. Inhibition of SuSy activity in transgenic potato plants resulted in a reduction in the total tuber dry weight and soluble tuber proteins (Zrenner et al., 1995). In tomato, SuSy activity has been shown to positively correlate with fruit growth rate and starch content, thus it was proposed to dominantly regulate the sucrose import into fruit (Wang et al., 1993). Overexpression of SuSy in poplar resulted in increased wood density and cellulose production, while repression of SuSy activity led to reduced wood density (Coleman et al., 2009; Gerber et al., 2014). Furthermore, carrot plants exhibited shorter and thinner roots, and obvious growth retardation when SuSy activity was suppressed (Tang and Sturm, 1999). SuSy also has been reported to participate in controlling the efficient partitioning of sucrose in mung bean seeds (Chopra et al., 2005).

SuSy has also been suggested to have a specific role in cell wall polymer synthesis, including the biosynthesis of both cellulose and callose (Amor et al., 1995). The widely cited model suggests that a plasma-membrane-localized SuSy is tightly associated with the CSCs to channel precursor UDP-glucose directly to the complex and ultimately synthesize cellulose (Amor et al., 1995; Haigler et al., 2001; Koch, 2004). In developing cotton fibers, SuSy was first reported to tightly bind to the plasma membrane through western blot analysis (Amor et al., 1995). This plasma membrane-associated form of SuSy has also been found in other species, such as soybean (Zhang et al., 1999; Komina et al., 2002), maize (Carlson and Chourey, 1996; Subbaiah and Sachs, 2001;

Hardin et al., 2004), sycamore (Pozueta-Romero et al., 2004), and wheat (Albrecht and Mustroph, 2003). In addition, immunohistochemistry studies of cotton fibers demonstrated that SuSy was abundant in sites where cellulose and callose were rapidly synthesized during secondary cell wall formation (Amor et al., 1995; Haigler et al., 2001; Salnikov et al., 2003). Similar results have been also reported in wheat roots and tracheary elements of *Zinnia elegans* (Salnikov et al., 2001; Albrecht and Mustroph, 2003). Haigler et al. (2001) proposed a model explaining how subcellular localization of SuSy regulates intracellular carbon portioning to cell wall synthesis in developing cotton fibers, where SuSy is largely associated with the plasma membrane during rapid secondary cell wall formation. When plants are under stress, cellulose synthesis will slow, and plasma membrane-associated SuSy (P-SuSy) becomes soluble SuSy (S-SuSy) to facilitate glycolysis and contribute to survival metabolic processes (Haigler et al., 2001). Cellulose synthesis will quickly resume if S-SuSy turns to P-SuSy when conditions improve (Haigler et al., 2001). Furthermore, cellulose and callose could be synthesized *in vitro* when detached and permeabilized cotton fibers were fed with sucrose (Amor et al., 1995). Fujii et al. (2010) isolated a sucrose synthase-like particle from mung bean plasma membrane that could bind, *in vitro,* to the purified rosettes, shown through immunogold labelling with an anti-SuSy serum. In addition, the incorporation of this catalytic unit into the rosette structures could enable the cellulose synthesis activity when supplied with sucrose plus UDP (Fujii et al., 2010). In co-immunoprecipitation experiments conducted in the developing xylem of *Populus*, SuSy was pulled down, among the other known cell wall-related proteins, with the cellulose synthase complex (Song et al., 2010). In contrast, through immunohistochemical analysis and immunogold labeling, Regmi et al. (2011) demonstrated that SuSy was exclusively localized to phloem, not xylem in the leaves of maize, rice and *Arabidopsis*.

Only in poplar leaves, SuSy was found to be confined to xylem (Regmi et al., 2016). Phloem-specific localization of SuSy has been observed in other plant organs, including leaves and fruits of citrus, and roots and silique walls of *Arabidopsis* (Martin et al., 1993; Nolte and Koch, 1993; Fallahi et al., 2008). In addition, Barratt et al. (2009) reported that SuSy was not important for cellulose production in *Arabidopsis* since the *sus1/sus2/sus3/sus4* quadruple mutants lacking most of SuSy activity displayed normal cell wall structure and cellulose content. Therefore, although there are multiple lines of evidence from species like cotton and poplar supporting the hypothesis that SuSy is directly associated with cellulose synthesis, the exact function of SuSy in some other species (*e.g. Arabidopsis*) remains unclear.

Furthermore, a range of studies has demonstrated that misregulation of SuSy has a profound effect on cellulose production. For instance, high SuSy activity was correlated with increased cellulose content in hybrid poplar and thickened secondary cell walls in transgenic tobacco (Coleman et al., 2009; Wei et al., 2015). In addition, overexpression of SuSy in hybrid poplar led to increased cell wall crystallinity and significantly higher wood density (Coleman et al., 2009). Enhanced fiber production was also apparent in cotton plants overexpressing SuSy, while suppression of SuSy resulted in a fiberless phenotype (Ruan et al., 2003; Xu et al., 2012; Bai et al., 2014). In contrast, when a mutant form of the mung bean SuSy (S11E) was overexpressed in poplar, overall morphology and cellulose content of all transgenic lines were similar to that of control plants (Konishi et al., 2004). It has also been shown that deficient SuSy activity in developing wood did not affect cellulose biosynthesis, but led to a decrease in wood density, which indicated that SuSy might play a role in defining carbon partitioning into wood (Gerber et al., 2014). Furthermore,

silencing of SuSy in alfalfa (*Medicago sativa*) resulted in no obvious phenotype and indistinguishable cell wall cellulose content (Samac et al., 2015). Therefore, the functional role of SuSy in cell wall synthesis remains unclear.

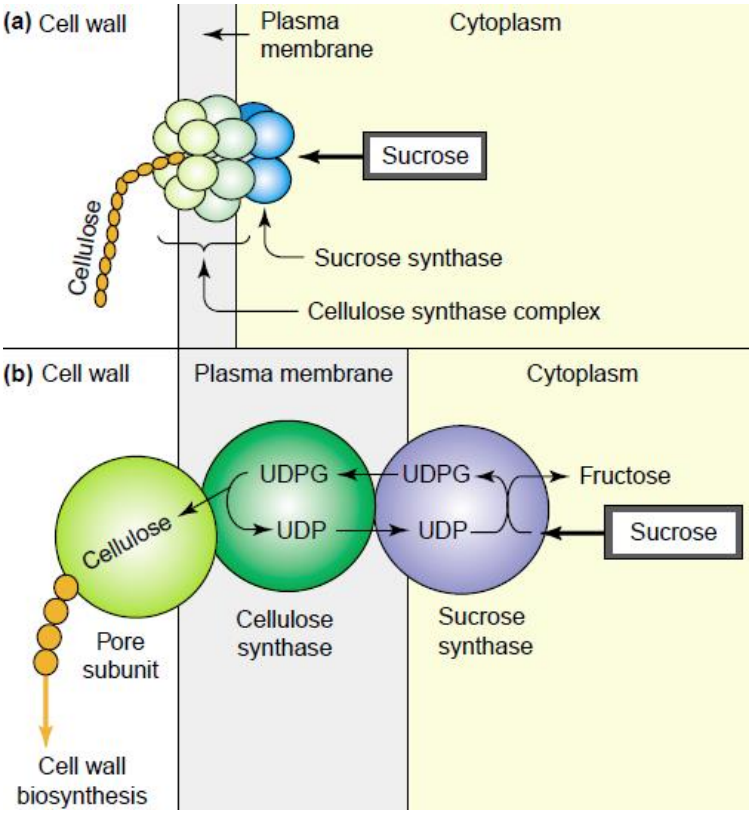

Figure 1.5 A proposed model showing the role of SuSy in the synthesis of cellulose (Koch, 2004). Plasma membrane-associated SuSy is shown to tightly interact with the cellulose synthase complex to facilitate the direct transfer of UDP-glucose from sucrose breakdown to cellulose biosynthesis. Reprinted with permission from Elsevier.

1.10 Goals and research objectives

The prevailing model of cellulose production suggests that a plasma-membrane localized sucrose synthase could associate with the cellulose synthase complexes to channel UDP-glucose derived from sucrose cleavage directly to cellulose synthesis. The primary goal of this project is to understand the functional role(s) of SuSy involvement in cell wall biosynthesis in the model plant *Arabidopsis thaliana*. Specifically, I set out to investigate whether a true interaction between SuSy and the CSCs exists during secondary cell wall formation as the model implies. In addition, I wanted to elucidate the functionality of each *Arabidopsis* SuSy during plant growth and development. To achieve these goals, the following four objectives were generated:

1.10.1 Investigation of the spatiotemporal expression and subcellular localization of *Arabidopsis* SuSy1 and SuSy4 during cell wall formation (Chapter 2)

The underlying hypothesis is that SuSy could directly interact with CSCs during cell wall formation. To test this hypothesis, *Arabidopsis* stem tissue was used as a model system to study cellulose biosynthesis as it is primarily composed of fibers. I first checked the transcript abundance of all six *Arabidopsis* SuSy genes in stem tissue, and selected SuSy1 and SuSy4 for further examination. I characterized the phenotypes of *sus1/sus4* double mutant under hypoxic conditions and investigated the complementation of mutant phenotypes by fluorescently tagged SuSy proteins. I employed a spinning disc confocal microscope to perform live-cell imaging on a variety of tissues of SuSy transgenic plants to determine the spatial localization of SuSy1 and SuSy4. In addition, I checked the subcellular localization of SuSy1 and SuSy4 in protoxylem tracheary

elements during secondary cell wall formation in plants containing an inducible master transcription factor which could control xylem fate.

1.10.2 Investigation of spatiotemporal localization of *Arabidopsis* SuSy2, SuSy3, SuSy5 and SuSy6 (Chapter 3)

The hypothesis is that *Arabidopsis* SuSy2, SuSy3, SuSy5 and SuSy6 are not directly involved in cell wall cellulose biosynthesis but instead, they likely serve different functional roles in plant growth and development. To test this hypothesis, I generated Yellow Fluorescent Protein (YFP) fusions of SuSy2, SuSy3, SuSy5 and SuSy6 to examine the spatiotemporal localization of SuSy proteins in different plant tissues via live-cell imaging. I also employed different staining dyes to determine the precise subcellular localization of the fluorescently tagged SuSy using confocal microscopy.

1.10.3 Characterization of *sus1/sus4/sus5/sus6* quadruple mutant phenotypes (Chapter 4)

The goal of the work described in this chapter was to investigate whether the newly created quadruple mutant of *Arabidopsis* SuSy (*sus1/sus4/sus5/sus6*; previously not examined) is morphologically and metabolically different from WT plants under normal growth conditions or with environmental stimulation. To achieve this goal, I created homozygous *sus1/sus4/sus5/su6* quadruple mutant by crossing the double mutant lines *sus1/sus4* and *sus5/sus6*. The T-DNA insertional mutants were screened and confirmed by genotyping using specific primers. Subsequently, I employed comprehensive characterization protocols to examine quadruple mutant

phenotypes in several aspects of growth and development, soluble sugar and starch content (chemical analyses), and cell wall morphology (microscopy and staining).

1.10.4 Investigation of the effect of phosphorylation on SuSy4 subcellular localization and functional properties (Chapter 5)

The underlying hypothesis is that phosphorylation of SuSy can affect its membrane association as well as the functional properties of this protein under hypoxic conditions. To test this, I employed site-directed mutagenesis to modulate the phosphorylation status of *Arabidopsis* SuSy4. YFP fusion constructs containing modified SuSy were generated and transformed into *sus1/sus4* double mutant plants. Subsequently, I examined the subcellular localization of both phosphomimetic and phosphoresistant SuSy4 in leaf longitudinal sections through a confocal microscope. In addition, I analyzed soluble sugar and starch content of rosette leaves after five days flooding treatment.

Chapter 2: Investigation of the spatiotemporal expression of *Arabidopsis* SuSy1 and SuSy4

2.1 Introduction

In the vast majority of terrestrial plants, assimilated carbon from photosynthesis is primarily transported as sucrose to non-photosynthetic tissues, where it serves an integral role as a carbon and energy source. In sink tissues, sucrose is essential for the maintenance of cellular metabolism, cell wall biosynthesis, and can be converted to starch for storage and later use. Two enzymes catalyze the entry of carbon skeletons from sucrose into cellular metabolism: sucrose synthase and invertases. While INVs irreversibly cleave sucrose into glucose and fructose, SuSy reversibly catalyzes the formation of fructose and UDP-glucose (Koch, 2004). SuSy predominantly occurs as a soluble form in the cytoplasm, but has also been found associated with the plasma membrane (Amor et al., 1995; Salnikov et al., 2001; Subbaiah and Sachs, 2001; Duncan et al., 2006). Both INVs and SuSy have been shown to play an important role in modulating sink strength, and SuSy is also key to facilitating starch biosynthesis, as well as respiration and phloem loading (Koch, 2004; Nolte and Koch, 1993; Munoz et al., 2005). In sink tissues, such as secondary xylem, SuSy is proposed to have a specific role in the synthesis of cell wall polymers, including cellulose and callose (Amor et al., 1995; Haigler et al., 2001).

Cellulose is the most abundant biopolymer on earth, and cellulose synthesis serves as a major carbon sink in plants. The prevailing model of cellulose production suggests that a plasma-

membrane localized SuSy interacts directly with the cellulose synthase complex to channel UDP-glucose, derived from sucrose cleavage, directly to cellulose synthesis (Amor et al., 1995). Theoretically, this model has several advantages. First, no additional energy is required for cellulose deposition, as the polymer can be synthesized directly from UDP-glucose released by SuSy (Haigler et al., 2001). Second, competition for UDP-glucose by other pathways can be avoided (Haigler et al., 2001). And third, free UDP, a known inhibitor of the cellulose synthase proteins which is released after glucosyl transfer, can be recycled immediately by SuSy (Ross et al., 1991). This model was originally based on cotton fibers, which deposit significant amounts of highly pure cellulose in the secondary cell wall (Haigler et al., 2001). Consistent with this model, some SuSy isoforms have been found to be tightly associated with the plasma membrane and abundant in sites where cellulose and callose are rapidly synthesized during cell wall formation (Amor et al., 1995; Haigler et al., 2001; Salnikov et al., 2001; Salnikov et al., 2003). In addition, SuSy was identified to be co-immunoprecipitated with CSCs in the developing xylem of poplar (Song et al., 2010). Moreover, multiple lines of evidence have demonstrated that misregulation of SuSy led to changed cellulose content in plant species such as poplar (Coleman et al., 2009), tobacco (Wei et al., 2015), and cotton (Ruan et al., 2003; Xu et al., 2012). In contrast, SuSy was shown to have no effect on cellulose production in *Arabidopsis* (Barratt et al., 2009). Therefore, it remains unclear how SuSy contributes to the overall cellulose synthesis machinery, or if it is truly essential for cellulose deposition.

The phloem of higher plants facilitates the long-distance translocation and partitioning of sucrose. In most plants, sucrose is actively loaded from the apoplast and SuSy has been suggested to be

closely linked with this energy-dependent process (Regmi et al., 2016). For instance, via immunohistochemistry studies, companion cell-specific localization of SuSy has been shown in the leaves of various plant species, including citrus (Nolte and Koch, 1993), rice (Regmi et al., 2016), maize (Yang and Russell, 1990; Regmi et al., 2016), and *Arabidopsi*s (Regmi et al., 2016). Companion cells are very metabolically active and distinguished by a dense cytoplasm containing numerous mitochondria, plastids and free ribosomes (Cayla et al., 2015), and are closely linked with sieve elements via plasmodesmata to supply energy and macromolecules to the sieve elements. In contrast, mature sieve elements are highly specialized for translocation. Although sieve elements lose their nuclei, ribosomes and vacuoles during maturation, they maintain smooth endoplasmic reticulum, plastids and P-protein (van Bel et al., 2002).

Although SuSy is believed to be a central enzyme for sucrose catabolism and individual isoforms have been reported to be necessary for normal plant growth and development in maize (Chourey et al., 1998), pea (Craig et al., 1999) and cotton (Ruan et al., 2003), the importance of SuSy in *Arabidopsis* has been questioned. Barratt et al. (2009) have shown that mutant plants lacking four of the six isoforms display normal growth, cellulose content and cell wall structure. Based on these findings, it was proposed that either INV compensates for the loss of SuSy activity or there is a significant redundancy within the SuSy multi-gene family. *Arabidopsis* contains six SuSy genes, which have been grouped into three pairs of closely related isoforms and each pair has a distinct expression profile (Baud et al., 2004; Bieniawska et al., 2007). For example, SuSy1 and SuSy4 are highly expressed in the stem, and have been proposed to be closely linked to cell wall biosynthesis (Bieniawska et al., 2007). In addition, it has been suggested that SuSy1 and SuSy4 together are

necessary for plants to cope with anaerobic stress, because *SuSy1* and *SuSy4* transcript abundance dramatically increases under hypoxic conditions, whereas the other isoforms are not affected (Baud et al., 2004).

In *Arabidopsis*, xylem vessels and fiber cells form a thick secondary cell wall and serve as the major sink for cellulose deposition. To assay whether SuSy is really a component of the cellulose synthase complex, YFP fusion constructs of AtSuSy1 and AtSuSy4 were generated, and fiber cells were targeted to explore the precise intracellular localization of SuSy via live-cell imaging using the confocal microscope, given that this is where the bulk of the cellulose is deposited. Surprisingly, neither SuSy1 nor SuSy4 was detectable in the developing xylem of several plant tissues, including roots, leaves, stems, and siliques. In marked contrast, SuSy1 and SuSy4 were identified to be confined to either companion cells or sieve elements of phloem.

2.2 Methodologies

2.2.1 Plant material, growth conditions, and flooding treatment

The *sus1/sus4* double knock out mutant line was described in Bieniawska et al. (2007), which was created by crossing *sus1* (SALK_014303) with *sus4* (GENT *sus*4) single mutant lines. Homozygous *Arabidopsis sus1/sus4* T-DNA line was identified by PCR genotyping using respective left T-DNA border primers (*sus1*: 5′ ATTTTGCCGATTTCGGAAC 3′, *sus4*: 5′ CCCCTGCGCTGACAGCCGGAACACG 3′) and respective flanking primers (*sus1*: LP 5′ CTCAAGAGTGCAAGGATCAGG 3′, RP 5′ ACGCTGAACGTATGATAACGC 3′; *sus4*: LP 5′

GAGACCAAGACCTGGAGTTTGGGAATACG 3′, RP 5′ ATCAAGTCAGGCTTCCCCTGCA-ACTCTTT 3′). PCR conditions were as follows: 5 minutes at 95 °C; 35 cycles of 30 seconds at 95 °C, 30 seconds at 57 °C, 90 seconds at 72 °C; 10 minutes at 72 °C. The absence of *SuSy1* and *SuSy4* transcript was confirmed by real-time quantitative RT-PCR using the primers listed in Table 2.1. Seeds of wild-type (WT) *Arabidopsis thaliana* ecotype Columbia-0 and *sus1/sus4* were sterilized with 70% (v/v) ethanol for 5 minutes, followed by 10% (v/v) bleach for 15 minutes, and finally rinsed with sterile distilled water. After 2-4 days at 4 °C in the dark, seedlings were germinated on half-strength Murashige and Skoog (MS) medium without sucrose, and transferred to soil 7 days post germination. All plants were grown in a growth chamber maintained at 21 °C, 16-h light, 8-h dark, 50% humidity, and a PPFD of 150-180 μmol m^{-2} s^{-1}. After 4 weeks of growth, a subset of plants was subject to a flooding treatment by adding and maintaining degassed water in the growth trays at a level just above the surface of the soil for five days. Water used for flood treatment was degassed by vacuum for overnight. Leaf diameters were measured at the widest part of the rosettes before and after the five days of flooding. At the end of flooding, rosette leaves were collected for soluble sugar and starch analyses.

2.2.2 RNA isolation and reverse transcript PCR

Stems of mature *Arabidopsis* plants were harvested after 6 weeks of growth and ground in liquid nitrogen. RNA was extracted using the TRIzol® reagent (Invitrogen) according to the manufacturer's instructions and treated with TURBO DNase™ (Ambion) to remove residual DNA. cDNA was synthesized using the iScript™ Select cDNA Synthesis Kit (BIO RAD) with

oligo-dT and random primers. The program conditions used to reverse translate cDNA were: 25 °C for 5 minutes, 60 °C for 60 minutes, and 85 °C for 5 minutes.

2.2.3 Real-time quantitative PCR

Real-time PCR was used to determine the transcript abundance all *SuSy* genes in WT stems. Three biological replicates were harvested for each treatment, and samples were run in triplicate with SsoFast™ EvaGreen® Supermix (BIO RAD) on a Bio-Rad CFX96 Touch Real-Time PCR Detection System using the primers listed in Table 2.1. The *Arabidopsis ubiquitin5* gene (*AtUBQ5*; At3g62250) was employed as a reference gene. The conditions for real-time analyses were: 95 °C for the 30 seconds, followed by 40 cycles of 95 °C for 5 seconds, 58 °C for 5 seconds, and 65 °C for 5 seconds. Relative expression was determined according to Levy et al. (2004) using the equation: $\Delta Ct=2^{-(Ct\textit{SuSy}-CtUBQ5)}$.

Table 2.1 Primers employed for the amplification of SuSy coding sequences and real-time PCR analyses

Gene	Orientation	Primer sequences (5′ to 3′) for coding sequences amplification	Primer sequences (5′ to 3′) for real-time PCR analyses
SuSy1	Forward	CACCATGGCAAACGCTGAACGTAT	TTGCCTGAACAAACCCGGAA
(At5g20830)	Reverse	ATCATCTTGTGCAAGAGGAAC	CCTCACAGCTAGAGCAACCC
SuSy2	Forward	ATGCCGACTGGTAGGTTCGAGACTAT	GCACAGCCTGATTGAGCAGT
(At5g49190)	Reverse	GTTCTCATCTGTTGCCAGCGGGATTG	GCTCACCATTTCGAGCACGG
SuSy3	Forward	ATGGCAAACCCTAAGCTCACTAGGG	CGCAGGAACGAAGAACACCG
(At4g02280)	Reverse	GTCATCGGCGGTTGAAGGAACAG	ATGGTCATGTCTGCACCGGG
SuSy4	Forward	CACCATGGCAAACGCAGAA	AAGGAATCGTTCGCAAATGG
At3g43190)	Reverse	CTCTTCATGAGCAAGAGGAACA	TTTCAGCGGCAACATCCTC
SuSy5	Forward	ATGGAAATGACATCTGGATCG	CGTTGGGTTTCCCGCTTTGA
(At5g37180)	Reverse	AGCACCAAACAACCTGAAACTC	GCCACCAAGTTTCCATCCGT
SuSy6	Forward	ATGTCATCTTCATCTCAAGCTATGC	CCTTCGTCAATGGGTTTCCCG
(At1g73370)	Reverse	ATACTCTTGAGCCGAGTTAGCACC	TCTTGCTCGTTGCGTCCTGA
ubiquitin5	Forward		CAGCTCCACAGGTTGCGTTA
(At3g62250)	Reverse		CAAGCCGAAGAAGATCAAGCA CAAG

2.2.4 Plasmid constructs

SuSy1 and *SuSy4* coding sequences were amplified from *Arabidopsis* stem cDNA employing iProof™ High-Fidelity PCR kit (Bio-Rad) using the primers listed in Table 2.1. The *SuSy1* and *SuSy4* coding sequences were first cloned into pDONR/Zeo, and subsequently transferred into a modified pBIN19 vector using Gateway™ technology. The *35S* promoter region of the binary vectors pBIN19 attR-YFP and pBIN19 YFP-attR was replaced respectively by either the *SuSy1* or

SuSy4 promoter fragments consisting of approximately 2000 base pairs of the upstream region from the translational start codon provided by Dr. Ji Young Park of the Mansfield lab (the full details are listed in Table 3.1). The kanamycin resistance gene was also replaced by a sulfadiazine resistance gene for the screening of putative transformants. C-terminal and N-terminal YFP fusions (*$SuSy1_{pro}$::SuSy1::YFP*, *$SuSy4_{pro}$::SuSy4::YFP*, *$SuSy1_{pro}$::YFP::SuSy1* and *$SuSy4_{pro}$::YFP::SuSy4*) were transformed into chemically competent DH5α *E. coli* and sequenced. All constructs were transformed independently into *sus1/sus4* double mutant or plant line containing *$35S_{pro}$::VND7::VP16::GR* (Yamaguchi et al., 2010) using *Agrobacterium tumefaciens* (strain GV3101). Positive lines were identified by growth on half-strength MS medium supplemented with 5 mg/L sulfadiazine, and the five lines with the brightest YFP signal were selected for further analyses.

2.2.5 Chlorophyll content analysis

Rosette leaves which were larger than 2 cm and showed signs of chlorosis were selected for analysis. The Chlorophyll Content Index (CCI) was measured on excised leaves, at the leaf tips where chlorosis was visually apparent, using a Chlorophyll Content Meter CCM-200 (OPTISCIENCE, USA) by determining the absorbance of plant leaves at two wavelengths (931 nm & 635 nm). The CCI is the ratio of transmission of radiation from a light emitting diode (LED) centered at 931 nm to transmission of radiation from an LED centered at 653 nm (CCM-200 user manual). Data were collected from three leaves of each plant and four individual plants representing each line.

2.2.6 Soluble carbohydrate analysis

After five days of the flooding treatment, rosette leaves of WT and mutant leaves were harvested and immediately flash-frozen in liquid nitrogen (harvest consistently occurred 2-4 hours after the end of dark period). Isolated leaves were ground using a mortar and pestle and freeze-dried overnight. Soluble sucrose was extracted from 10-12 mg of freeze-dried tissue using 1 mL methanol:chloroform:water (12:5:3) incubated at 4 °C overnight. On the following day, samples were centrifuged for 10 minutes at 6,000 rpm, and the supernatant was transferred to a new tube. The extraction was repeated two more times to collect any residual sugar, and the supernatants were pooled. The pellet was dried at 55 °C overnight and used for subsequent starch analysis. To partition the solvents, 1 mL of deionized water was added to the supernatants prior to vortexing and centrifuging for 4 minutes at 4,000 rpm. The top phase containing soluble sugars was subsequently collected. 2 mL of this phase was then dried in a vacuum centrifuge overnight, and the pellet re-suspended in 0.5 mL deionized water and filtered through a 0.45 μm syringe filter into a high-performance liquid chromatography (HPLC) vial. The soluble sugar concentration was quantified by an anion-exchange HPLC (ICS-5000; Dionex, Sunnyvale, CA) fit with a Dionex™ CarboPac™ PA1 column and a pulsed amperometric detector and a gold electrode. Sugars were eluted with 16 mM NaOH, 2 mM NaOAc at a flow rate of 0.8 mL/minute. The concentration of soluble sugar was determined using a calibration standard curve generated with known sucrose concentrations.

2.2.7 Starch analysis

For starch measurement, the residue pellet from soluble sugar extraction was weighed and hydrolyzed in 1 mL 4% H_2SO_4 at 121 °C for 5 minutes. After centrifuging at 500 rpm for 5 minutes, the supernatant containing liberated glucose was subsequently collected. 760 µL sample and 40 µL fucose stock (5 mg/mL; used as internal standard) were weighed and passed through 0.45 µm syringe filter into HPLC vial. Glucose content was determined by HPLC fit with a CarboPac^{TM} PA1 column and an electrochemical detector. Carbohydrate was eluted using water at the flow rate of 1 mL/minute. The starch content was quantified using a calibration standard curve generated with known glucose concentrations.

2.2.8 Microscopy

Live-cell imaging was performed on a Leica DMI 6000 B inverted microscope with a Perkin Elmer Ultraview VoX Spinning Disk scan head with excitation/emission wavelengths of 514 nm/540 nm respectively, for visualization of all SuSy-YFP fusions. Images were captured on a Hamamatsu 9100-02 CCD camera using Volocity 6.3 software (Improvision) and processed using Image J software (National Institutes of Health; http://rsb.info.nih.gov/ij/). Cell wall staining was conducted using propidium iodide (PI) by incubating 7-day-old seedlings in 10 µg/mL PI (dissolved in water) for 5 minutes, followed by thorough washing and mounted in water prior to imaging. PI was subsequently detected using the 561 nm laser lines and the 595 nm emission filters. Sieve plates were labelled using 0.01% aniline blue (in water) for 10 minutes in the dark and then rinsed with water, mounted in water prior to imaging (Thompson and Wolniak, 2008).

Aniline blue was subsequently detected by the 405 nm laser and observed with the 540 nm emission filters.

2.2.9 Tissue collection and preparation

For visualizing thin cross-sections of stems and petioles, inflorescence stems from 5-week-old *Arabidopsis* plants (approximately 3 cm from the base of a stem) and rosette leaves (both smaller sink leaves and larger source leaves) were hand-sectioned using a double-sided razor blade. A sliding benchtop microtome (American Optical, Model #860) was employed to cut 60-100 μm-thick longitudinal sections of petiole and silique containing vascular bundles. SuSy transgenic seedlings were grown on half-strength MS medium for 7 days in the condition described above, and entire seedlings were mounted in water prior to imaging. Seedlings containing both *35S$_{pro}$::VND7::VP16::GR* and SuSy YFP fusions were germinated on germination media (1× MS, 1% sucrose, 1× Gamborg's Vitamin mix, 0.05% MES, 0.8% agar at pH 5.8) for 5 days. 10 μM dexamethasone (diluted in half-strength MS liquid solution, Sigma) was added to the plates for 12 to 24 hours to induce the differentiation of protoxylem tracheary elements.

2.3 Results

2.3.1 Expression of SuSy in *Arabidopsis* stems

Since the *Arabidopsis* stem is largely composed of fibers, which in turn is dominated by cellulose biosynthesis, the stem is a very suitable model to study cellulose biosynthesis in *Arabidopsis*. *SuSy1* and *SuSy4* have previously been identified as the most highly expressed stem isoforms (Bieniawska et al., 2007). Consistent with these findings, our assessments of the transcript

abundance of all six *SuSy* genes were measured relative to UBQ5 in 6-week-old *Arabidopsis* stems using real-time quantitative PCR, and showed that *SuSy1* exhibited the highest transcript levels (Figure 2.1). *SuSy4* transcripts were 15% lower than *SuSy1*, but twice that of *SuSy6*. In contrast, *SuSy2* and *SuSy3* expression was barely detectable, while *SuSy5* was very low. Therefore, as the dominant genes expressed in the stem, *SuSy1* and *SuSy4*, were selected to test their putative roles in cellulose synthesis and deposition.

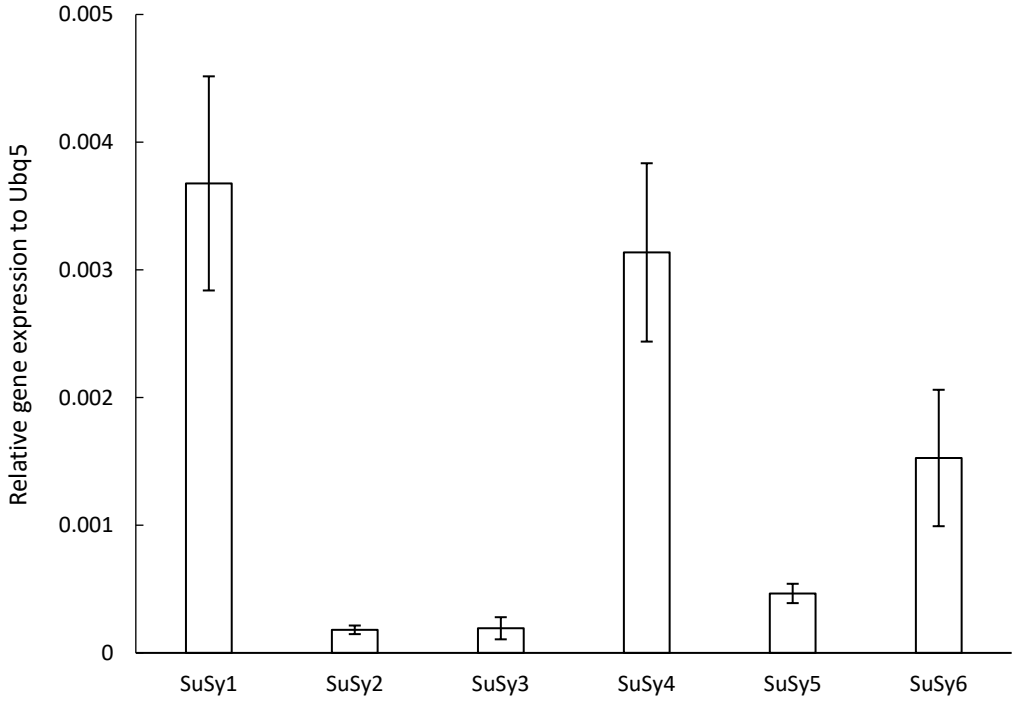

Figure 2.1 Transcript abundance of all six *Arabidopsis* SuSy isoforms in stems of 6-week-old plants. Transcripts were measured by real-time quantitative PCR using primers listed in Table 2.1. Means ± SE are calculated from three biological replicates.

2.3.2 Phenotypes of *sus1/sus4* double knock out mutant plants

Under normal growing conditions, *sus1/sus4* exhibited no obvious growth phenotypes compared to WT plants, except for a mild prevalence of chlorosis (Figures 2.2). In addition, soluble sugar and starch content of inflorescence stems and rosette leaves showed no significant difference from WT (Figure 2.3, Figure 2.4 and Figure 2.5). In contrast, under hypoxic conditions, reduced growth rates (Table 2.2) and significantly elevated soluble sugar and starch content (Figure 2.6 and Figure 2.7) were observed in the rosette leaves of *sus1/sus4* mutant, which is largely consistent with the report of Bieniawska et al. (2007). *sus1/sus4* and WT plants were subject to five days continuous flooding, alongside plants grown in well-aerated conditions as a control. The maximum rosette leaf size was measured at the beginning and the end of treatment. After five days of flooding, the overall increase in rosette size in WT plants was 1.16 ± 0.09 cm, while *sus1/sus4* double mutants were more severely affected by hypoxia, showing on average, an increase in rosette size of 0.44 ± 0.06 cm (Table 2.2). Compared to untreated plants, the final rosette size of flooded WT was reduced by 4.7% and *sus1/sus4* was reduced by 60.2%.

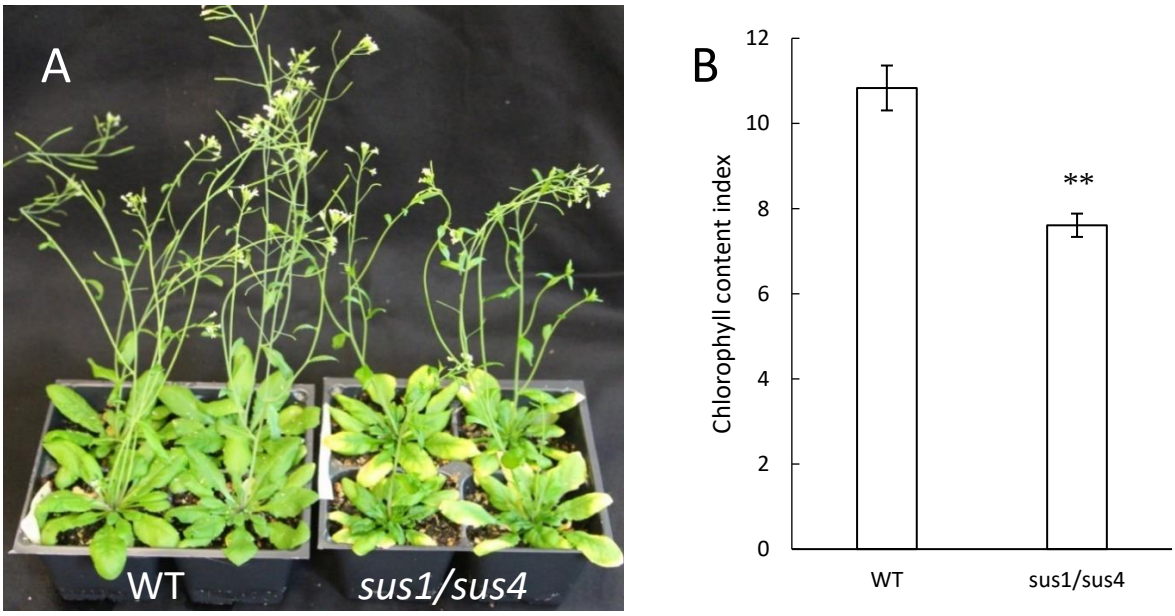

Figure 2.2 Representative 6-week-old WT and *sus1/sus4* mutant plants grown under the same conditions, clearly showing chlorosis in *sus1/sus4* double mutants (A). Chlorophyll Content Index (CCI) of the rosette leaf of *sus1/sus4* and WT (B). Results are the means ± SE of three replicates from each of four individual plants (n=4). Asterisks indicate significant difference (*p*-value < 0.01) from WT plants using a Student *t*-test.**

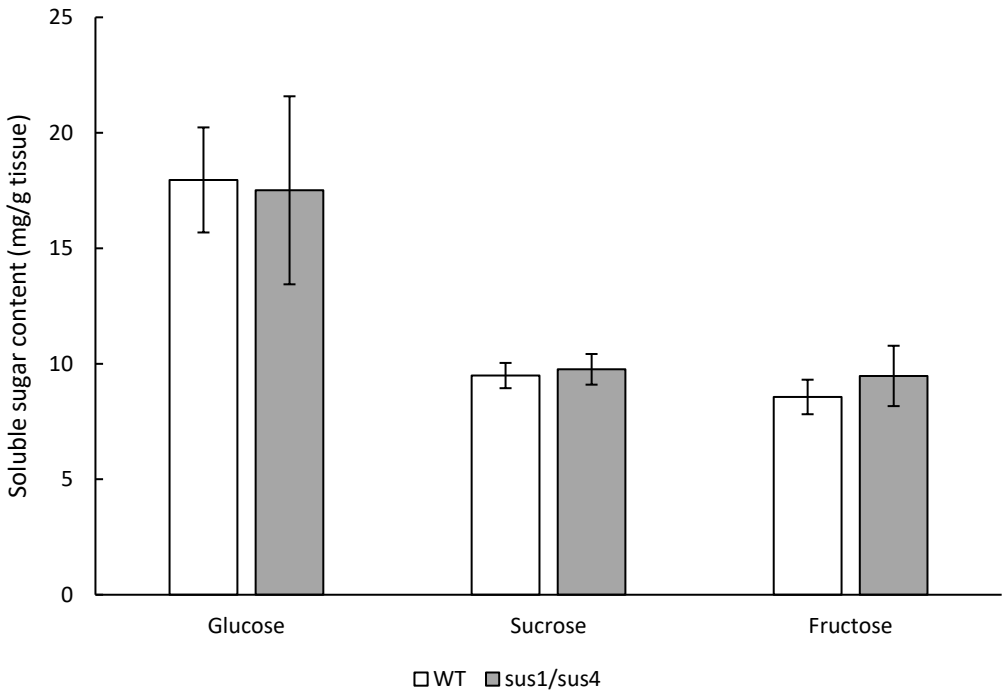

Figure 2.3 Soluble sugar content of rosette leaves from 6-week-old *Arabidopsis*. White bars represent WT plants, while grey bars represent *sus1/sus4* double mutants. Data are means ± SE calculated from four individual plants per line. There is no significant difference from WT according to a Student *t*-test.

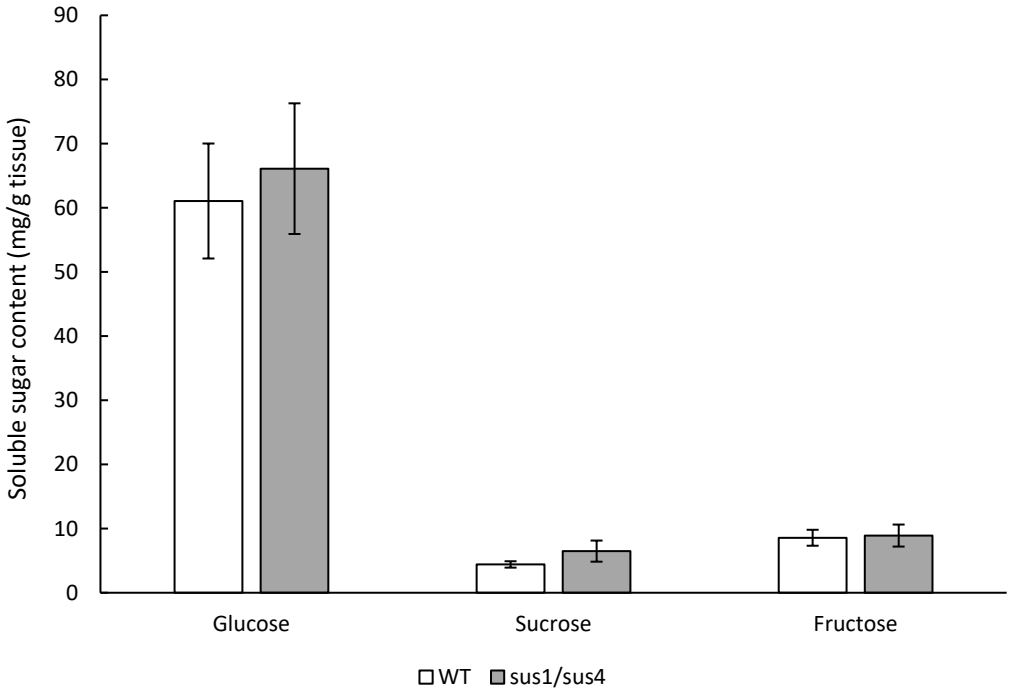

Figure 2.4 Soluble sugar content of inflorescence stems from 6-week-old *Arabidopsis*. White bars represent WT plants while grey bars represent *sus1/sus4* double mutants. Data are means ± SE calculated from four individual plants per line. There is no significant difference from WT according to a Student *t*-test.

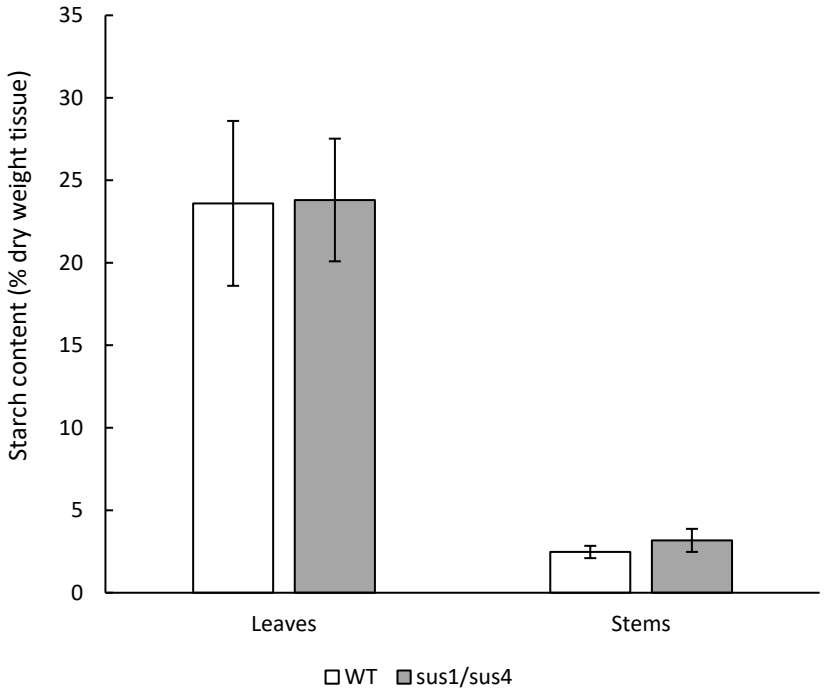

Figure 2.5 Starch content of stems and rosette leaves from 6-week-old *Arabidopsis*. White bars represent WT plants, while grey bars represent *sus1/sus4* double mutants. Data are means ± SE calculated from four individual plants per line. There is no significant difference from WT according to a Student *t*-test.

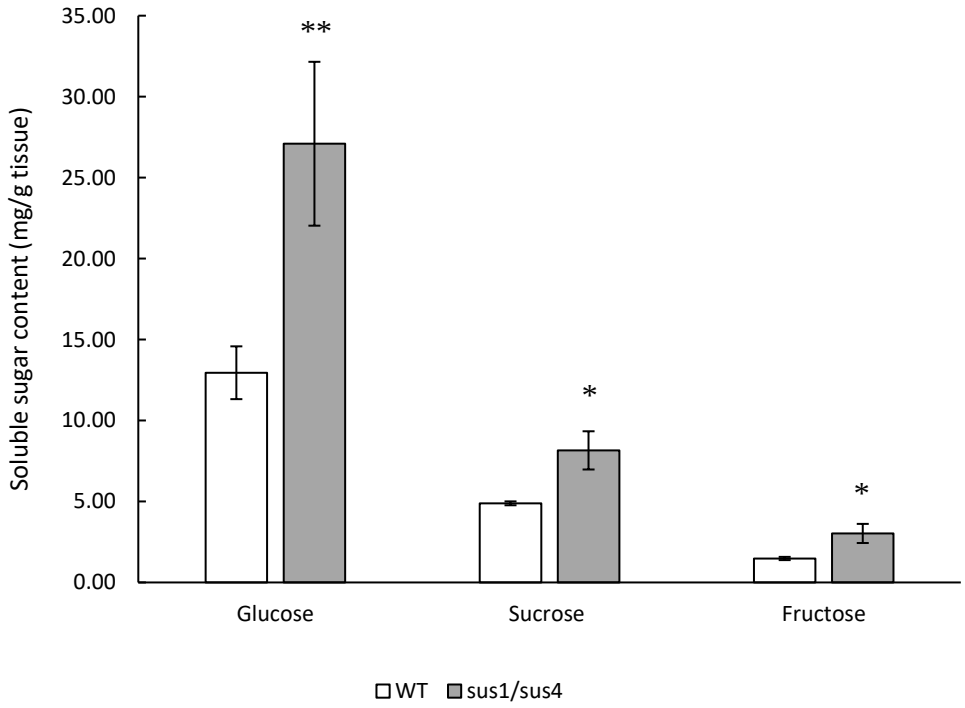

Figure 2.6 Leaf soluble sugar content of 4-week-old *Arabidopsis* after five days flooding. White bars represent WT, while grey bars represent *sus1/sus4* double mutants. Data are means ± SE calculated from four individual plants per line. Asterisks indicate significant difference (* *p*-value < 0.05, ** *p*-value < 0.01) from WT plants using a Student *t*-test.

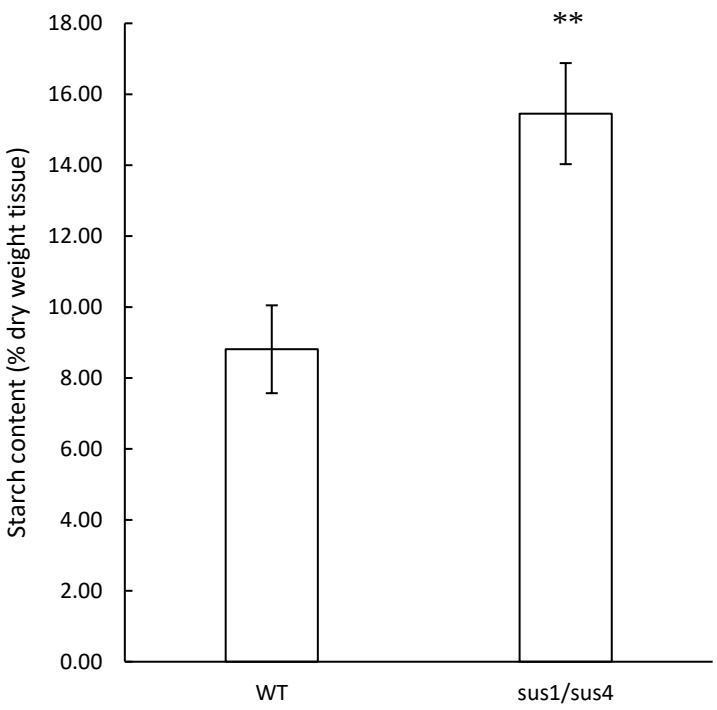

Figure 2.7 Leaf starch content of 4-week-old *Arabidopsis* following five days flooding. Data are means ± SE calculated from four individual plants per line. Asterisks indicate significant difference (*p*-value < 0.01) from WT plants using a Student *t*-test.**

Table 2.2 Partial complementation of *sus1/sus4* mutant rosette leaf growth phenotype by SuSy1- or SuSy4-YFP fusion constructs. 4-week-old WT, *sus1/sus4,* and two independently transformed transgenic SuSy1 and SuSy4 lines were subjected to flooding by maintaining degassed water above the surface of the soil for five consecutive days. The control plants represent plants without flooding and were watered only when necessary. Rosette leaf sizes were measured on the 1st and 5th day of growth. Mean (SE) values are calculated from at least three individual plants per line. Asterisks indicate significant difference (* corrected *p*-value < 0.05, ** corrected *p*-value < 0.01) of rosette size gain (Column A and Column B) using the Benjamini-Hochberg (Benjamini and Hochberg, 1995) corrected Student *t*-test.

Line	Flooding			Control			
	Rosette size at first day	Rosette size after 5 days	Size gain (A)	Rosette size at first day	Rosette size after 5 days	Size gain (B)	% reduction in rosette size gain (1-A/B)×100
WT	3.24(0.08)	4.40(0.10)	1.16(0.09)	3.06(0.14)	4.27(0.13)	1.21(0.07)	4.71
sus1/sus4	2.90(0.11)	3.34(0.09)	0.44(0.06)**	2.80(0.26)	3.90(0.14)	1.10(0.12)	60.23
*SuSy1$_{pro}$::SuSy1::YFP*1	2.96(0.16)	3.66(0.09)	0.70(0.12)**	2.97(0.37)	3.93(0.44)	0.97(0.13)	27.59
*SuSy1$_{pro}$::SuSy1::YFP*2	2.50(0.15)	3.13(0.15)	0.63(0.09)**	2.65(0.23)	4.00(0.07)	1.35(0.14)	53.09
*SuSy4$_{pro}$::SuSy4::YFP*1	3.15(0.06)	3.88(0.13)	0.73(0.10)**	2.60(0.11)	3.53(0.05)	0.93(0.14)	21.62
*SuSy4$_{pro}$::SuSy4::YFP*2	3.10(0.17)	4.03(0.22)	0.93(0.12)	2.68(0.13)	3.70(0.25)	1.03(0.19)	9.76

2.3.3 SuSy1 and SuSy4 are not present in the VND7-induced tracheary elements

Arabidopsis SuSy1 (At5g20830) and *SuSy4* (At3g43190) coding sequences were cloned and fused to either a C-terminal or N-terminal YFP fluorescence tag. Constructs were placed under the regulation of the respective *Arabidopsis SuSy1* or *SuSy4* promoters. To examine the interaction of SuSy1 and SuSy4 with CesA during secondary cell wall formation, a vascular-related NAC domain 7 (VND7) inducible protoxylem tracheary element (TE) differentiation system was employed. Previous study has demonstrated that the overexpression of *Arabidopsis* VND7

transcript factor could induce the transdifferentiation of seedling cells into protoxylem TE (Kubo et al., 2005). In this system, VND7 is paired with an inducible transcriptional activator, the viral protein 16 (VP16) coupled with a glucocorticoid receptor (GR; Yamaguchi et al., 2010). Upon induction with dexamethasone (DEX), even the epidermal cells in *Arabidopsis* seedlings could differentiate into TE, which permits high-resolution imaging of proteins expressed in the TE. All SuSy YFP fusions were transformed into *Arabidopsis* line carrying VND7-VP16-GR and transgenic plants showed good signal confined to the vasculature of seedling roots (Figure 2.8). However, no YFP signal of either SuSy1 and SuSy4 was detected in the induced TE cells (Figure 2.9), indicating that SuSy1 and SuSy4 are not upregulated during protoxylem TE secondary cell wall formation.

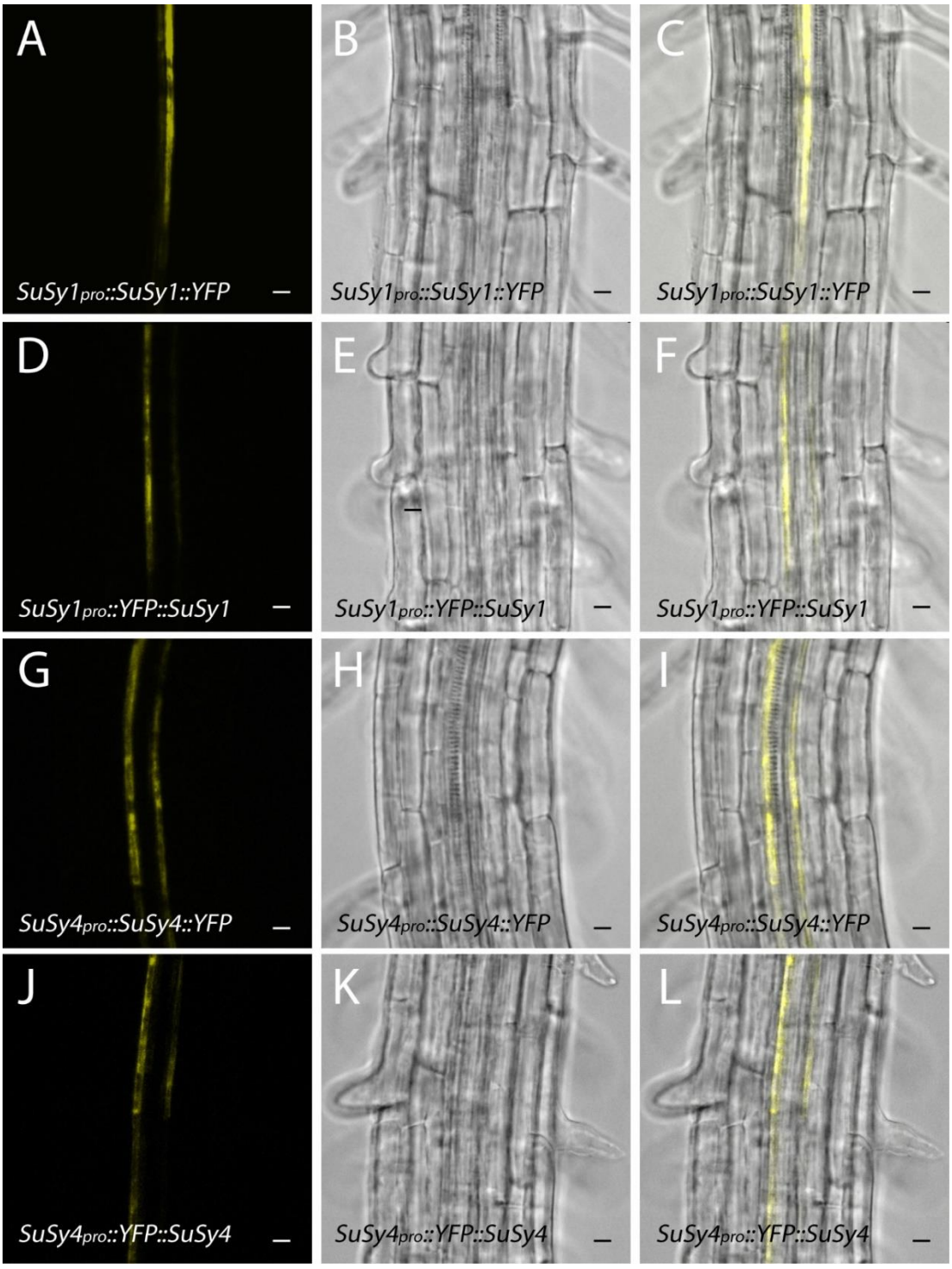

Figure 2.8 Localization of SuSy1 and SuSy4 YFP fusions in the roots of 7-day-old seedlings. Images showing that N-terminal and C-terminal YFP fusion proteins of AtSuSy1 (A-F) and AtSuSy4 (G-L) were detected in the

vasculature of roots. (A, D, G, J) YFP fluorescence panels, (B, E, H, K) bright field images, (C, F, I, L) merged images of YFP fluorescence and bright field images. Bars=10 µm.

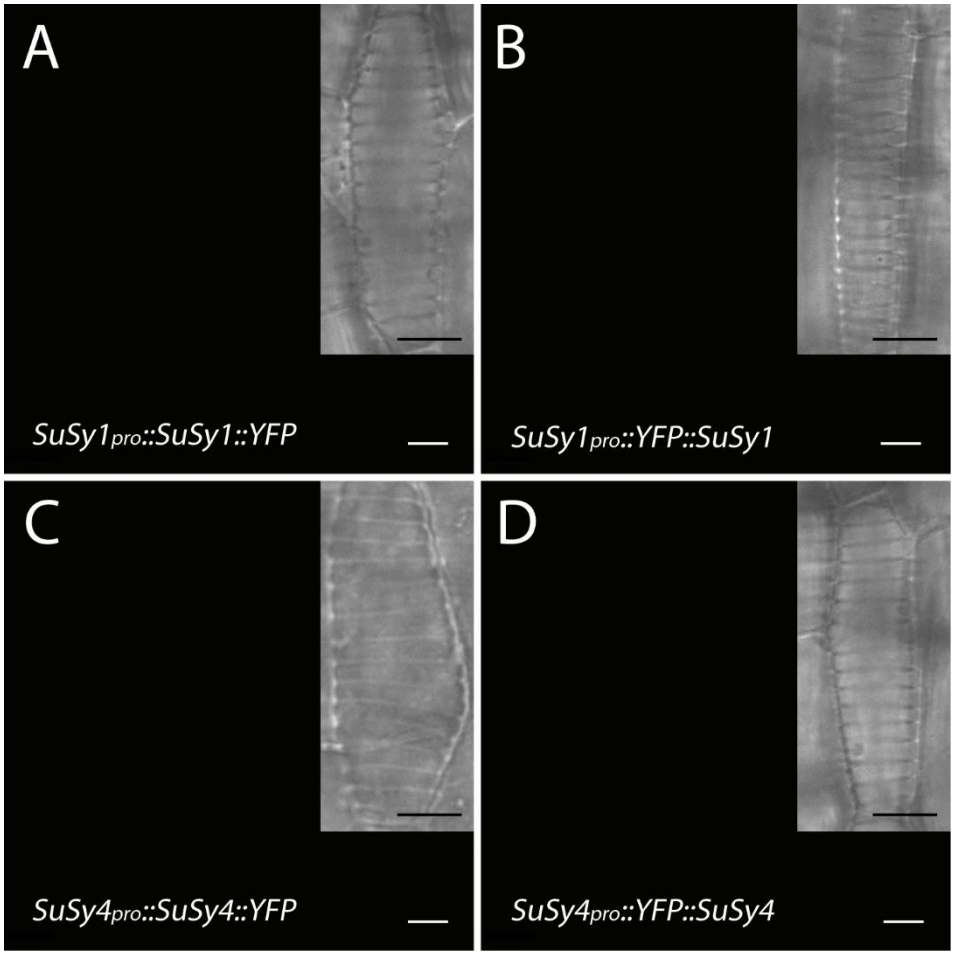

Figure 2.9 No YFP signal was detected in the VND7-induced *Arabidopsis* seedlings tracheary elements. In the 5-day-old *Arabidopsis* seedlings carrying both VND7-VP16-GR and SuSy-YFP, after induction with DEX, YFP signal of SuSy1 and SuSy4 was not detectable in the transdifferentiated protoxylem TE cells. A-D are YFP fluorescence panels and inserted images are bright field images showing transdifferentiated TE. Bars=10 µm.

2.3.4 Spatiotemporal localization of SuSy1 and SuSy4

The same four constructs were also transformed into *sus1/sus4* double mutants and all transgenic lines showed strong YFP fluorescence. Lines expressing C-terminal YFP fusions were used for further research, and the functionality of fusion proteins was tested by examining the level of the functional complement of the *sus1/sus4* loss-of-function mutants. In general, individual SuSy-YFP fusions partially rescued the *sus1/sus4* phenotypes: demonstrating partial recovery of the observed leaf chlorosis (Figure 2.10) and the reduced growth rate (Table 2.2). Complete recovery of the cellular soluble sucrose was observed under hypoxic conditions (Figure 2.11). However, three out of four SuSy transgenic lines failed to recover starch content (Figure 2.12). Subsequently, live-cell imaging was performed to visualize the distribution of SuSy1 and SuSy4 via spinning disk confocal microscopy. Consistent with previous results in the VND system, the YFP signal was not detectable in the xylem of any organ examined, including leaves (Figure 2.13), stems (Figure 2.14), siliques (Figure 2.15) and roots (Figure 2.16). Instead, SuSy1 and SuSy4 fusion proteins were consistently shown to be abundantly present in phloem tissue. In the roots of 7-day-old-seedlings, protoxylem cells were stained with propidium iodide and the fluorescently-tagged SuSy signal was observed specifically in the phloem poles (Figures 2.16). In addition, unlike SuSy1, SuSy4 signal was present at the root tips (Figure 2.17). SuSy1 and SuSy4 were also found in the funiculus, and only SuSy1 was shown to be present in the unloading domain of seeds at the end of a funiculus (Figure 2.18).

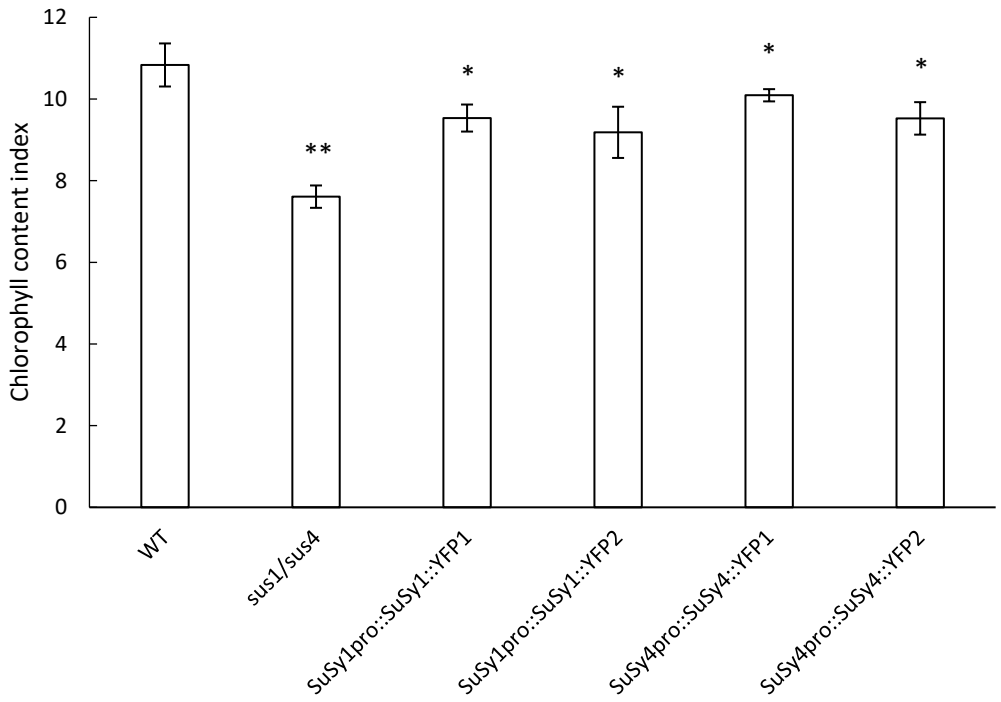

Figure 2.10 Chlorophyll Content Index (CCI) of the rosette leaves from *sus1/sus4*, WT, and SuSy transgenic plants grown under the same conditions. Results are the means ± SE of three technical replicates from each of four individual plants (n=4). Asterisks indicate significant difference (* corrected *p*-value < 0.05, ** corrected *p*-value < 0.01) from WT plants using a Benjamini-Hochberg corrected Student *t*-test.

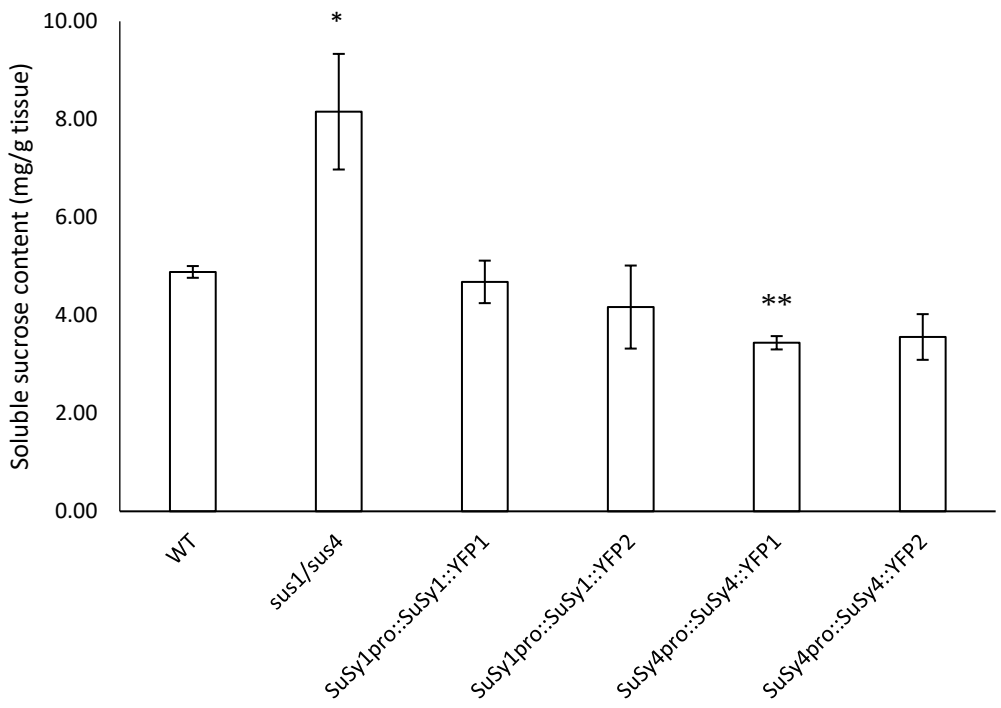

Figure 2.11 Leaf soluble sucrose content of 4-week-old *sus1/sus4*, WT and transgenic lines containing SuSy-YPF after five days flooding. Data are means ± SE calculated from four individual plants per line. Asterisks indicate significant difference (* corrected *p*-value < 0.05, ** corrected *p*-value < 0.01) from WT plants using a Benjamini-Hochberg corrected Student *t*-test.

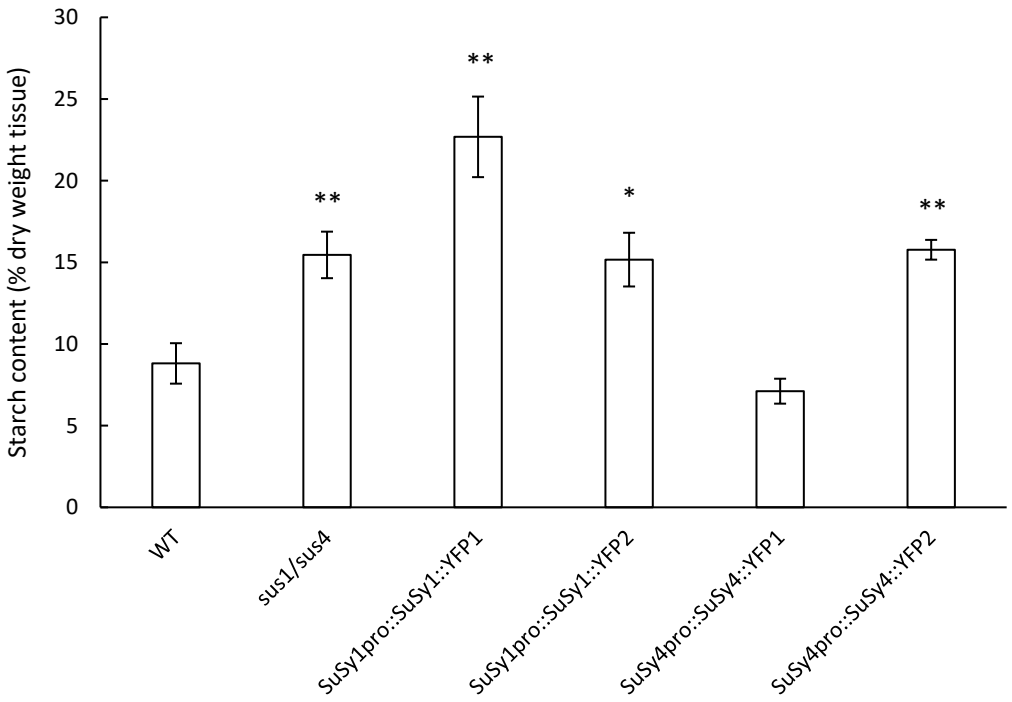

Figure 2.12 Leaf starch contents of 4-week-old *sus1/sus4*, WT and transgenic lines after five days flooding. Data are means ± SE calculated from four individual plants per line. Asterisks indicate significant difference (* corrected *p*-value < 0.05) from WT plants using a Benjamini-Hochberg corrected Student *t*-test.

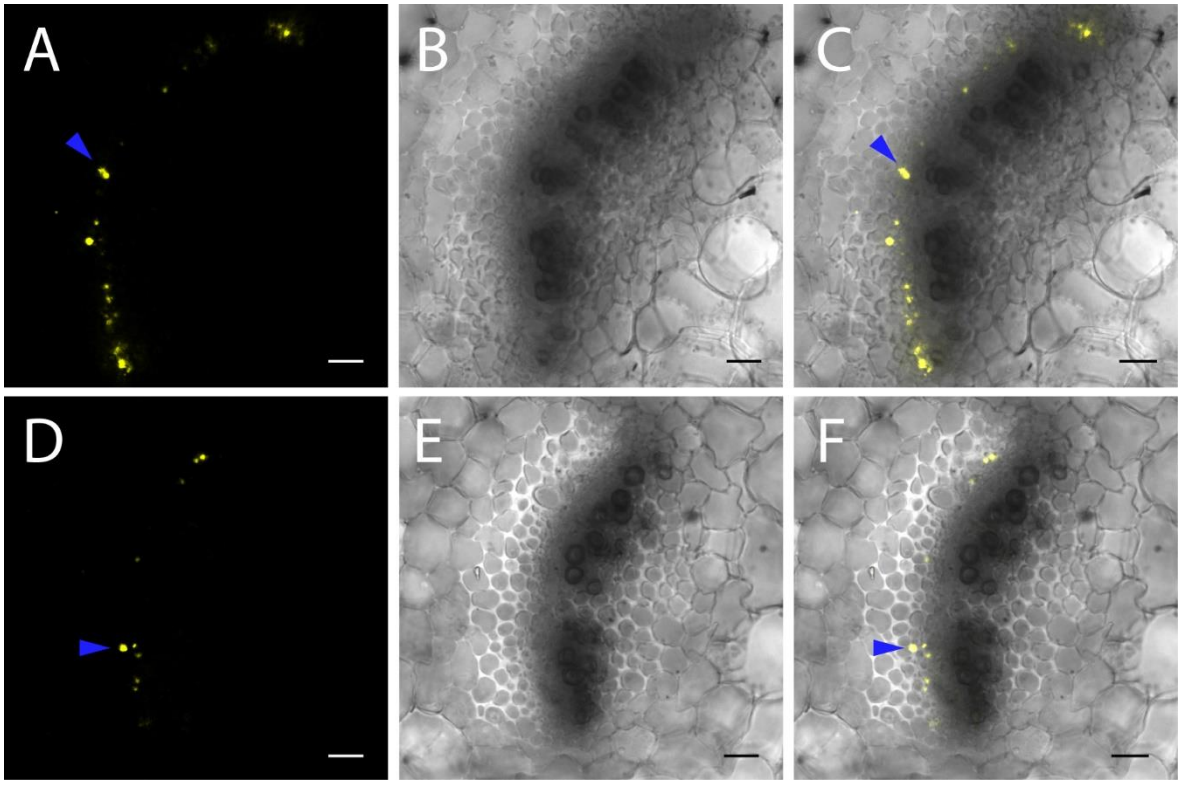

Figure 2.13 Confocal images of AtSuSy1-YFP and AtSuSy4-YFP in the cross sections of leaf petioles of transgenic *Arabidopsis*. Images showing YFP signal of SuSy1 (A-C) and SuSy4 (D-F) in the phloem of petioles (Arrowheads). (A, D) YFP fluorescence panels, (B, E) bright field images, and (C, F) merged images of YFP fluorescence and bright field images. Bars=50 µm.

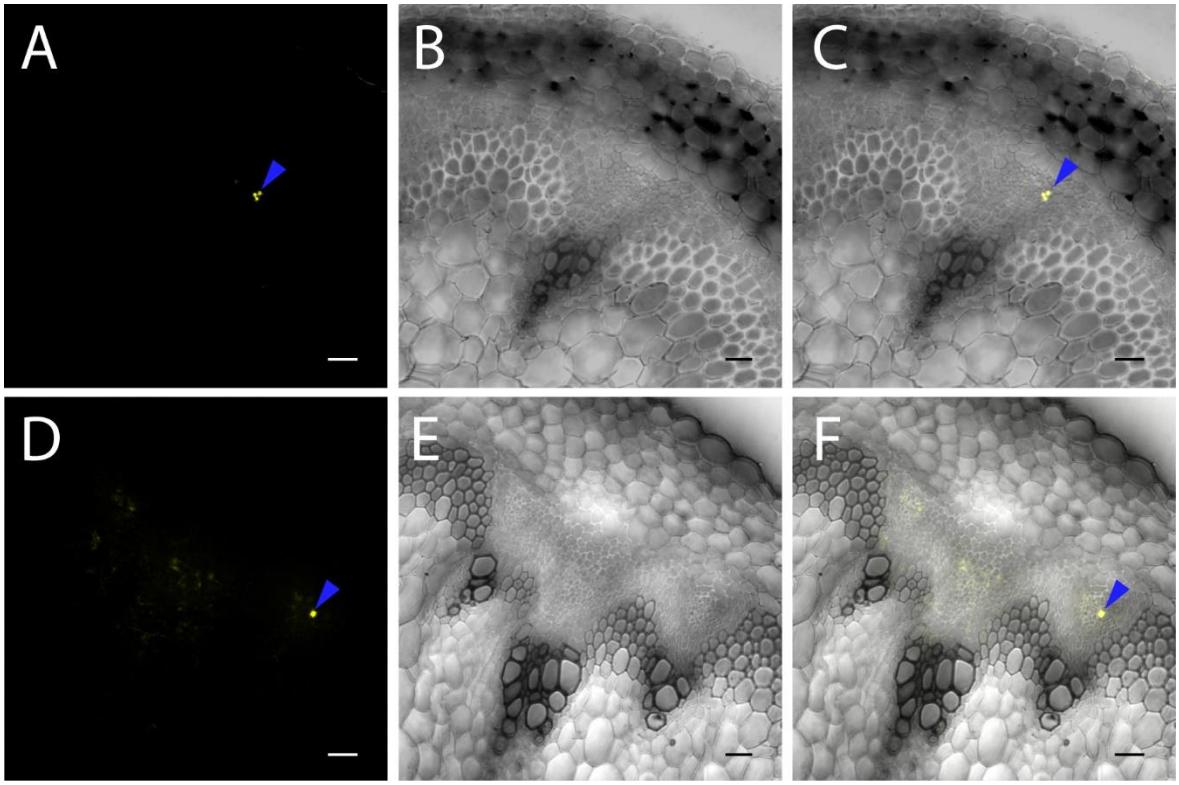

Figure 2.14 AtSuSy1-YFP and AtSuSy4-YFP were localized in the phloem of stems of transgenic *Arabidopsis* plants. Images showing YFP signal of SuSy1 (A-C) and SuSy4 (D-F) in the phloem of inflorescence stem cross sections (Arrowheads). (A, D) YFP fluorescence panels, (B, E) bright field images, and (C, F) merged images of YFP fluorescence and bright field images. Bars=50 µm.

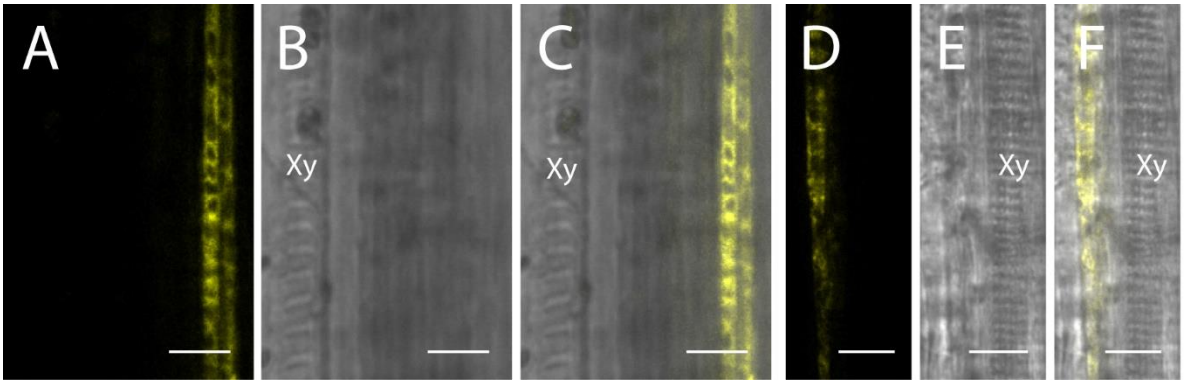

Figure 2.15 Phloem localization of AtSuSy1-YFP and AtSuSy4-YFP in silique walls. Longitudinal sections of silique walls showing SuSy1 (A-C) and SuSy4 (D-F) in the phloem and not in protoxylem cells (Xy). A and D represent channels of YFP fluorescence, while B and E are bright field images, and C and F are merged images of YFP panels and bright field images. Bars=10 µm.

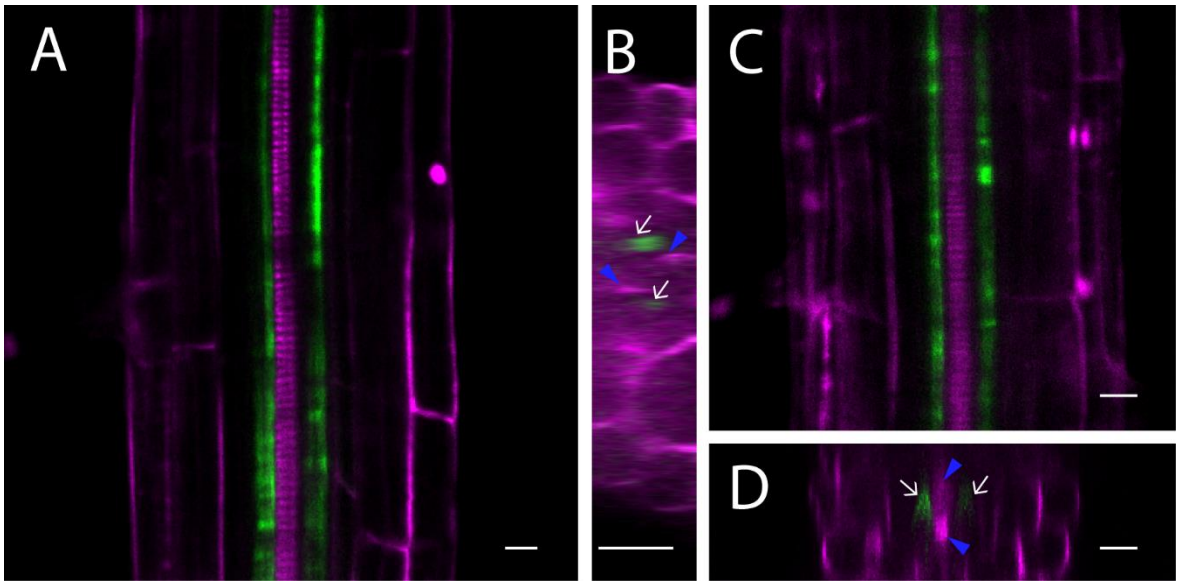

Figure 2.16 Phloem localization of AtSuSy1-YFP and AtSuSy4-YFP in the roots of 7-day-old *Arabidopsis* seedling. YFP labelling of AtSuSy1 (A) and AtSuSy4 (C) in the phloem of roots. Sections showing AtSuSy1 (B) and AtSuSy4 (D) were confined to the phloem poles (white arrows). Propidium iodide staining (magenta) was used to label protoxylem (blue arrowheads). Bars=10 µm.

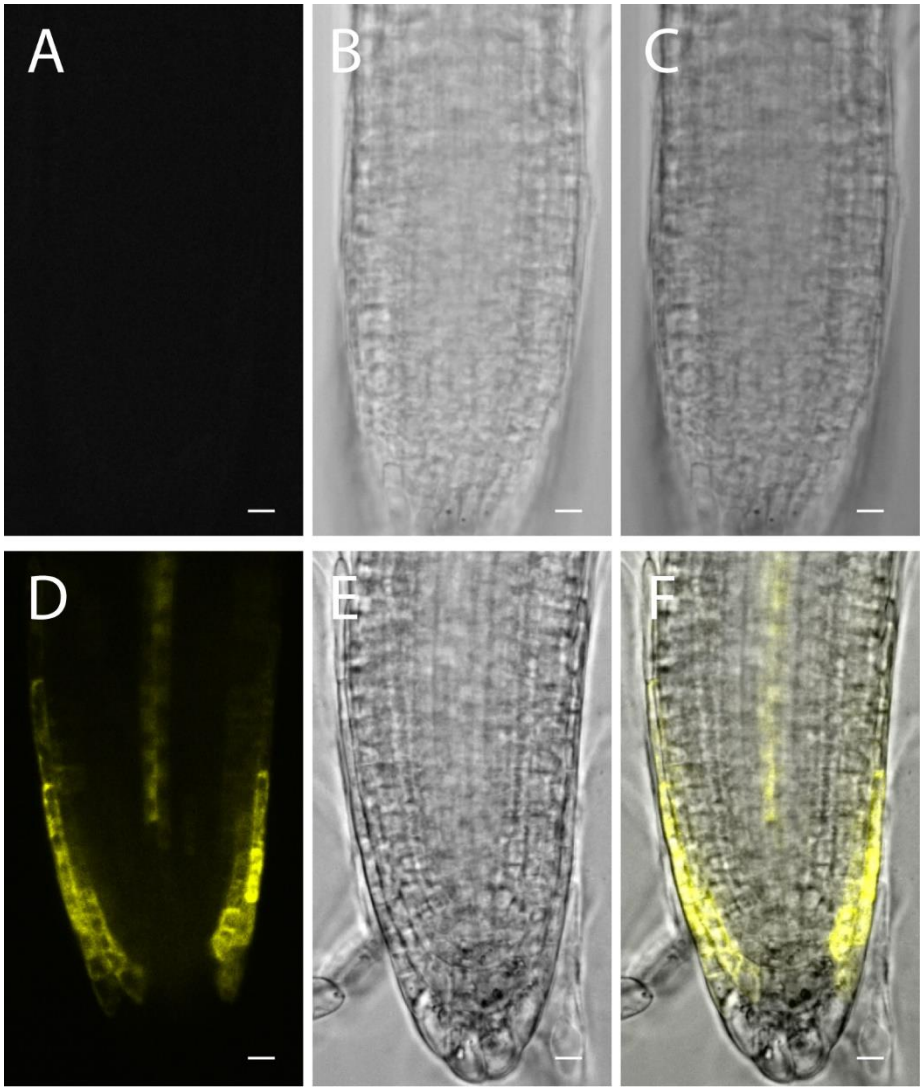

Figure 2.17 Localization of AtSuSy1-YFP and AtSuSy4-YFP in the roots of 7-day-old seedlings. Images showing AtSuSy4 (D-F) present in the root tips, while AtSuSy1 (A-C) was not detectable. (A, D) YFP fluorescence panels, (B, E) bright field images, (C, F) merged images of YFP fluorescence and bright field images. Bars=10 µm.

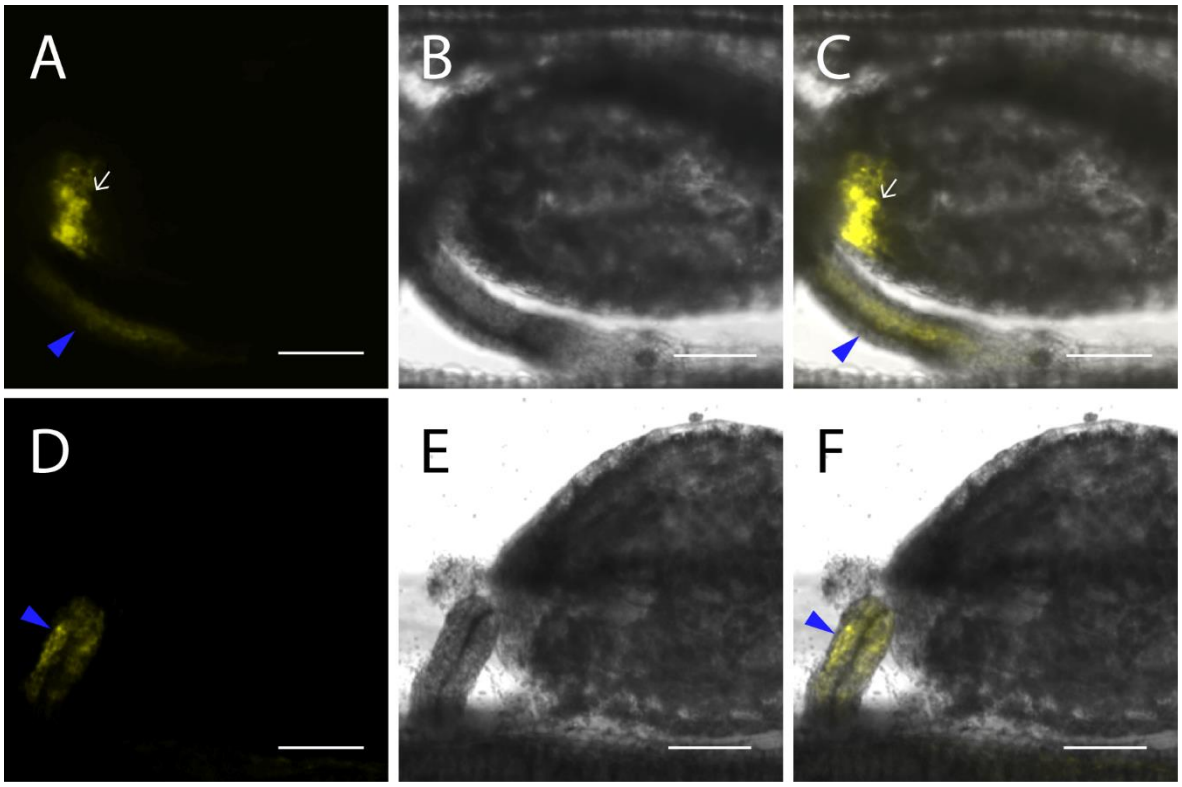

Figure 2.18 Different spatial localization of AtSuSy1-YFP and AtSuSy4-YFP in *Arabidopsis* seeds. AtSuSy1 was detected in the funiculus (arrowheads) and unloading zone (arrows) of seeds (A-C), and AtSuSy4 was found in the funiculus (D-F) as indicated by arrowheads (I and J). (A, D) YFP fluorescence panels, (B, E) bright field images, (C, F) merged images of YFP fluorescence and bright field images. Bars=50 µm.

2.3.5 SuSy1 and SuSy4 were confined to companion cells

To further examine the precise localization of SuSy1 and SuSy4 proteins, thin longitudinal sections of leaf petioles that allowed single cell imaging were employed. SuSy1 and SuSy4 were extensively detected in cells showing the morphology typical of companion cells (Figures 2.19 A and B), which differ from sieve elements as they inherently contain nuclei and vacuoles. To support this observation, the identity of these cells was confirmed with aniline blue staining, which

specifically labels the callose enriched sieve plates of sieve elements (Figure 2.19 C and D). Interestingly, both SuSy-YFP fusion proteins were consistently observed to be streaming within the cytoplasm of the companion cells, as shown by time-lapse video (Movie S1).

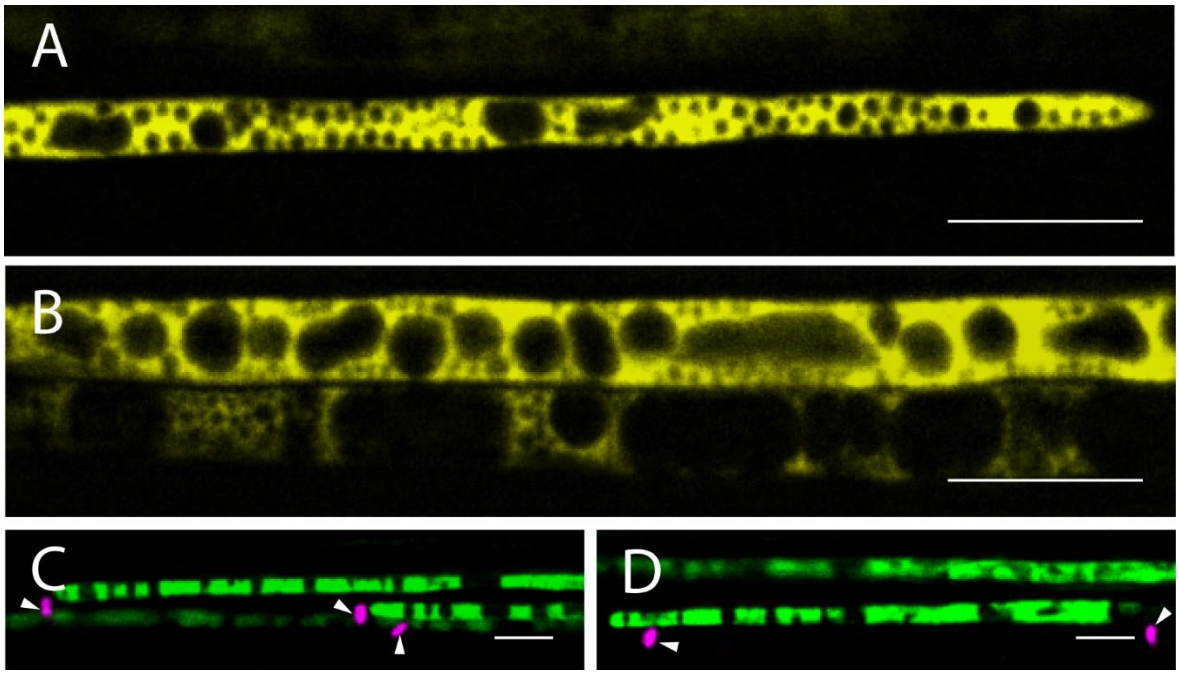

Figure 2.19 AtSuSy1-YFP and AtSuSy4-YFP were specifically localized to the companion cells. Longitudinal sections of transgenic *Arabidopsis* leaf petioles showing AtSuSy1 (A) and AtSuSy4 (B) in companion cells containing numerous intracellular organelles. Associated sieve plates were stained with aniline blue (arrowheads) in panels showing YFP signal of AtSuSy1 (C) and AtSuSy4 (D). Bars=10 µm.

2.4 Discussion

Previous studies (Amor et al., 1995; Haigler et al., 2001; Koch, 2004), including several textbook models (Taiz and Zeiger, 2010) have proposed that SuSy is part of, or interacts directly with, the cellulose synthase complex at the plasma membrane to channel UDP-glucose derived from sucrose

directly to growing cellulose polymer synthesized into the apoplast. To investigate the putative model, we used *Arabidopsis* xylem, located near the base of growing stem, a tissue with a high demand for UDP-glucose for the biosynthesis of cellulose (among other carbohydrates), to localize SuSy isoforms. We employed the VND7 inducible protoxylem tracheary element differentiation system to track SuSy protein during secondary cell wall formation. Surprisingly, no YFP signal associated with SuSy1 and SuSy4 was detected in induced TE cells. Live-cell imaging of fluorescently-tagged SuSy was thus carried out in several xylem-producing plant tissues including stems, leaves, siliques, and roots using confocal microscopy. Our results clearly demonstrated that neither SuSy1 nor SuSy4 was detectable in xylem, and more importantly, they were exclusively expressed in the phloem.

Consistent with Bieniawska et al. (2007), *sus1/sus4* double mutant plants exhibited no obvious growth phenotype when grown in well-aerated conditions, with the exception of slight levels of chlorosis, but showed significantly reduced growth rate and accumulation of soluble carbohydrates when subjected to flooding. Similar phenomena were also apparent in maize mutants lacking SuSy activity, which showed root death only during anoxic growth conditions (Ricard et al., 1998). In addition, elevation of SuSy transcript abundance and activity in response to hypoxic conditions has been reported in *Arabidopsis* (Baud et al., 2004; Bieniawska et al., 2007), as well as in wheat (Albrecht and Mustroph, 2003) and potato (Biemelt et al., 1999). This specific response (SuSy induction) has been proposed to be biologically beneficial under these conditions, as it offers an energetically more efficient way to supply UDP-glucose to biological processes: requiring a single enzymatic step via SuSy, while sucrose hydrolysis via invertases requires several additional

biochemical conversions for the formation of UDP-glucose (Canam et al., 2006). Thus, under anaerobic stress and limited ATP supply, the SuSy pathway of sucrose cleavage may be favoured in some plants. Evidence supporting this claim includes the observed rapidly decreasing ratio of INV-SuSy activity when maize roots (Zeng et al., 1999) and rice seedlings (Guglielminetti et al., 1995) were exposed to low levels of oxygen. Moreover, leaf chlorosis has been associated with inhibition of phloem loading (Zhang et al., 2014). In this study, leaf chlorosis was obvious in six-week-old *sus1/sus4* plants, indirectly supporting the putative role of these two SuSy isoforms in phloem loading in *Arabidopsis*.

In support of this claim, our live-cell imaging data clearly shows that SuSy1 and SuSy4 were exclusively localized to phloem companion cells, and were not present in the xylem of the tissues examined. Moreover, it was apparent that both isoforms were actively streaming in the cytoplasm of these cells (Movie S1). The current findings confirm early observations of SuSy1 activity within phloem cells (Martin et al., 1993). Furthermore, companion cell-specific localization of SuSy has been previously reported in leaves of rice (*Oryza sativa*), maize (*Zea mays*), *Arabidopsis*, and citrus (*Citrus paradise*) by immunohistochemistry studies (Nolte and Koch, 1993; Fallahi et al., 2008; Regmi et al., 2016). Our current study uniquely examined the tissue and subcellular localization of all (this Chapter and Chapter 3) SuSy isoforms. These findings, therefore, provide further insight into the potential role of SuSy in the energy-dependent sucrose loading. In *Arabidopsis*, sucrose is believed to be actively loaded into the phloem from the apoplast via a plasma membrane-localized AtSUC2 H^+-sucrose symporter inherent to companion cells (Stadler and Sauer, 1996). This symporter has been proposed to be important not only for phloem loading

in the source tissues, but also for sucrose retrieval during long-distance transport (Truernit and Sauer, 1995; Stadler and Sauer, 1996; Gottwald et al., 2000). Our data suggest that the distribution pattern of the SuSy isoforms is similar to that of AtSUC2 (and other potential H^+-sucrose symporters). Therefore, a more likely role for SuSy1 and SuSy4 is the production of ATP required for active sucrose loading. In addition, we provide evidence that SuSy1 was highly expressed in the symplastic unloading zone at the end of a funiculus (Figure 2.18). In *Arabidopsis*, sucrose unloading at the terminal ends of phloem tissue has been reported to be mainly symplastic, as observed in anthers (Imlau et al., 1999), developing seeds (Imlau et al., 1999; Stadler et al., 2005a), and root tips (Stadler et al., 2005b). Though the exact function of SuSy in this passive diffusion mechanism is not clear, one possibility is that the sucrose concentration, modulated by SuSy, may regulate the efficiency and extent of symplastic carbohydrate unloading. Only SuSy4 activity was detected in the root tips, where it may regulate the cell division by changing cell osmolarity.

Chapter 3: Investigation of spatiotemporal localization of *Arabidopsis* SuSy2, SuSy3, SuSy5 and SuSy6

3.1 Introduction

Sucrose derived from photosynthesis is broken down either by sucrose synthase or invertase. SuSy alone has been implicated in different functional roles in cellular metabolism, including supplying carbon for plant respiration, synthesis of secondary metabolites, synthesis of starch and the precursor for the biosynthesis of cellulose and callose (Haigler et al., 2001; Munoz et al., 2005; Verbancic et al., 2018). In addition, SuSy activity is thought to be important for determining sink strength. In the widely cited model of cellulose biosynthesis, SuSy is suggested to be tightly associated with cellulose synthase complex at the plasma membrane to channel UDP-glucose directedly to cellulose biosynthesis (Amor et al., 1995; Koch, 2004; Verbancic et al., 2018).

Arabidopsis contains six SuSy genes that exhibit distinct spatiotemporal expression profiles. It has been reported that SuSy2 is specifically induced in seeds at early maturation phase, but barely detectable in other tissues (Bieniawska et al., 2007; Nunez et al., 2008). Similarly, SuSy3 has been shown to be highly expressed in seeds during late maturation phase and has also been detected in the root vasculature (Bieniawska et al., 2007; Angeles-Nunez and Tiessen, 2010). Furthermore, in rosette leaves, SuSy3 has been shown to be confined to the guard cells of stomata, as shown by GUS staining (Bieniawska et al., 2007). In addition, the transcript abundance of SuSy3 has been shown to be induced by environmental stresses, including dehydration and sugar feedings (Baud

et al., 2004). In contrast, SuSy5 and SuSy6 were shown to be more widely expressed and no transcriptional difference was detected in response to stress (Baud et al., 2004). Moreover, it has consistently been reported that no single mutant of *Arabidopsis* SuSy exhibited an obvious growth phenotype and double mutant plants lacking homologous pairs (similar isoforms) were also not significantly different from WT plants (Bieniawska et al., 2007). The importance of SuSy in *Arabidopsis* growth and development has been questioned, as quadruple mutants (*sus1/sus2/sus3/sus4*) were indistinguishable from WT in all aspects of growth, cellulose content and cell wall structure (Barratt et al., 2009). However, Fallahi et al. (2008) reported that *SuSy2* and *SuSy3* were functional in seeds, since single knockouts of *SuSy2* and *SuSy3* exhibited different metabolic profiles at specific stages of seed development. Thus, SuSy2 and SuSy3 have been subsequently implicated in maintaining metabolite homeostasis and starch biosynthesis of seeds. In contrast, SuSy5 and SuSy6 have been shown to be confined to phloem sieve elements where they are proposed to play a specific role in callose synthesis (Barratt et al., 2009).

Seeds are an important sink of plants, and seed development is a vital process in the life cycle of higher plants. Three distinct stages of seed development have been characterized, including: morphogenesis, maturation and metabolic quiescence of the embryo (Baud et al., 2002; Figure 3.1). During early morphogenesis (until 6 days after flowering), the embryo establishes the basic architecture of a plant through a series of cell divisions. In the second phase of development (maturation), embryo cells undergo a period of cellular expansion, differentiation, as well as the synthesis of storage compounds, including nitrogen (proteins) and carbon compounds (lipids and starch; Baud et al., 2002). Finally, the embryo becomes metabolically quiescent and cellular

respiration is shut down, which enables seeds to be stored for a long period of time (Kermode et al., 1985). *Arabidopsis* seeds are composed of three parts: seed coat, endosperm and embryo. During the early stage of embryogenesis, rapid cell division occurs to establish the morphology of the embryo. The morphogenesis phase ends at five or six days after flowering (DAF), when the embryo reaches the heart stage (Mayer et al., 1991). From the torpedo stage (7 DAF) to the mature cotyledon stage (10 DAF), the endosperm is almost absorbed by the enlarged embryo, which finally occupies all free space within the integument (Baud et al., 2002). In contrast, during the maturation phase, the embryo undergoes cell expansion and accumulation of storage product, characterized by a rapid increase in seed dry weight (Baud et al., 2002; Fait et al., 2006). The seed coat consists of five cell layers (Western et al., 2000; Haughn and Chaudhury, 2005), and during differentiation, epidermal cells synthesize and deposit mucilage in the apoplast adjacent to the radial and tangential cell walls, forming a donut-shaped mucilage pocket surrounding a volcano-shaped cytoplasmic column. Later, a cellulose-rich secondary cell wall (columella) is subsequently deposited beneath the mucilage pocket, replacing the cytoplasm. Starch accumulates temporarily in the seed coat and embryo to be remobilized later for use in the biosynthesis of lipid, storage protein, and mucilage (da Silva et al., 1997; Lin et al., 2006; Angeles-Nunez and Tiessen, 2010). The endosperm plays a key role in providing nutrients for embryo growth during seed development or to seedlings during early germination and establishment (Yan et al., 2014). Development of the endosperm can be divided into several phases, including the formation of nuclear endosperm, cellularization, differentiation, maturation, and cell death (Kang et al., 2008; Yan et al., 2014). At seed maturity, the endosperm is absent in seeds of some species, but in *Arabidopsis* a thin layer of endosperm tissue is retained (aleurone layer; Muller et al., 2006; Lee et al., 2012).

In the previous chapter (Chapter 2), I suggested that AtSuSy1 and AtSuSy4 were not observed in xylem and not directly associated with cellulose biosynthesis, but were specifically localized to phloem companion cells of all tissues examined in *Arabidopsis*. To examine the possibility that in the absence of SuSy1 or SuSy4, one of the other four SuSy isoforms acts redundantly and thus provides UDP-glucose in xylem and therefore facilitates cellulose biosynthesis as the largely accepted model implies, I investigated the spatiotemporal localization of YFP fusions of SuSy2, SuSy3, SuSy5 and SuSy6 via live-cell imaging. In addition, I performed immunofluorescent labelling on the cross sections of *Arabidopsis* stem and petiole with an anti-soybean SuSy immune serum to confirm the results of live-cell imaging. The data showed that none of the four SuSy isoforms was detectable in the developing xylem of the tissues examined, including roots, leaves, stems, and siliques. In contrast, SuSy5 and SuSy6 were identified to be confined to the sieve elements of phloem, and SuSy2 and SuSy3 were confirmed to be highly expressed in developing seeds. In addition, SuSy signal was observed in phloem tissue through the immunolocalization studies. Our results bring into question the current model of cellulose biosynthesis in *Arabidopsis*, and help to define a functional and biological role for SuSy in *Arabidopsis* development.

3.2 Methodologies

3.2.1 Genomic DNA extraction

50-200 mg of fresh tissue was ground in liquid nitrogen and immediately immersed in 1 mL CTAB buffer (2% (w/v) CTAB [Sigma], 1.4 M NaCl, 20 mM EDTA, 100 mM Tris-HCl, 1% PVP, 2-mercaptoethanol, pH 8.0). Samples were incubated at 65 °C for 30 to 60 minutes and then

centrifuged at 13,000 rpm for 10 minutes. The supernatant was subsequently transferred to a new tube and one volume of phenol:chloroform:isoamyl alcohol was added to each tube, mixed thoroughly and centrifuged at 13,000 rpm for 10 minutes. The supernatant was collected and half a volume of isopropanol was added to precipitate the DNA by centrifugation. The resulting pellet was washed with 500 µL 70% ethanol and air dried for approximately 30 minutes. Finally, the pellet was suspended in deionized water and stored at -20 °C for later use. The quick DNA extraction method was employed to screen *Arabidopsis* homozygous mutants and transgenic plants, according to Edwards et al. (1991).

3.2.2 RNA isolation and RT-PCR

Stems of mature *Arabidopsis* plants were harvested after 6 weeks of growth and ground in liquid nitrogen in a mortar and pestle. RNA was extracted using the TRIzol® reagent (Invitrogen) according to the manufacturer's instructions and treated with TURBO DNase™ (Ambion) to remove residual DNA. For RNA isolation from silique tissues, which are abundant in lipids and starch, the PureLink® Plant RNA Reagent (Invitrogen) was employed according to the manufacturer's instructions. cDNA was synthesized using the iScript™ Select cDNA Synthesis Kit (BIO RAD) with oligo-dT and random primers. The program conditions used to reverse translate into cDNA were: 25 °C for 5 minutes, 60 °C for 60 minutes, and 85 °C for 5 minutes.

3.2.3 Plasmid construction

Synthesized cDNA isolated from the siliques of *Arabidopsis thaliana* Columbia-0 was used to clone SuSy2 and SuSy3 coding sequences, while SuSy5 and SuSy6 were cloned from cDNA

synthesized from stem tissue using primers listed in Table 2.1. All DNA sequences were cloned into pDONR/Zeo vectors and sub-cloned into pH7YWG2 vectors containing YFP at the C-terminus. The 35S promoter of pH7YWG2 vectors was replaced by the respective *SuSy* native promoters, which contained approximately 2000 base pairs of the upstream region from the translational start codon that were amplified from *Arabidopsis* genomic DNA. If the region between the start codon of *SuSy* to the stop codon of the adjacent upstream gene was less than 2000 base pairs, the entire region was cloned. Restriction enzyme sites were added to the promoter fragments for sub-cloning (the full details are listed in Table 3.1). All the constructs (*SuSy2*$_{pro}$*::SuSy2::YFP*, *SuSy3*$_{pro}$*::SuSy3::YFP*, *SuSy5*$_{pro}$*::SuSy5::YFP* and *SuSy6*$_{pro}$*::SuSy6::YFP*) were transformed independently into WT plants using *Agrobacterium tumefaciens* (strain GV3101). Positive transformants were selected by positive growth on half-strength MS medium supplemented with 20 mg/L hygromycin.

Table 3.1 Primers used for amplification of SuSy promoter fragments

Gene	Promoter size	Restriction sites added	Orientation	Primer sequences (5′ to 3′)
SuSy1	2090 bp	*Cla*I	Forward	TCTATCGATAAGTCAAGGTTAATC
		*Avr*II (*Xmaj*I)	Reverse	GCGCCT AGGTGATCCAAAAAAGA
SuSy2	600 bp	*Pme*I (*Mss*I)	Forward	CTCGTTTAAACCGACTAAAGAATTCTG
		*Spe*I	Reverse	CGCACTAGTGATTTTTTCTCAGAGG
SuSy3	1394 bp	*Pme*I	Forward	CTCGTTTAAACCCGGATTGCCTCTATA
		*Spe*I	Reverse	GCGACTAGTGAATATTCAGATGATCA
SuSy4	1960 bp	*Cla*I	Forward	GTGATCGATTTCTTCAACAAAGCCCTTCA
		*Avr*II (*Xmaj*I)	Reverse	CCTAGGTTCAAACACAATCACAAAGC
SuSy5	1731 bp	*Sac*I	Forward	CTAGAGCTCAATGCTCATTGCTCG
		*Spe*I	Reverse	GCGACTAGTTGTGTTATGTACCTTG
SuSy6	686 bp	*Pme*I	Forward	CTCGTTTAAACACACAACAACGAAAGAG
		*Spe*I	Reverse	CGCACTAGTAGAAACAACTGAAGATTC

3.2.4 Microscopy

Both live-cell imaging and immunohistochemistry analyses were performed on a Leica DMI 6000 B inverted microscope fitted with a Perkin Elmer Ultraview VoX Spinning Disk scan head with excitation/emission wavelengths of 514 nm/540 nm for visualization of all SuSy-YFP, and 488 nm/525 nm for detection of Alexa 488. Images were captured on a Hamamatsu 9100-02 CCD camera using Volocity 6.3 software (Improvision), and processed using Image J software (National Institutes of Health; http://rsb.info.nih.gov/ij/). The plasma membrane was labelled with a 10 μM FM^{TM} 4-64 dye (Invitrogen) for 1 minute and then imaged directly, while the sieve plates were labelled using 0.01% aniline blue for 10 minutes in the dark and then rinsed and mounted in water

prior to imaging (Thompson and Wolniak, 2008). FM4-64 was subsequently detected using the 561 nm laser lines and the 595 nm emission filters, and aniline blue was excited by a 405 nm laser and observed with the 540 nm detection filters.

3.2.5 Tissue collection and preparation

For visualizing thin cross-sections of stems and petioles, inflorescence stems from 5-week-old *Arabidopsis* plants (approximately 3 cm from the base of a stem) and rosette leaves (both smaller sink leaves and larger source leaves) were hand-sectioned using a double-sided razor blade. In addition, a sliding benchtop microtome (American optical, Model #860) was employed to cut 60-100 μm-thick longitudinal sections of petioles and siliques containing vascular bundles. *Arabidopsis* seedlings were grown on half-strength MS medium for 7 days in the condition described previously, and entire seedlings were mounted in water prior to imaging. To obtain a thin cross section of *Arabidopsis* seed, the whole silique was sectioned using a double-sided razor blade. Seeds of different stages were peeled using a needle, and were mounted in water under a coverslip. The intact embryo was separated from the seed coat by gently pressing the coverslip. The embryo was rinsed thoroughly in water prior to imaging. Plasmolysis was performed by incubating intact embryos in 0.8 M mannitol for 10 minutes prior to imaging.

3.2.6 Western blotting

Approximately 200 mg *Arabidopsis* stems and rosette leaves were ground in liquid nitrogen and used for protein extraction following a previously described procedure (Wang et al., 2006). Briefly, samples were extracted with 1 mL 10% trichloroacetic acid in acetone, mixed well, and centrifuged

at 13,000 rpm for 3 minutes at 4 °C. The supernatant was removed and 1 mL of 80% methanol containing 0.1 M ammonium acetate was added. Samples were subsequently centrifuged at 13,000 rpm for 3 minutes at 4 °C and the supernatant discarded. Residual acetone was removed after air drying at room temperature for at least 10 minutes. 1.2 mL of 1:1 phenol (pH 8.0, Sigma)/SDS buffer (30% sucrose, 2% SDS, 0.1 M Tris, pH 8, 5% 2-mercaptoethanol) was subsequently added to the tubes and incubated for 5 minutes. After centrifuging for 3 minutes at 13,000 rpm, the upper phase of phenol was transferred to a new tube and mixed with 1 mL methanol containing 0.1 M ammonium acetate. Samples were stored at -20 °C overnight and protein was collected by centrifugation for 5 minutes at 13,000 rpm. Pellets were subsequently washed with 100% methanol and then with 80% acetone, followed by centrifugation as above. Finally, the protein was air-dried and suspended in SDS sample buffer (1% SDS in 0.1× phosphate buffer saline). Proteins were quantified using DC™ Protein Assay (Bio-Rad) and diluted in SDS loading buffer. 15 µg denatured protein was loaded onto an 8% SDS polyacrylamide gel (PAGE) using Mini Protean® Tetra Cell system (Bio-Rad) and separated using 110 volts for 120 minutes. Proteins were subsequently transferred to a nitrocellulose membrane using a Mini Protean® 3 Cell (Bio-Rad) at 20 V overnight.

After two, 5-minute washes in TBS plus Tween-20 (TTBS; 20 mM Tris, pH 7.6, 138 mM NaCl with 0.01% Tween-20), the membrane was transferred to a blocking solution containing 5% (w/v) nonfat dry milk (NFDM) in TTBS for one hour. The membrane was rinsed three times for 5 minutes with TTBS, and subsequently incubated with an anti-SuSy immune serum raised against soybean root nodule SuSy (Zhang et al., 1999; Fedosejevs et al., 2014). The primary antibody was

suspended in TTBS solution containing 1% (w/v) NFDM at a 1:5000 dilution and incubated at room temperature for 1 hour. After washing for four times for 5 minutes in TTBS, the membrane was incubated in a 1:20,000 dilution of Trial Superclonal™ secondary antibody (Goat anti-Rabbit IgG, Thermo Fisher) conjugated with enhanced chemiluminescent (ECL) horseradish peroxidase (HRP) for 1 hour. Finally, after four washes for 5 minutes with TTBS, the signal was developed on CL-Xposure™ film (Thermo Fisher), with a SuperSignal West Pico Chemiluminescent Substrate kit (Thermo Fisher) following the manufacturer's instructions.

3.2.7 Immunohistochemistry

Arabidopsis inflorescence stem and petiole sections were cut and immediately immersed in a formaldehyde fixative (pH 7.0, 50 mM PIPES, 4% formaldehyde) for 2 hours. Samples were subsequently washed twice for 15 minutes with 50 mM PIPES buffer and dehydrated in a graded ethanol series. Tissues were infiltrated in LR white resin (London Resin Company, Berkshire, UK) and sectioned with a Leica Ultracut UCT Ultramicrotome (Leica Microsystems GMbH, Wetzlar, Germany). To survey the morphology of each sample, thick sections (300 nm) were stained with 1% toluidine blue in 1% sodium borate and viewed under a Leica DMR microscope equipped with a QICAM digital camera (QIMAGING). For immunofluorescent labelling, new sections were cut and mounted on poly-L-lysine-coated slides (Electron Microscopy Science), and subsequently blocked with 5% NFDM in Tris-buffered saline containing 20 mM Tris, 500 mM NaCl and 0.2% Tween-20 (TBST) for 30 minutes. After a brief spray with TBST, sections were incubated with an anti-soybean SuSy primary antibody as described above at a 1:20 dilution for 1 hour at room temperature. Sections were rinsed twice for 10 minutes with TBST and incubated in a 1:200

dilution of secondary anti-rabbit Alexa 488 antibody (Molecular Probes, Eugene, OR, USA) at room temperature for 1 hour. Finally, after rinsing twice for 10 minutes with TBST, sections were mounted in 70% glycerol and viewed under a Perkin Elmer spinning-disk confocal microscope. A concurrent negative control was performed at 1:20 dilution using pre-immune rabbit serum.

3.3 Results

3.3.1 Spatiotemporal localization of SuSy2, SuSy3, SuSy5, and SuSy6

In order to examine the possibility that any one of the other four SuSy isoforms may be localized to the xylem and enable the production of UDP-glucose directly from sucrose to facilitate cellulose biosynthesis, C-terminal YFP fusion constructs of *SuSy2*, *SuSy3*, *SuSy5* and *SuSy6* were generated (*SuSy2*$_{pro}$*::SuSy2::YFP*, *SuSy3*$_{pro}$*::SuSy3::YFP*, *SuSy5*$_{pro}$*::SuSy5::YFP*, *SuSy6*$_{pro}$*::SuSy6::YFP*) and independently transformed into WT *Arabidopsis*, grown, and subsequently analyzed by confocal microscopy. Live-cell imaging of seedling root tissues showed that SuSy3, SuSy5, and SuSy6 were exclusively in the phloem (Figure 3.1 and Figure 3.2), while SuSy2 was absent or undetectable (Figure 3.2). Similarly, cross sections from both the base and the top of the stem clearly showed a phloem-specific localization of SuSy5 and SuSy6 (Figure 3.3). Furthermore, the same distribution of SuSy5 and SuSy6 was found in leaf petioles and silique walls (Figure 3.4 and Figure 3.5). In contrast, neither SuSy2 nor SuSy3 was detectable in the vascular bundles of the stems (Figure 3.6), leaf petioles and silique walls (data not shown), but abundant in the developing seeds (Figure 3.7, Figure 3.8 and Figure 3.9). Only SuSy3 was highly expressed in the guard cells of leaf stomata, and the signals were confined to the cytoplasm (Figure 3.10). These observations suggest that SuSy protein is not present in the xylem of *Arabidopsis* plants.

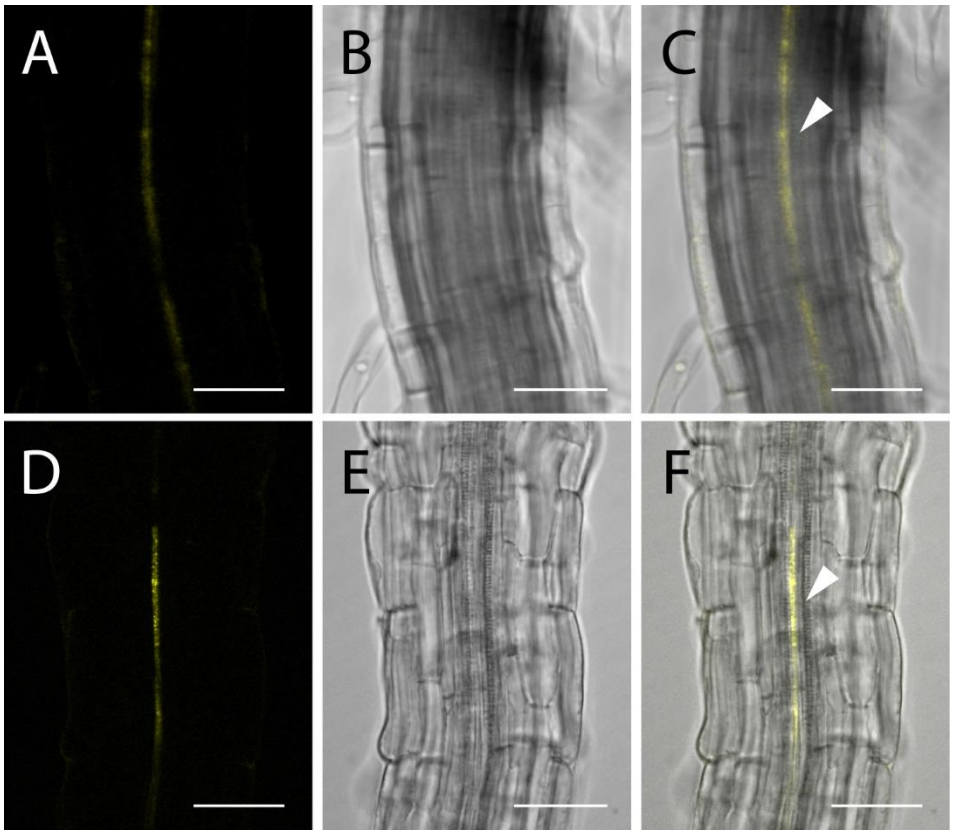

Figure 3.1 Localization of AtSuSy5-YFP and AtSuSy6-YFP in 7-day-old *Arabidopsis* seedling roots. YFP signals of SuSy5 (A-C) and SuSy6 (D-F) were detected in phloem and arrowheads indicate protoxylem. (A, D) YFP fluorescence panels, (B, E) bright field images, and (C, F) merged images of YFP fluorescence and bright field images. Bars=50 µm.

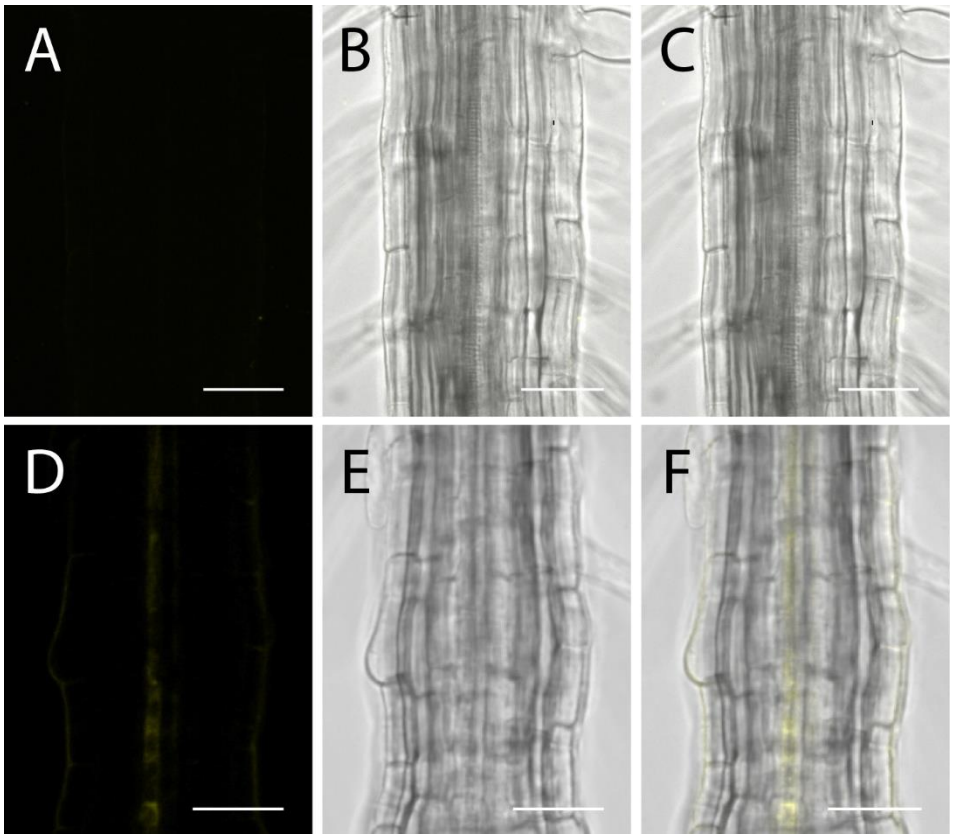

Figure 3.2 Localization of AtSuSy2-YFP and AtSuSy3-YFP in 7-day-old *Arabidopsis* seedling roots. YFP signal of SuSy2 (A-C) was not detected in roots and SuSy3 (D-F) was confined to the phloem of roots. (A, D) YFP fluorescence panels, (B, E) bright field images, and (C, F) merged images of YFP fluorescence and bright field images. Bars=50 µm.

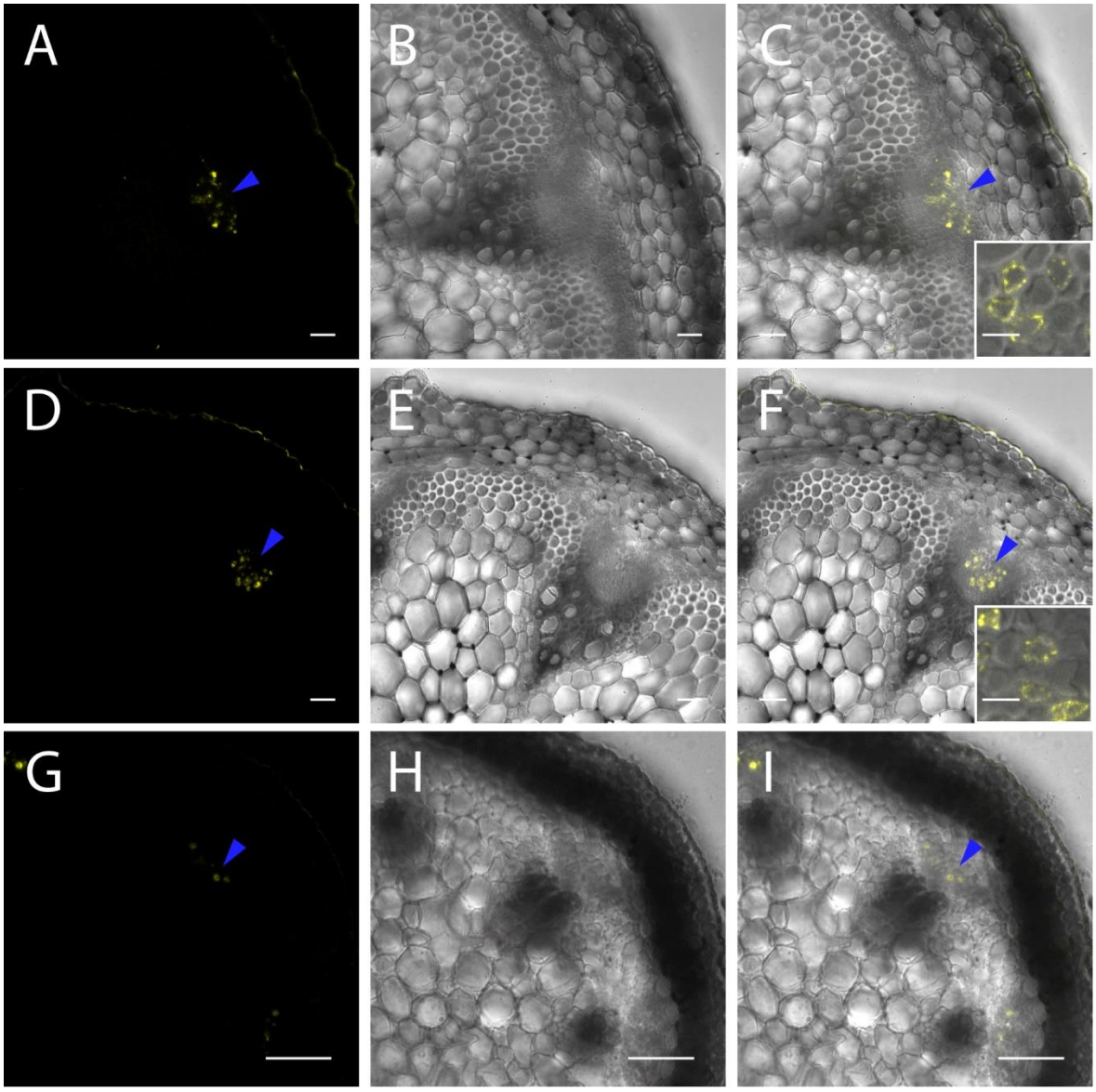

Figure 3.3 AtSuSy5-YFP and AtSuSy6-YFP were localized to the phloem of *Arabidopsis* stem cross sections. Sections were cut 1 cm from the base of the stem of 6-week-old *Arabidopsis* plants, SuSy5 (A-C) and SuSy6 (D-F) were specifically localized to the phloem (arrowheads). Insert images are phloem cells shown in higher magnification and scale bars represent 5 µm. (G-I) Sections of the primary stem showing the localization of SuSy6 in the phloem (arrowheads). (A, D, G) YFP fluorescence panels, (B, E, H) bright field images, and (C, F, I) merged images of YFP fluorescence and bright field images. Bars=50 µm.

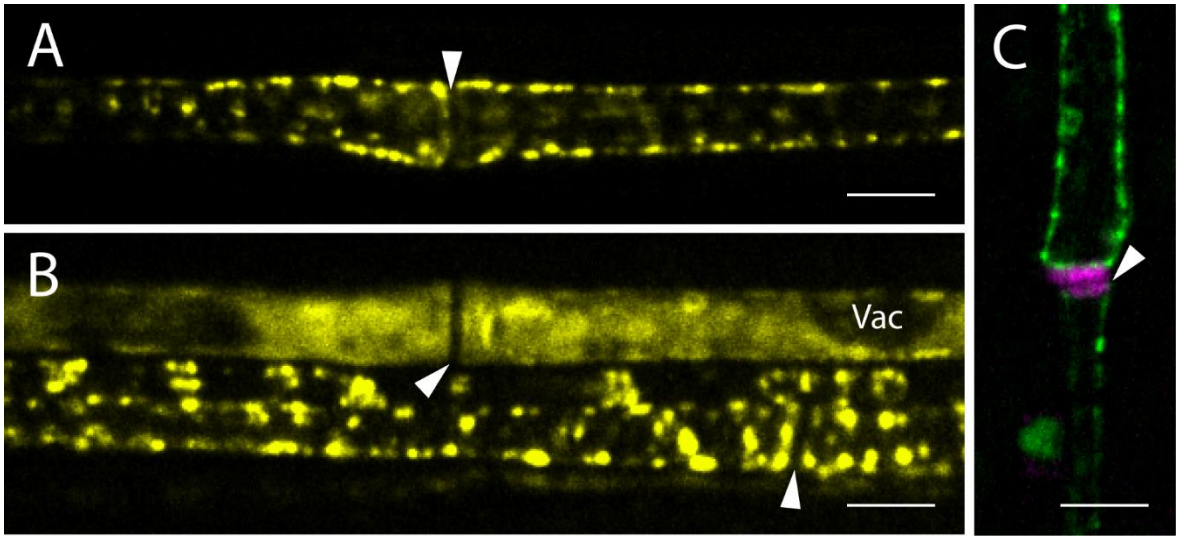

Figure 3.4 AtSuSy5-YFP and AtSuSy6-YFP were confined to the sieve elements of *Arabidopsis* petioles. Longitudinal sections of leaf petioles showing AtSuSy5 in mature sieve elements (A) and immature sieve elements (B) containing vacuoles (Vac). AtSuSy6 was localized to mature sieve elements (C), where magenta signal indicates the sieve plates (arrowheads) stained with aniline blue. Bars=5 µm.

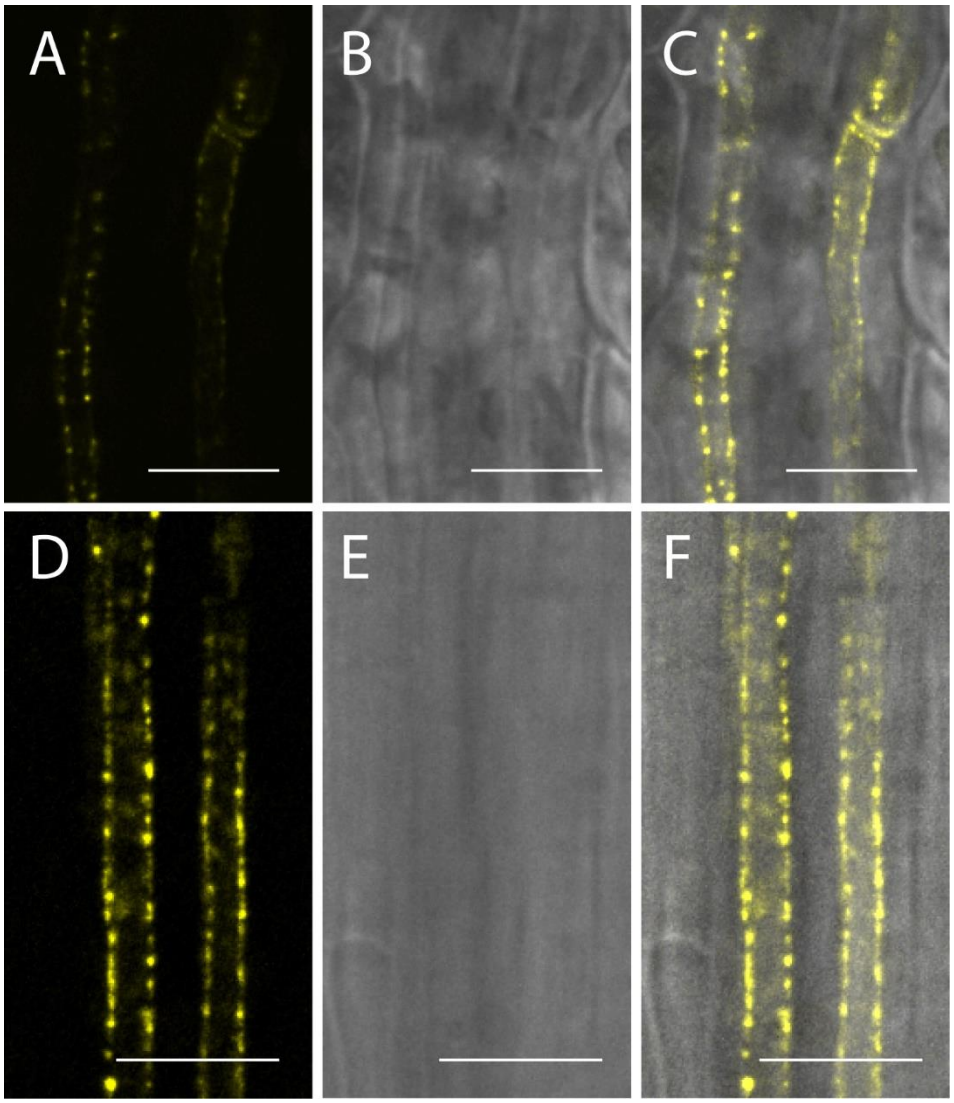

Figure 3.5 AtSuSy5-YFP and AtSuSy6-YFP were found in the sieve elements of *Arabidopsis* silique. Longitudinal sections of silique walls showing YFP signals of SuSy5 (A-C) and SuSy6 (D-F) in phloem sieve elements. (A, D) YFP fluorescence panels, (B, E) bright field images, and (C, F) merged images of YFP fluorescence and bright field images. Bars=10 µm.

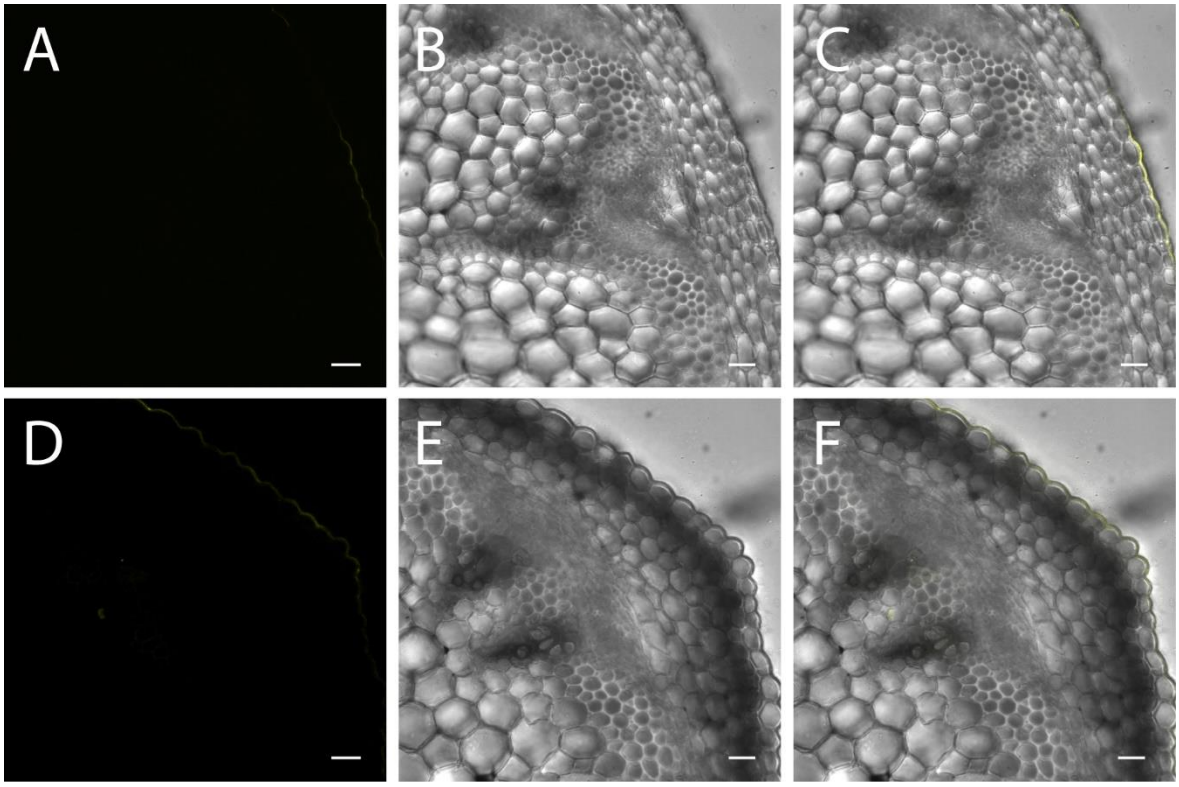

Figure 3.6 No YFP signal for SuSy2 and SuSy3 was apparent in the vascular bundles of *Arabidopsis* inflorescence stems. Images showing lack of AtSuSy2 (A-C) and AtSuSy3 (D-F) fluorescence in the cross-sections of 6-week-old inflorescence stem. (A, D) YFP fluorescence panels, (B, E) bright field images, and (C, F) merged images of YFP fluorescence and bright field images. Bars=50 µm.

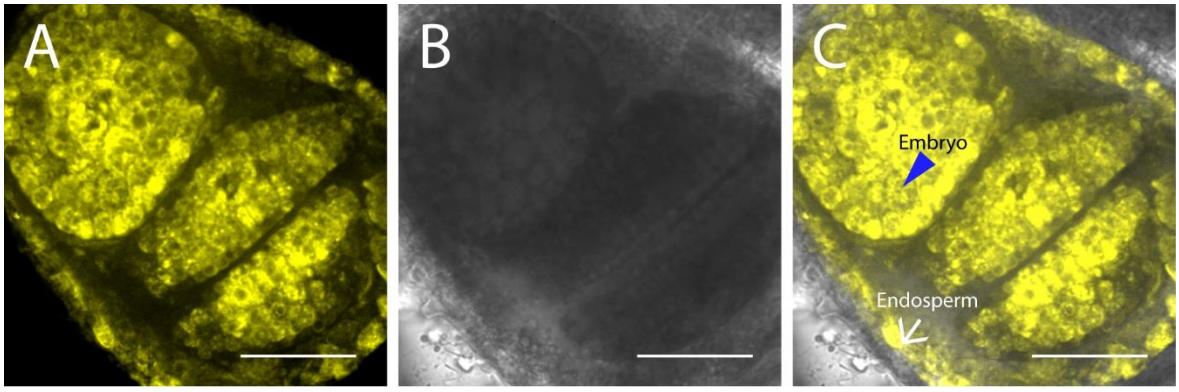

Figure 3.7 AtSuSy2-YFP was apparent in the seeds of transgenic *Arabidopsis* plants. Cross sections of seed at 13 DPA showing SuSy2 in the embryo (arrowheads) and endosperm (arrows). (A) YFP fluorescence panels, (B) bright field images, and (C) merged images of YFP fluorescence and bright field images. Bars=50 µm.

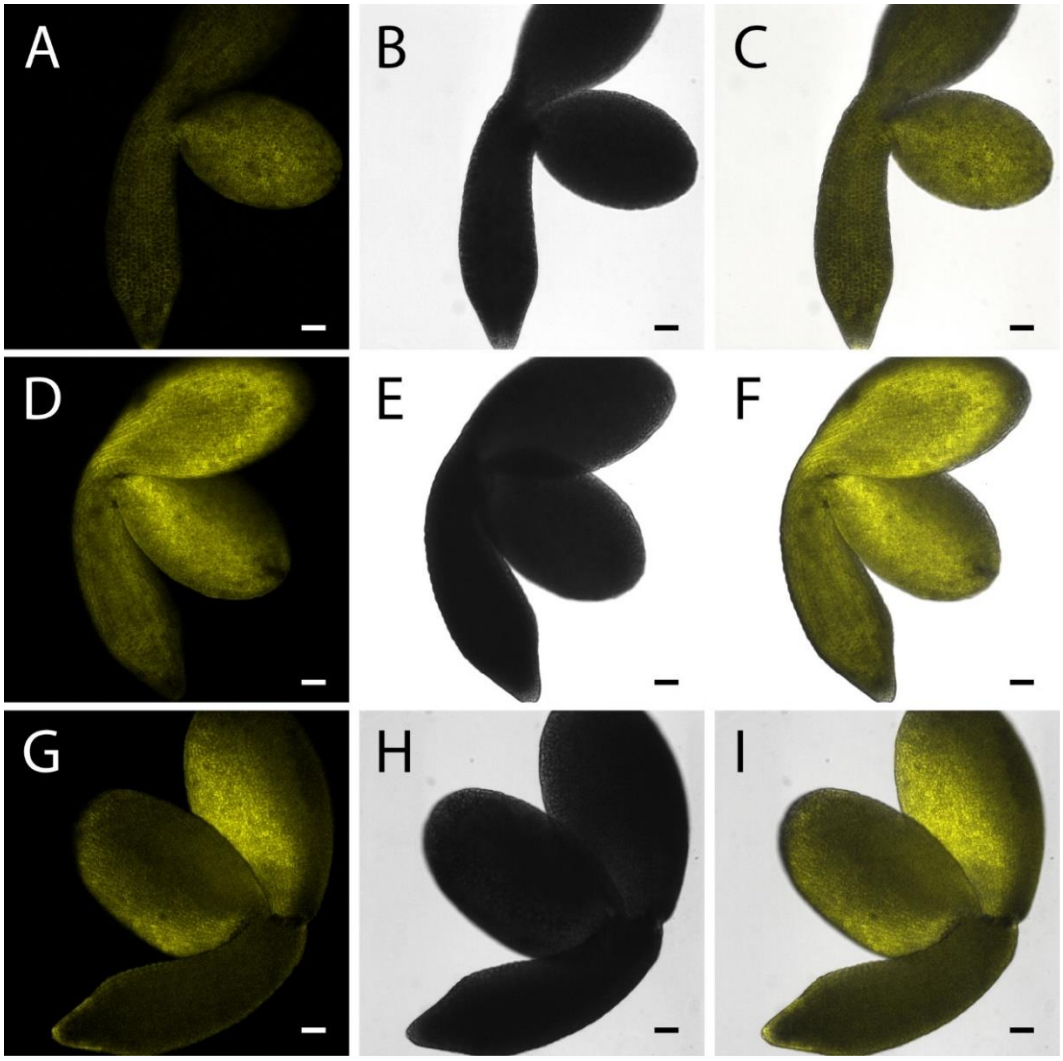

Figure 3.8 AtSuSy2-YFP was clearly observed in the developing embryo of *Arabidopsis* from 10 DPA to 17 DPA. (A, D, G) YFP fluorescence panels, (B, E, H) bright field images, and (C, F, I) merged images of YFP fluorescence and bright field images. Bars=50 µm.

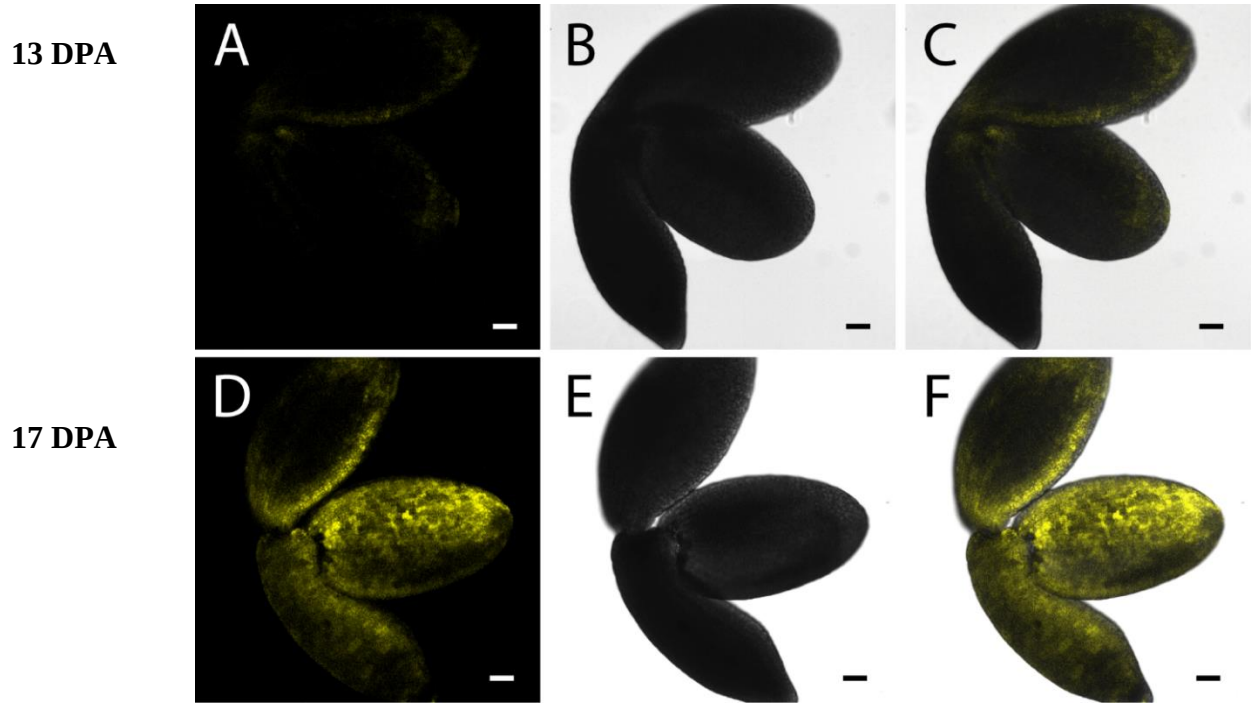

Figure 3.9 AtSuSy3-YFP was apparent in the developing embryo of *Arabidopsis* at 13 DPA and 17 DPA. (A, D) YFP fluorescence panels, (B, E) bright field images, and (C, F) merged images of YFP fluorescence and bright field images. Bars=50 µm.

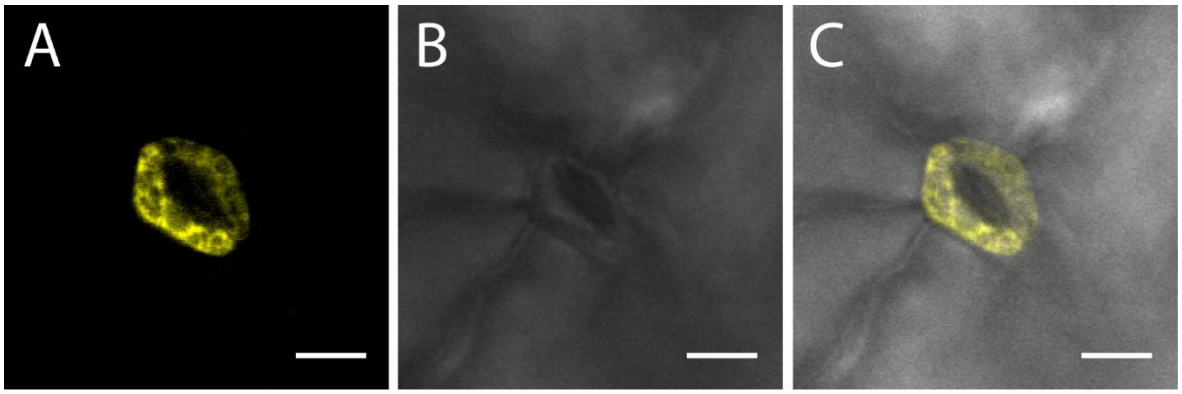

Figure 3.10 AtSuSy3-YFP was present in the guard cells of *Arabidopsis* leaf stomata. Images showing SuSy3 in the cytoplasm of guard cells. (A) YFP fluorescence panels, (B) bright field images, and (C) merged images of YFP fluorescence and bright field images. Bars=10 µm.

3.3.2 SuSy5 and SuSy6 are restricted to sieve elements.

Again, longitudinal sections of leaf petioles were examined to determine the sub-cellular localization of SuSy5 and SuSy6. Consistent with Barratt et al. (2009), SuSy5 and SuSy6 were only apparent in the sieve elements, including both immature sieve elements containing vacuoles and mature elements that are fully functional (Figure 3.4). These observations were further confirmed by aniline blue staining of sieve plates (Figure 3.4 C). Interestingly, in the mature sieve elements, YFP fusions appeared to be parietally positioned and largely accumulate as puncta, and were distributed along the entire sieve element (Figure 3.4 A and C). In addition, SuSy5-YFP and SuSy6-YFP fusions were immobile, as shown by time-lapse video (Movie S2). In contrast, fluorescence occurred uniformly in the cytoplasm when the sieve element was immature (Figure 3.4 B). Employing the styryl dye FM4-64, which specifically labels the plasma membrane (Bolte et al., 2004), the precise localization of SuSy5 and SuSy6 was determined. SuSy5 and SuSy6 were restricted to the inner side of the plasma membrane, indicating a cytoplasmic localization of these two proteins (Figure 3.11). This observation was most evident at the sieve plates, where the plasmodesmata were also stained by FM4-64 (Figure 3.11 C and F).

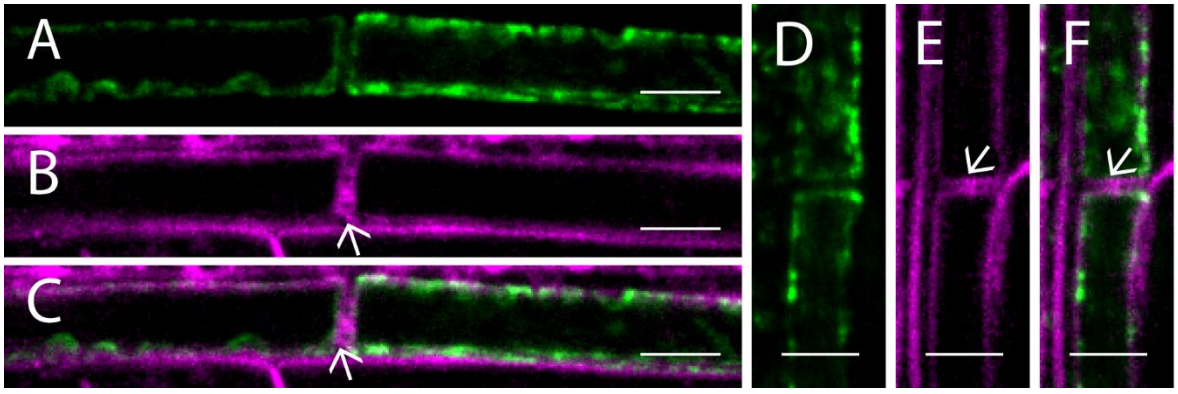

Figure 3.11 Cytoplasmic localization of AtSuSy5-YFP and AtSuSy6-YFP in sieve elements. Longitudinal sections of *Arabidopsis* leaf petioles showing the subcellular localization of SuSy5 (A-C) and SuSy6 (D-F) in the sieve elements stained with FM4-64. YFP signal of AtSuSy5 and AtSuSy6 are shown in panels A and D while plasma membrane stained with FM4-64 shown in B and E. Merged images of SuSy-YFP and plasma membrane stained with FM4-64 are shown in C and F. Plasmodesmata are indicated by arrows. Bars=5 µm.

3.3.3 SuSy2 and SuSy3 are highly expressed in developing seeds

To investigate the specific localization of SuSy2 in seeds, live-cell imaging was performed on the cross sections of seed at 13 days post anthesis (DPA). Consistent with previous studies (Nunez et al., 2008), SuSy2 was apparent in the embryo and endosperm (Figure 3.7). Surprisingly, no signal was detected in the outer integuments of seed coat from 7 DPA to 13 DPA, when the mucilage was secreted and secondary cell wall was deposited (Figure 3.12). In contrast, SuSy3 activity was found in the embryo (Figure 3.9), but not in the endosperm and seed coat. To further study the expression patterns of SuSy2 and SuSy3 in embryos during seed development, intact embryos from 7, 10, 13 and 17 DPA were obtained and employed for live-cell imaging. SuSy2 activity was not detectable at 7 DPA, but was abundant throughout the embryo from 10-17 DPA (Figure 3.8). The signal faded quickly after 17 DPA. In contrast, SuSy3 activity was not detectable at 7 and 10

DPA, while only a weak signal was observed at 13 DPA and the protein was present in abundance throughout the embryo at 17 DPA (Figure 3.9). SuSy2 seemed to be largely localized to the inner face of plasma membrane at 10 DPA, as shown by the colocalization of YFP signals with the plasma membrane labelled by FM4-64 (Figure 3.13 C-E). Only a small amount of YFP signal was detected in the cytoplasm, which was probably due to the formation of a large vacuole in embryo cells during cell expansion (Figure 3.13 E). In addition, SuSy2 activity was not found at the cell wall after plasmolysis (Figure 3.13 F). At 13 DPA when *Arabidopsis* seeds are fully mature, SuSy2 was largely present in the cytoplasm of embryo cells (Figure 3.14 A and B). Similarly, at 17 DPA, SuSy3 activity was detected only in the cytoplasm (Figure 3.14 C and D).

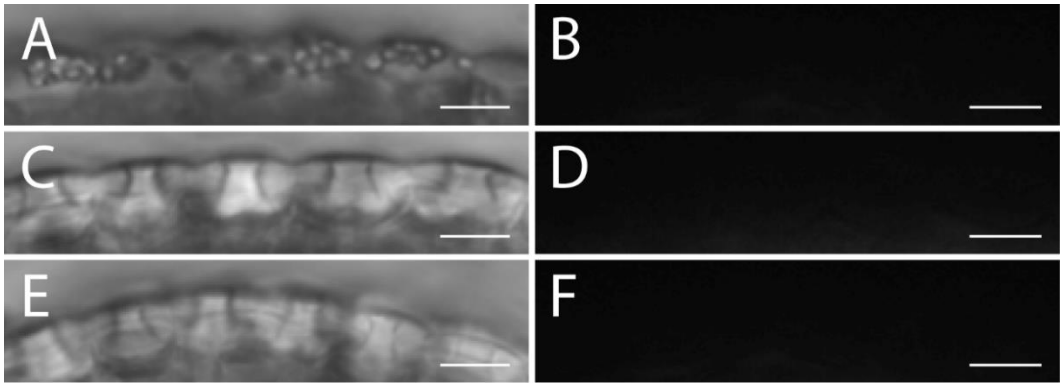

Figure 3.12 AtSuSy2-YFP was not apparent in the epidermis of *Arabidopsis* seed coat from 7 DPA to 13 DPA. (A) Starch-containing amyloplasts accumulated in the cells of outer integuments at 7 DPA. (C) Epidermal cells synthesized and secreted a large quantity of mucilage, and secondary cell wall was subsequently deposited at 10 DPA. (E) At the end of seed maturation, the structure of epidermal cell was preserved by the mucilage and columella. (A, C, E) bright field images, and (B, D, F) YFP fluorescence panels. Scale bars=10 µm.

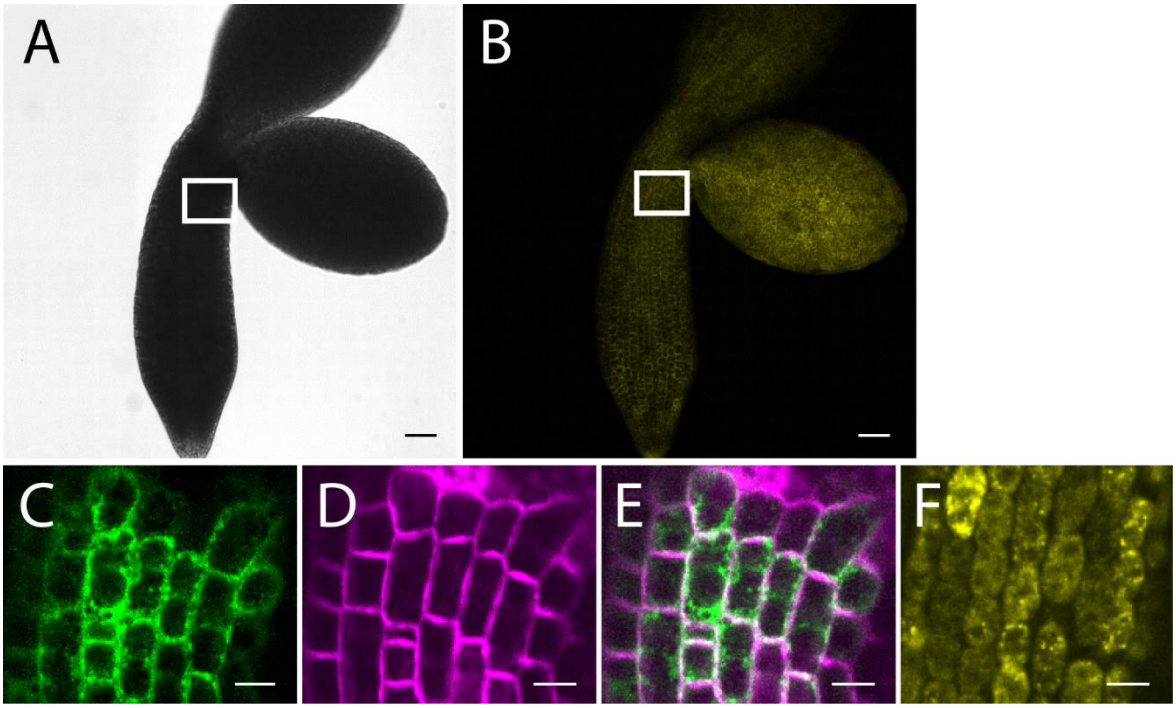

Figure 3.13 AtSuSy2-YFP was largely localized to the inner face of plasma membrane in embryo cells at 10 DPA. The area indicated by the corresponding white box is represented in panels C-F. YFP signal of AtSuSy2 is shown in panels B and C, while plasma membrane stained with FM4-64 (Magenta) is shown in D. Merged images of SuSy2-YFP and plasma membrane stained with FM4-64 are shown in (E) while YFP signal of SuSy2 was apparent in the cytoplasm after plasmolysis (F). Bars= 50 µm in A and B, 10 µm in C-F.

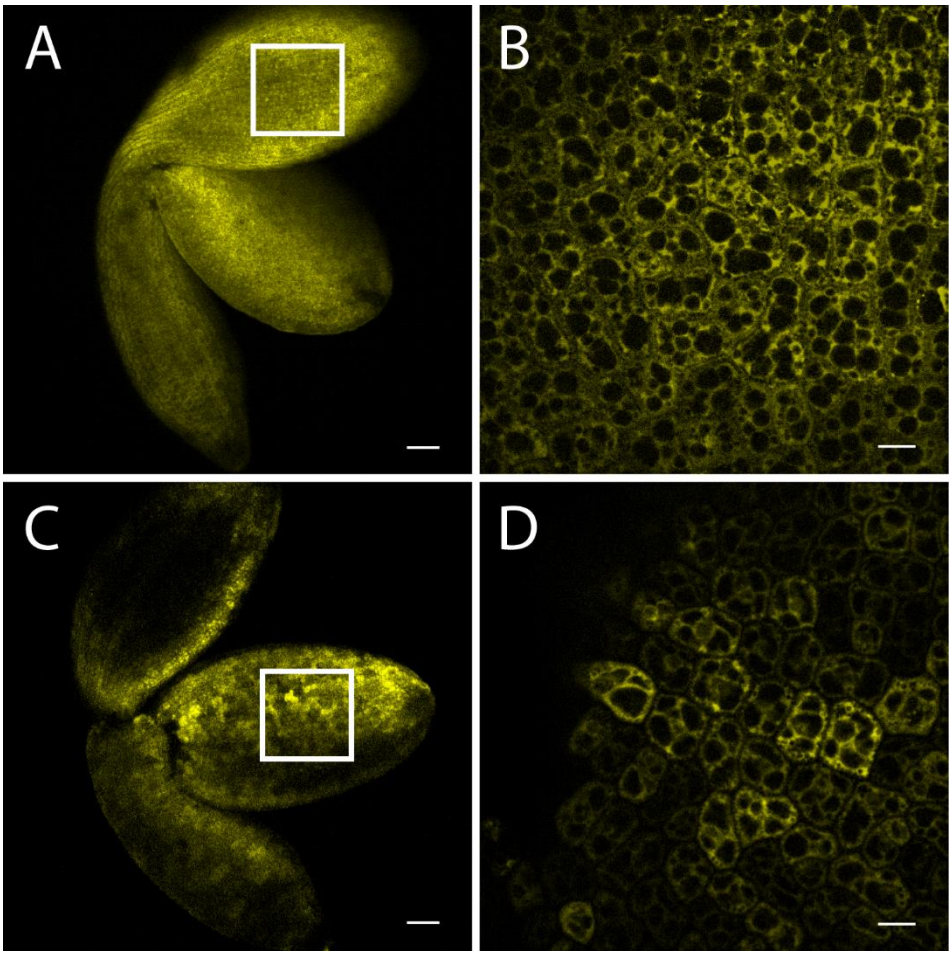

Figure 3.14 AtSuSy2-YFP and AtSuSy3-YFP were present in the cytoplasm of *Arabidopsis* embryo cells. The areas indicated by the corresponding white boxes in panel A and C are represented separately in panels B and D. Images show that at 13 DPA and 17 DPA, SuSy2 (B) and SuSy3 (D) were confined to the cytoplasm of embryo cells. Bars= 50 µm in A and C, 10 µm in B and D.

3.3.4 Immunolabelling supports SuSy localization to the phloem.

To confirm the results of live-cell imaging, immunofluorescent labelling was performed on cross sections of *Arabidopsis* stems and petioles with an anti-soybean SuSy immune serum. Using Western blotting, we first tested the cross-reactivity of the SuSy serum against total proteins

extracted from *Arabidopsis* stems and leaves. A single dominant band at ~90 kDa was apparent (Figure 3.15 G), which is consistent with the predicted size of the six *Arabidopsis* SuSy genes which encode polypeptides of 92-106 kDa (all sharing high amino acid identity). Subsequent immunolocalization was carried out, and SuSy was only observed in the phloem (Figure 3.15 C and F). In contrast, no signal was detected at the same spot using the pre-immune serum (Figure 3.15 B and E). Fluorescence in xylem was likely due to non-specific binding, since a similar signal intensity was observed in the pre-immune negative control.

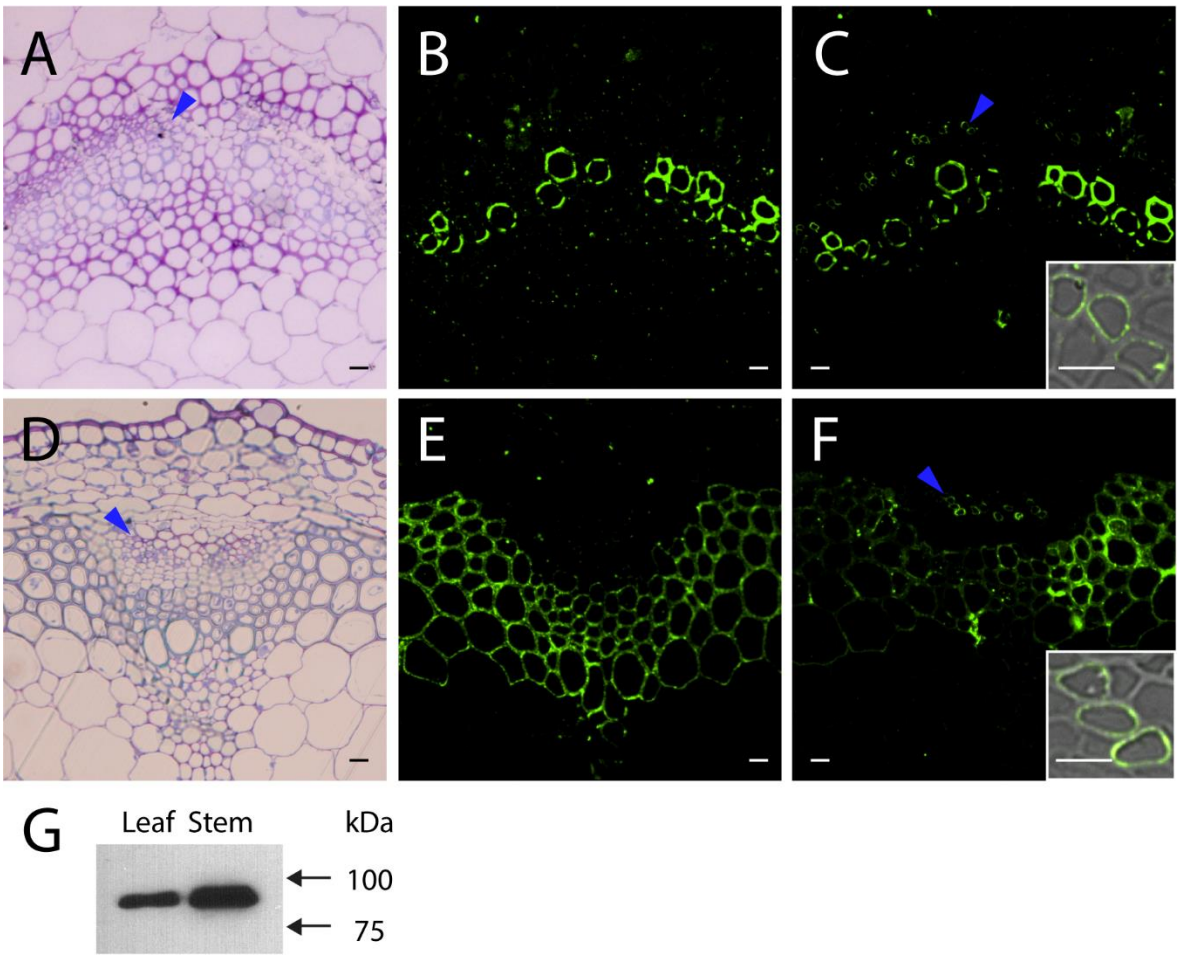

Figure 3.15 Immunofluorescent labelling of *Arabidopsis* petioles and stems confirming phloem localization of SuSy. Morphology of the cross-sections of leaf petioles (A) and stems (D) stained with toluidine blue. Sections treated with pre-immune serum (B and E) or anti-soybean SuSy immune serum (C and F) show the localization of SuSy in the phloem. Fluorescence in the xylem of panels B, C, E and F was likely due to non-specific binding. Areas indicated by the arrowheads are represented in insert images, showing the phloem labelling in higher magnification. (G) Western blot showing the cross-reactivity of anti-soybean SuSy immune serum against total protein extracted from *Arabidopsis* stems and leaves. Bars=20 µm in A-F, 5 µm in insert images.

3.4 Discussion

In contrast to the companion cell specificity of SuSy1 and SuSy4, we show that SuSy5 and SuSy6 were confined to phloem sieve elements, consistent with Barratt et al. (2009). However, our high-resolution imaging expands these findings to show that SuSy5 and SuSy6 occurred predominantly as immobile puncta at the margin of sieve tubes, and were not co-localized at the plasma membrane. These unique observations may be explained by the ultrastructure of a sieve element, which has lost its nuclei, ribosome and vacuole during maturation, but still contains smooth endoplasmic reticulum, plastids and P-protein (Knoblauch and van Bel, 1998; Cayla et al., 2015). These organelles are usually embedded in an amorphous ground matrix that attaches to the plasma membrane or P-protein filaments (Froelich et al., 2011). Thus, we propose that SuSy5 and SuSy6 are likely trapped in this parietal protein layer (see lack of movement in Movie S2), and play a specific role in the cellular metabolism of sieve elements. Sieve plates provide connection among adjacent sieve elements, and the callose lining of sieve plate pores is essential for normal phloem transport (Barratt et al., 2011). SuSy5 and SuSy6 are therefore suggested to facilitate callose synthesis, as double mutants displayed defects in callose lining of the sieve plates (Barratt et al., 2009). Our subcellular localization supports these claims. In addition, via immunofluorescence, SuSy has been shown to colocalize with H^+-ATPases in sieve elements of castor bean tumor (Wächter et al., 2003). A sucrose transporter, AtSUC3, has been identified in the phloem sieve elements and proposed to be responsible for the retrieval of sucrose during phloem transport (Meyer et al., 2004). Therefore, we postulate that SuSy5 and SuSy6 may also be involved in providing energy for this sucrose retrieval.

In this study, we provide evidence that SuSy2-YFP and SuSy3-YFP were not present or detectable in the vasculature of inflorescence stems, silique walls, and leaf petioles, but were specifically and strongly expressed in seeds. Previous studies evaluating SuSy transcript abundance and enzyme activity showed that SuSy2 and SuSy3 were specifically induced in defined phases during seed development, but barely detectable in other organs (Bieniawska et al., 2007; Fallahi et al., 2008; Nunez et al., 2008). Our findings are consistent with SuSy2 and SuSy3 having a role in seed development. In addition, the results show that SuSy2 was not detectable in the epidermal cells of seed coat from 7 DPA to 13 DPA, when pectin-enriched mucilage is synthesized and deposited in the apoplast and secondary cell walls are subsequently formed beneath the mucilage. SuSy2 does not seem to be involved in mucilage and cell wall synthesis, which is consistent with previous data in current work (Chapter 2).

Our results show that SuSy2-YFP was specifically found in the embryo and endosperm, and the transcript was highly induced at 10 DPA. After 17 DPA, the relative amount of SuSy2 fusion proteins decreased dramatically. In contrast, SuSy3 was only apparent in the embryo during the late maturation phase of seed development (after 13 DPA), and the signal was not detectable in endosperm or seed coat. These data are consistent with previous studies showing the distinct expression profile of SuSy2 and SuSy3 in developing seeds (Baud et al., 2004; Bieniawska et al., 2007; Angeles-Nunez and Tiessen, 2010). Furthermore, SuSy2 seemed to be restricted to the inner face of plasma membrane of embryo cells at the beginning of expression and then was largely confined to the cytoplasm. SuSy3 was always found in the cytoplasm of embryo cells. It has been reported that single knockouts of SuSy2 and SuSy3 showed decreased starch content and

accumulation of sucrose in the defined phase of seed development, indicating that SuSy2 and SuSy3 are not fully redundant genes (Angeles-Nunez and Tiessen, 2010). In *Arabidopsis*, the endosperm serves as both a mechanical barrier to inhibit embryonic growth and a nutrient source for seed germination and seedling establishment (Yan et al., 2014). At 10-12 DPA, the cellularized endosperm is rapidly consumed by the expanding embryo and starch temporarily accumulates in the embryo (Angeles-Nunez and Tiessen, 2010). Thus, SuSy2 may play a role in starch biosynthesis in embryo cells and facilitate the carbon remobilization from endosperm to embryo. By 13 DPA, cell division declines and the embryo reaches its maximum size, and the endosperm disappears and is replaced by a single cell layer of aleurone. In addition, starch is remobilized to the biosynthesis of lipid and storage protein from 12-18 DPA (Angeles-Nunez and Tiessen, 2010). At this stage, SuSy activity in the embryo may be crucial to generating precursors for lipid and storage protein biosynthesis from sucrose. Therefore, SuSy2 and SuSy3 activity may be important to modulate the sink strength of seeds and thus have a profound effect on embryo development.

In addition, our imaging shows that SuSy3 was identified in the phloem of seedling roots where it may serve a similar role to the other SuSy. SuSy3 was shown to be present in the guard cells of leaf stomata, which is consistent with Bieniawska et al. (2007), where SuSy3 was detected specifically in leaf stomata by GUS histochemical staining. Furthermore, Daloso et al. (2016) have demonstrated that upregulation of AtSuSy3 in tobacco plants led to increased stomatal aperture and conductance, transpiration rate and growth. Therefore, SuSy3 is proposed to manipulate guard cell metabolism. Based on these findings, we suggest that SuSy2 and SuSy3 are not likely to be

associated with cellulose synthesis, but are important to seed development and stomatal metabolism, as has previously been implied.

In contrast to the proposed model of cellulose synthesis, our general results demonstrate that no single fluorescently-tagged *Arabidopsis* SuSy was detectable in the xylem of the organs examined. More importantly, all SuSy proteins other than SuSy2 and SuSy3 were restricted to the phloem of tissues examined. These findings suggest that the bulk of cellulose biosynthesis does not use UDP-glucose channelled directly from particulate SuSy, but instead relies on the free pool of cytoplasmic UDP-glucose. In *Arabidopsis*, free UDP-glucose may be generated partially by the activity of SuSy, but is more likely formed via UDP-glucose pyrophosphorylase converting glucose released by invertases. This hypothesis is supported by the recent study by Anderson et al. (2018), who showed that *Arabidopsis* mutant lacking two cytosolic invertase isoforms exhibited abnormal cellulose biosynthesis and significantly reduced UDP-glucose content. SuSy could still impact cellulose deposition indirectly, by modulating carbon allocation and sink strength. Thus, the current model should be re-considered in *Arabidopsis*, as well as in other species reporting phloem-specificity of SuSy. However, it is still possible that in certain plant species the proposed association between SuSy and cellulose synthase exists in certain cell types, such as cotton fibers and developing poplar xylem, which have extremely high-rates of cellulose synthesis. In these systems, overexpression of SuSy genes has manifested in improved wall biosynthesis, resulting in elevated cellulose production (Coleman et al., 2009; Xu et al., 2012). However, this does not necessarily have to come from a direct interaction between SuSy and the cellulose synthase

complex. Therefore, our results highlight the need to re-examine this model in several species, especially those generating significant quantities of cellulose in a relatively short period of time.

In summary, *Arabidopsis* SuSy is specifically localized to seeds and phloem, not xylem, which questions the current model of cellulose biosynthesis in this species. Furthermore, it would appear that the predominant role of SuSy in *Arabidopsis* is phloem loading and unloading, and SuSy is also implicated in seed development and stomatal metabolism. Our findings suggest that SuSy is likely to play an important role in regulating carbon partitioning and modulating sink strength. They enhance our understanding of the pathway by which carbon, from sucrose, is supplied to cell wall biosynthesis, especially cellulose synthesis in *Arabidopsis* (and potentially other species).

Chapter 4: Characterization of *sus1/sus4/sus5/sus6* quadruple mutant phenotypes

4.1 Introduction

In several plant species, SuSy is generally believed to be the dominant enzyme catalyzing the breakdown of sucrose. Compared to invertase, SuSy is less energy intensive, as only half of the ATP is consumed for the conversion of sucrose to hexose phosphates via the SuSy pathway. In addition, the reaction route of SuSy is reversible and allows for feedback regulation. Several papers have reported that individual isoforms of SuSy are required for normal growth and development in many crop plants including potato tubers (Zrenner et al., 1995), cotton fibers (Ruan et al., 2003), tomato fruit (D'Aoust et al., 1999), maize endosperm (Chourey et al., 1998) and pea embryo (Craig et al., 1999). In contrast, no obvious growth phenotypes were observed in *Arabidopsis* when individual isoforms of SuSy were eliminated (Bieniawska et al., 2007). It has been shown that single knockout mutants of SuSy were not significantly different from WT plants in many aspects including soluble sugar and starch content, cellulose content, seed weight and lipid content (Bieniawska et al., 2007). Only very mild phenotypes were reported in SuSy2 and SuSy3 single mutants. For instance, T-DNA insertion lines of SuSy2 and SuSy3 were not different from WT plants in final seed size and composition, but showed different metabolic profile at specific stages of seed development (Angeles-Nunez and Tiessen, 2010). Double mutants lacking similar isoform pairs (*sus1/sus4, sus2/sus3, sus5/sus6*) also displayed normal growth, starch and cellulose content, seed weight and composition when grown under normal conditions (Bieniawska et al., 2007).

However, under hypoxic conditions, the double knockouts of SuSy1 and SuSy4 displayed growth retardation and soluble sugar accumulation (Bieniawska et al., 2007). Additionally, mutants lacking both SuSy5 and SuSy6 showed sieve plates deficient in a callose lining (Barratt et al., 2009).

Previous studies failed to find a phenotype for *sus1/sus2/sus3/sus4* quadruple mutants which are deficient in SuSy activity in all cell types except phloem (Barratt et al., 2009). These plants lacking four of six isoforms of SuSy were morphologically and chemically indistinguishable from WT plants (Barratt et al., 2009). In marked contrast, mutant plants missing two closely related isoforms of neutral and alkaline invertase displayed severe growth phenotypes including reduced growth rate, shorter roots, and a dwarf phenotype (Barratt et al., 2009). In addition, root cells of *cinv1/cinv2* mutants showed abnormal cell division and the tendency to collapse (Barratt et al., 2009). Therefore, the functional role of SuSy has been questioned, and INV was highlighted to be the primary enzyme in *Arabidopsis* (Barratt et al., 2009). However, Baroja-Fernández et al. (2012) demonstrated that the residual SuSy activity in the *sus1/sus2/sus3/sus4* quadruple mutants was sufficient to support normal growth and development of *Arabidopsis* when SuSy activity was measured under optimal conditions by kinetic assay. Therefore, it has been proposed that either redundancy exists within the *Arabidopsis* SuSy family or INV compensates for the missing SuSy activity.

In Chapter 2, I have shown that AtSuSy1 and AtSuSy4 were exclusively expressed in the companion cells of phloem tissue in various plant organs. They were therefore proposed to

facilitate phloem loading and sugar retrieval during long-distance transport. Similarly, AtSuSy5 and AtSuSy6 were shown to be confined to phloem sieve elements and may be involved in the uptake of solutes along the pathway. In addition, I demonstrated that these two isoforms were actually localized to the cytoplasm, but present as immobile puncta. In contrast, SuSy2 and SuSy3 were not detectable in the vasculature of many tissues, but were specifically induced in the developing seeds. Based on these observations, I postulate that the functional roles of SuSy1, SuSy4, SuSy5 and SuSy6 may be largely redundant in *Arabidopsis*, and mutants lacking these four specific isoforms may exhibit an obvious phenotype.

In this chapter, I generated the *sus1/sus4/sus5/sus6* quadruple mutant by crossing homozygous plants of *sus1/sus4* with *sus5/sus6*. Comprehensive phenotypic characterization was subsequently conducted on the *sus1/sus4/sus5/sus6* quadruple mutant compared to WT, *sus1/sus4*, and *sus5/sus6* plants. The evaluation included rosette leaf size, inflorescence stem height, cell wall morphology and thickness, dry seed weight, leaf soluble sugar content with and without flooding. In brief, the results showed that *sus1/sus4/sus5/sus6* quadruple mutant was not significantly different from WT plants in all aspects examined. However, when grown in half-strength MS media supplemented with high concentration of sucrose, *sus1/sus4/sus5/sus6* exhibited most obvious inhibition of seedling growth.

4.2 Methodologies

4.2.1 Genomic DNA extraction

To screen *sus1/sus4/sus5/sus6* homozygous mutants, a rapid genomic DNA extraction protocol was employed (Edwards et al., 1991). Approximately 20 mg fresh leaf tissue was ground with an epitube pestle and extracted with 400 μL extraction buffer (0.2 M Tris-HCl, 25 mM EDTA, 0.25 M NaCl, 0.5% SDS, PH=7.5). After 3 minutes of centrifugation (13,000 rpm), the supernatant was transferred to a new epitube and mixed with 350 μL isopropanol. Samples were incubated at -20 °C for at least 10 minutes, and subsequently centrifuged for 5 minutes at 13,000 rpm. The supernatant was discarded and the pellet was washed with 500 μL 70% ethanol, followed by centrifugation for 2 minutes. Finally, the pellet was air dried for 10 to 20 minutes and resuspended in 15 μL distilled water. DNA concentration was measured with a NanoDrop^{TM} Lite spectrophotometer (Thermo Fisher), and the DNA was stored at -20 °C until use.

4.2.2 Plant materials

sus5/sus6 and *sus1/sus4* double mutants were originally described in Bieniawska et al. (2007). *sus5/sus6* homozygous lines were confirmed by PCR using respective left T-DNA border primer (*sus5 and sus6*: 5′ ATTTTGCCGATTTCGGAAC 3′) and respective flanking primers (*sus5*: LP 5′ GGAGATTCACCAAGTTCTACAC 3′, RP 5′ GGATATATCTTTGTTTGGCCAG 3′; *sus6*: LP 5′ TGACACGGTTAATACCGGAAG 3′, RP 5′ ATCCATCTGAATTTCCCCTTG 3′). PCR conditions were as follows: 5 minutes at 95 °C; 35 cycles of 30 seconds at 95 °C, 30 seconds at 57 °C, 90 seconds at 72 °C, followed by 10 minutes at 72 °C. The *Arabidopsis* homozygous *sus5/sus6* T-DNA line was crossed with the *sus1/sus4* homozygous mutant. After two generations of back-

crossing, homozygous plants of *sus1/sus4/sus5/sus6* quadruple mutant were identified and confirmed by PCR genotyping.

4.2.3 Plant growth conditions, rosette leaf size measurement and flooding treatment

All plants were grown in a growth chamber maintained at 21 °C, 16-h light, 8-h dark, 50% humidity, and a PPFD of 150-180 μmol m^{-2} s^{-1}. After 4 weeks of growth, WT, *sus1/sus4/sus5/sus6* quadruple mutant, *sus1/sus4*, and *sus5/sus6* double mutant plants were subject to a flooding treatment by adding and maintaining degassed water in the growth trays at a level just above the surface of the soil for 5 days. In addition, a subset of the same plant lines was grown in a well-aired condition. Leaf diameters were measured at the widest part of the rosettes from eight individual plants after 4 weeks growth. Rosette leaves with or without flooding treatment were collected at the same time for soluble sugar analysis.

4.2.4 Soluble carbohydrate analysis

Arabidopsis rosette leaves were harvested and immediately flash-frozen in liquid nitrogen (harvest consistently occurred 2-4 hours after the end of dark period). Isolated leaves were ground using a mortar and pestle and freeze-dried overnight. Sucrose was extracted from 10-12 mg of freeze-dried tissue using 1 mL methanol:chloroform:water (12:5:3) incubated at 4 °C overnight. On the following day, samples were centrifuged for 10 minutes at 6,000 rpm, and the supernatant was transferred to a new tube. The extraction was repeated two more times to collect any residual sugar, and the supernatants pooled. The pellet was dried in a 55 °C oven overnight and used later for starch analysis. To partition the solvents, 1 mL of deionized water was added to the supernatants

prior to vortexing and centrifuging for 4 minutes at 4,000 rpm. After phase separation, the top phase containing soluble sugars was collected. 2 mL of this phase was then dried in a vacuum centrifuge overnight, and the pellet re-suspended in 0.5 mL deionized water and filtered through a 0.45 μm syringe filter into an HPLC vial. The soluble sugar concentration was quantified by an anion-exchange HPLC (ICS-5000; Dionex, Sunnyvale, CA) fit with a Dionex™ CarboPac™ PA1 column and a pulsed amperometric detector and a gold electrode. Sugars were eluted with 16 mM NaOH, 2 mM NaOAc at a flow rate of 0.8 mL/minute. The concentration of soluble sucrose was determined using a calibration standard curve generated with known sucrose concentrations.

4.2.5 *Arabidopsis* root length and seedling size measurement

For root length analysis, WT, *sus1/sus4/sus5/sus6* quadruple mutant, *sus1/4*, and *sus5/6* double mutant seeds were plated on half-strength MS plates lacking sucrose after cold treatment for 2 to 4 days at 4 °C (considered as the 0 days after germination). Seedlings were grown vertically for 7 days at 23 °C, under 16/8 hours light/dark regime. Pictures showing all the seedlings with a ruler were analyzed in Image J (National Institutes of Health; http://rsb.info.nih.gov/ij/).

To investigate the response of *sus1/sus4/sus5/sus6* mutant to sugar and osmotic stress, seedlings were grown on half-strength MS plates supplied with sucrose or mannitol. At 3 days after germination, seedling size was measured from root tip to hypocotyl apex using Image J, as described above.

4.2.6 Plant height measurement and cell wall measurement

Plant height was measured from the flower apex to the base of the stem using 7-week-old *Arabidopsis* plants. Thin cross-sections were cut 3 cm from the base of the stem using a sterile razor blade and were subsequently incubated in 0.02% toluidine blue solution for 2 minutes at room temperature. After thoroughly washing, respective stem cross-sections from WT and *sus1/sus4/sus5/sus6* quadruple mutant were mounted in water prior to imaging. Cell wall morphology and thickness were subsequently analyzed on a Leica DMR microscope equipped with a QICAM digital camera (QIMAGING).

4.2.7 Dry seed weight measurement

Arabidopsis seeds were harvested when they were fully mature and dried in a desiccator at room temperature for a week prior to weighing in lots of 100 individual seeds. Data were collected from four independent plants and three samples from each plant.

4.3 Results

Homozygous *sus1/sus4/sus5/sus6* quadruple mutants were generated and confirmed by PCR using specific primers (Figure 4.1). Further analyses were performed to investigate the impact on growth and development of the *sus1/sus4/sus5/sus6* quadruple mutant in comparison with WT plants, *sus1/sus4*, and *sus5/sus6* double mutants. In general, the *sus1/sus4/sus5/sus6* quadruple mutant showed no obvious visual phenotype when grown under normal growth conditions. After 4 weeks growth, *sus1/sus4/sus5/sus6* plants were not significantly different from WT in rosette leaf size, and only minor chlorosis was observed at the rosette leaf tip of quadruple mutant plants, similar to

that of the *sus5/sus6* double mutant, while the *sus1/sus4* mutant leaves exhibited more severe chlorosis (Figure 4.2). In addition, *sus1/sus4/sus5/sus6* mutant plants were indistinguishable from WT in inflorescence stem height (Figure 4.3) and dry seed weight (Figure 4.4). Stem cross-sections were cut 3 cm from the base of the stem and were stained with toluidine blue. The morphology and cell wall thickness were visualized under a light microscope. Images showed that quadruple plants were not visibly different from WT in cell wall structure or thickness (Figure 4.5).

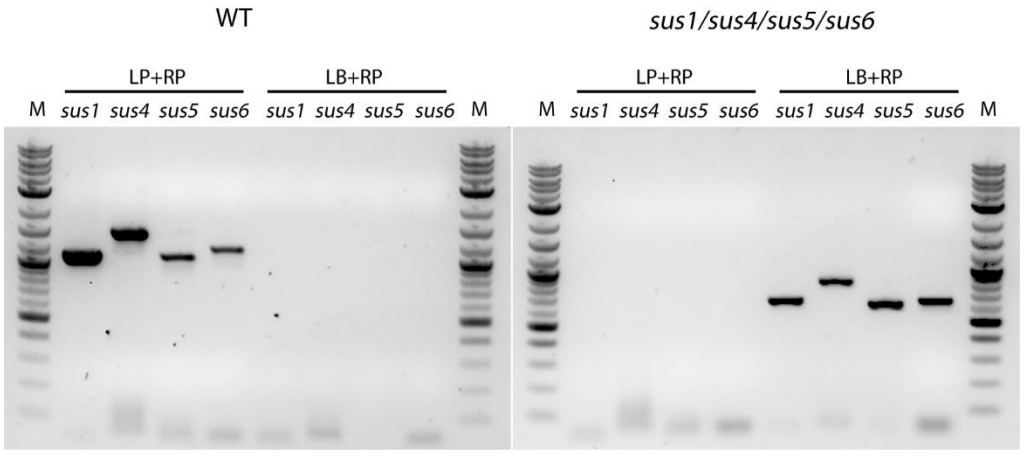

Figure 4.1 PCR analysis of genomic DNA from WT and *sus1/sus4/sus5/sus6* homozygous plants using gene-specific primers (LP + RP) and left border T-DNA primers (LB + RP). M represents 2-Log DNA ladder marker (NEB).

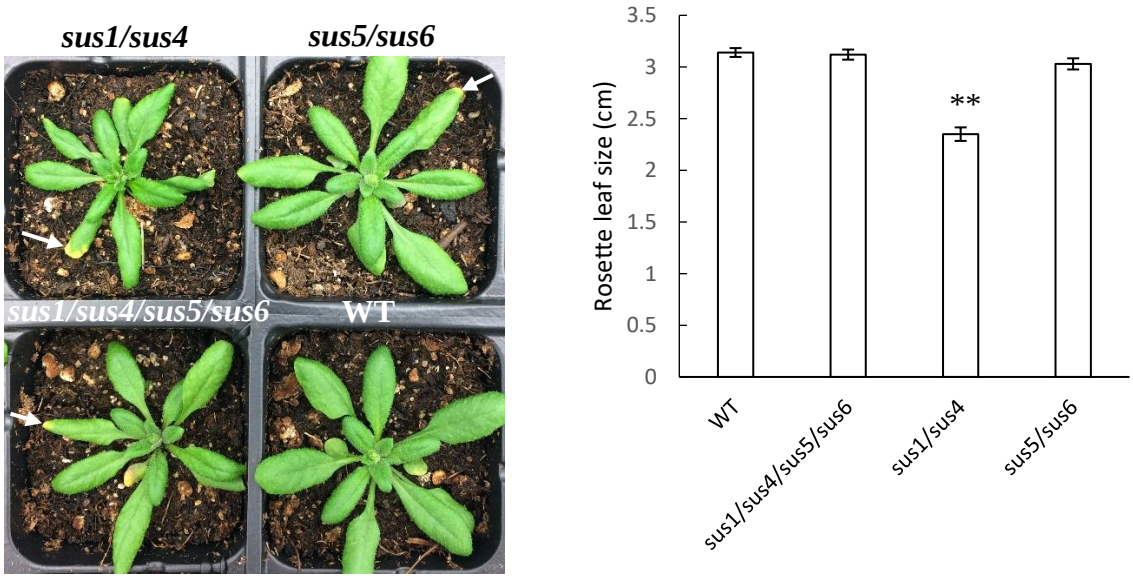

Figure 4.2 Morphology and rosette leaf size of 4-week-old *sus1/sus4/sus5/sus6, sus1/sus4, sus5/sus6,* and WT plants grown under the same conditions. Only mild chlorosis was observed in the leaf tip of the quadruple mutant indicated by arrows (Images on the left). The bar graph on the right shows the means ± SE rosette leaf diameters from eight individual plants. Asterisks indicate significant difference (*p*-value < 0.01) from WT plants using a Benjamini-Hochberg Student *t*-test.**

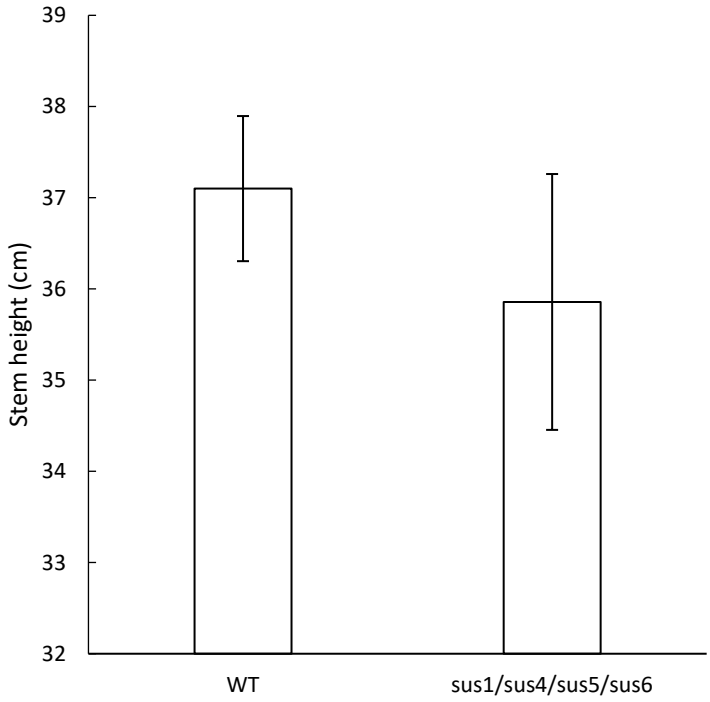

Figure 4.3 Inflorescence stem height of 7-week-old *sus1/sus4/sus5/sus6* and WT plants. Results are the means ± SE of seven individual plants. There is no significant difference from WT according to a Student *t*-test.

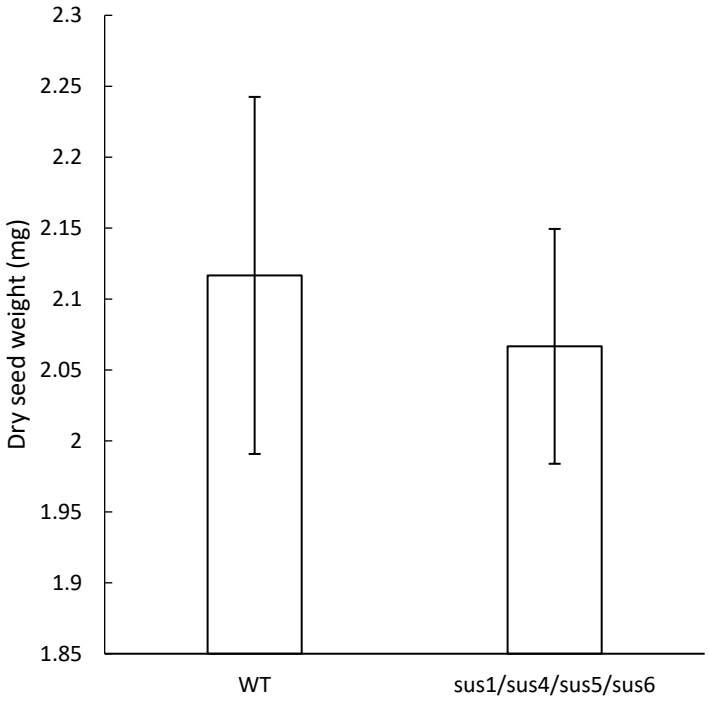

Figure 4.4 Dry seed weight of *sus1/sus4/sus5/sus6* and WT plants. Results are the means ± SE of three replicates from four individual plants and each replicate contains 100 individual seeds (n=4). There is no significant difference from WT according to a Student *t*-test.

sus1/sus4/sus5/sus6 **WT**

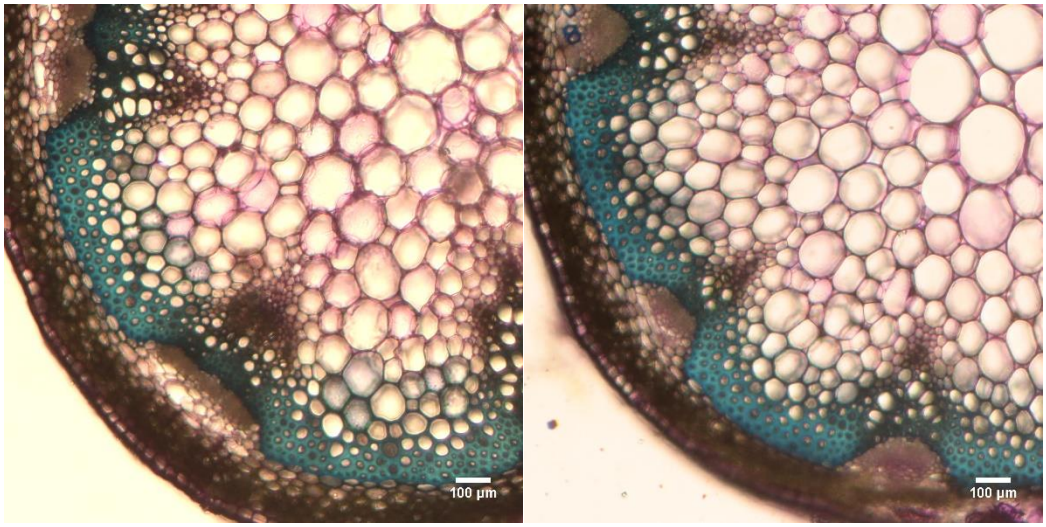

Figure 4.5 Cell wall morphology of 7-week-old *sus1/sus4/sus5/sus6* and WT plants. Sections were cut 3 cm from the base of the stem and stained with 0.02% toluidine blue for 2 minutes at room temperature. Images show that morphology and cell wall thickness of *sus1/sus4/sus5/sus6* mutant is visually indistinguishable from WT plants under a light microscope. Bars=100 µm.

In addition, analysis of soluble sugar was carried out on the rosette leaves with or without flooding. In general, soluble sugar content increased after flooding treatment in all plants. Similar to previous results (Chapter 2), elevated soluble sugar content was more dramatic in the *sus1/sus4* double mutant after five days flooding (Figure 4.6 and Figure 4.7). Statistical analysis indicated that soluble fructose content was significantly elevated in only the *sus1/sus4* mutant compared to WT plants. In general, the soluble sugar content of the *sus1/sus4/sus5/sus6* quadruple mutant was not significantly different from WT plants under neither well-aerated nor hypoxic conditions (Figure 4.6 and Figure 4.7).

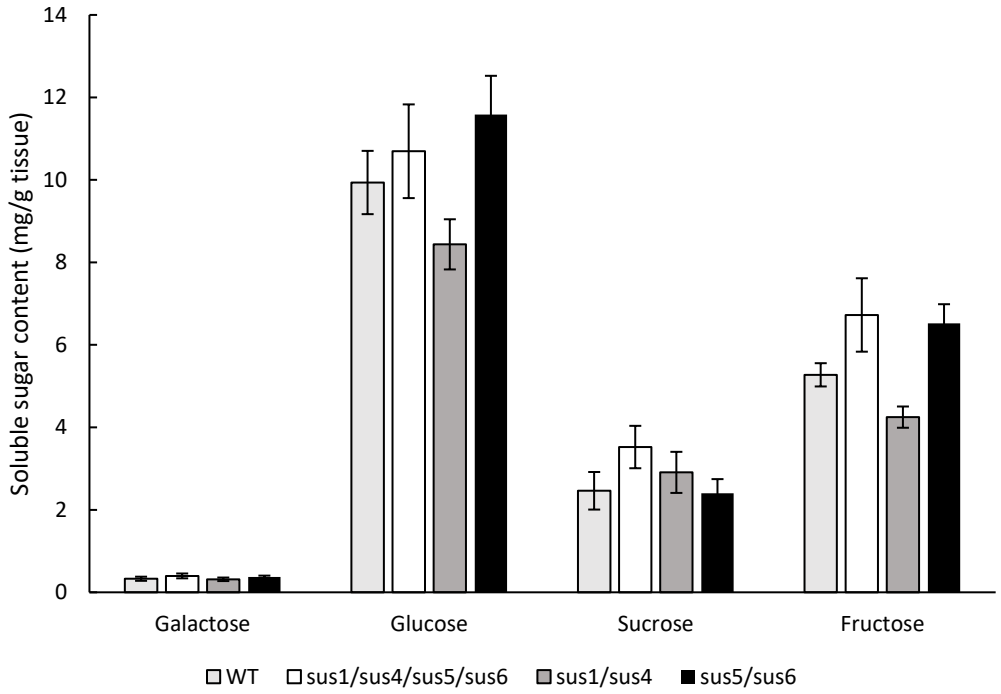

Figure 4.6 Leaf soluble sugar content of 4-week-old WT, *sus1/sus4/sus5/sus6* quadruple mutant, *sus1/sus4*, and *sus5/sus6* double mutant plants grown under well-aerated conditions. Data are means ± SE calculated from at least four individual plants per line. There is no significant difference from WT according to the Benjamini-Hochberg corrected Student *t*-test.

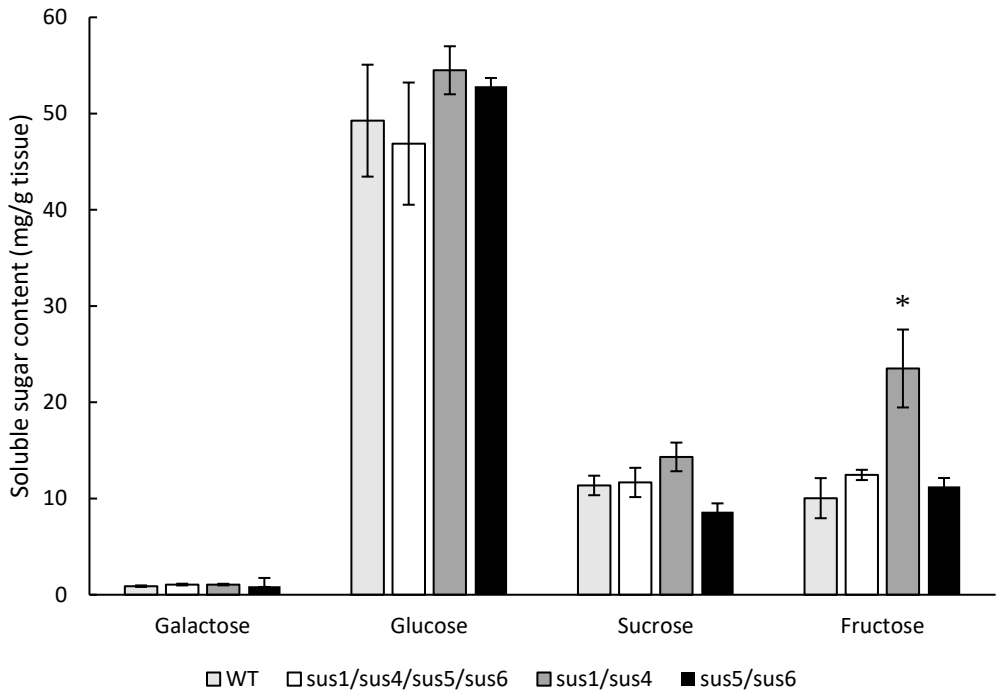

Figure 4.7 Leaf soluble sugar content of 4-week-old WT, *sus1/sus4/sus5/sus6* quadruple mutant, *sus1/sus4*, and *sus5/sus6* double mutant plants after five days flooding. Data are means ± SE calculated from at least four individual plants per line. Asterisks indicate significant difference (* corrected *p*-value < 0.05) from WT plants using the Benjamini-Hochberg corrected Student *t*-test.

Sucrose and hexose are important for plant growth and development since they play roles not only as nutrients but also as signalling molecules (Koch, 1996). SuSy catalyzes the reversible reaction of sucrose cleavage and has been proposed to be involved in phloem loading and unloading (Chapter 2 and Chapter 3). Therefore, I further examined the growth response of *sus1/sus4/sus5/sus6* quadruple mutant, WT, *sus1/4*, and *sus5/6* double mutant plants to different concentrations of sucrose. All the seeds were harvested at the same time and germinated on the plates supplied with 0%, 2% and 6% sucrose respectively. At 3 days after germination, whole

seedling size of the *sus1/sus4/sus5/sus6* mutant was not obviously different from other plants when grown in half-strength MS medium lacking sucrose or supplied with 2% sucrose (Figure 4.8). However, when treated with 6% sucrose, SuSy quadruple and double mutants showed significantly inhibited seedling growth. Seedling sizes of *sus1/sus4/sus5/sus6*, *sus1/sus4*, and *sus5/sus6* were respectively 65%, 72% and 85% of that of WT (Figure 4.8). Inhibition of seedling growth in *sus1/sus4/sus5/sus6* was more obvious than *sus1/sus4* and *sus5/sus6* double mutants. This growth defect observed in high-concentrated sucrose conditions may be due to the osmotic stress induced by sucrose. To separate the effect of sucrose and osmotic stress on seedling growth, all plants were also grown on plates supplemented with 1% and 3% mannitol which caused constant osmotic stress similar to that of sucrose supplementation. No obvious growth differences were observed between quadruple mutant seedlings and all the other plants with 1% and 3% mannitol treatment (Figure 4.9), suggesting that the inhibited seedling growth is not caused by osmotic stress.

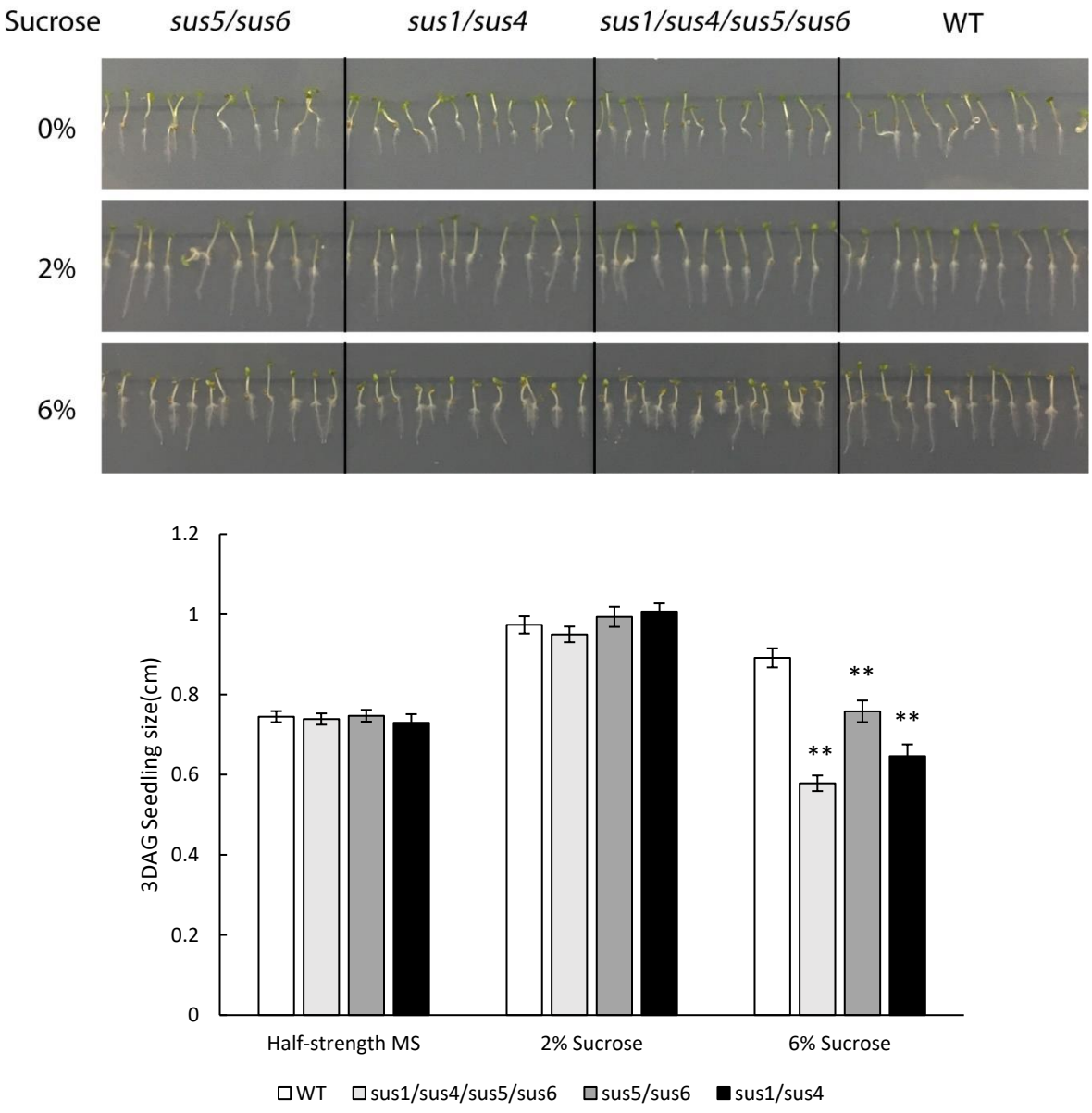

Figure 4.8 Seedling size of *sus1/sus4/sus5/sus6*, *sus1/sus4*, *sus5/sus6*, and WT plants grown in half-strength MS plates supplied with 0%, 2% and 6% sucrose. Images show that 3 days after germination, no obvious growth difference was observed when seedlings were grown in medium lacking sucrose or supplied with 2% sucrose. In contrast, the seedling size (total length of radicle and hypocotyl) of *sus1/sus4/sus5/sus6*, *sus1/sus4*, *sus5/sus6* mutants was smaller than WT plants with the supplementation of 6% sucrose. Data in the bar graph are means

± SE calculated from at least twenty-five seedlings. Asterisks indicate significant difference (corrected *p*-value < 0.01) from WT plants using the Benjamini-Hochberg corrected Student *t*-test.**

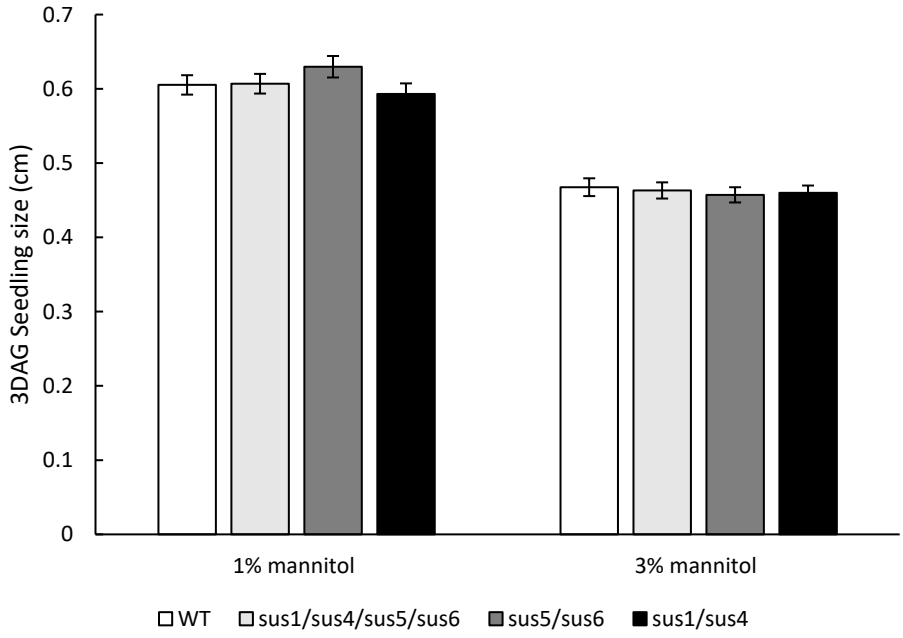

Figure 4.9 Seedling size of *sus1/sus4/sus5/sus6, sus1/sus4, sus5/sus6* and WT plants grown in half-strength MS plates supplied with 1% and 3% mannitol. Images show plants at 3 days after germination, no obvious growth differences were observed when seedlings were treated with 1% and 3% mannitol. Data in the bar graph are means ± SE calculated from at least thirty seedlings. There is no significant difference in seedling size from WT plants according to the Benjamini-Hochberg corrected Student *t*-test.

4.4 Discussion

In previous chapters (Chapter 2 and Chapter 3), I demonstrated that four isoforms of SuSy (SuSy1 and SuSy4, SuSy5 and SuSy6) were specifically localized to the phloem tissue and proposed that they play a common role in phloem loading and unloading. However, under normal growth

conditions, the morphology of the quadruple mutant lacking these four SuSy isoforms was not significantly different from WT plants in terms of rosette leaf size, inflorescence stem height, cell wall thickness and dry seed weight. These results indicate that the missing activity of these four SuSy isoforms does not dramatically affect phloem functionality, since the quadruple mutant showed normal growth and development. This is presumably due to the fact that invertases compensate for the loss of SuSy activity. Functional redundancy may largely exist between SuSy and INV in *Arabidopsis* plants and it has been reported that CINV could also play an important role in phloem unloading and modulating sucrose partitioning (Eschrich, 1980; Ruan et al., 2010). Consistent with Chapter 2, *sus1/sus4* double mutant showed severe chlorosis at the tip of rosette leaves, while no chlorosis was observed in WT plants. However, the *sus1/sus4/sus5/sus6* quadruple mutant and *sus5/sus6* double mutant only exhibited minor chlorosis. With five days flooding, *sus1/sus4* double mutants displayed more obviously elevated soluble sugar content than WT plants. In contrast, the quadruple mutant lacking SuSy1, SuSy4, SuSy5 and SuSy6 activity was not significantly different from WT plants in soluble sugar content under hypoxic conditions. These results suggest that when SuSy activity is lacking in the phloem, the quadruple mutant probably induces an alternative pathway to complement the more severe phenotype. This compensation would have to come from INV activity.

Our results also show that the quadruple mutant, WT, *sus1/sus4*, and *sus5/sus6* double mutant plants respond differently to high sucrose content in the media. Seedling growth of *sus1/sus4/sus5/sus6* was not obviously different from other plant lines in half-strength MS plates or media supplied with 2% sucrose. However, the *sus1/sus4/sus5/sus6* quadruple mutant and

double mutant (*sus1/sus4* and *sus5/sus6*) seedlings displayed significantly smaller sizes than WT plants in presence of 6% sucrose. This is probably because that within the early stage of seedling establishment, when the cotyledons are not open or fully expanded, exogenous sucrose could be absorbed by seedling roots and serve as the resource for plant growth and development. Sucrose metabolism supplies the substrate for biochemical processes and the synthesis of metabolically and structurally important compounds. Likely, the external sucrose is first taken up with water and enters the stele by crossing endodermis. It is further loaded into the phloem for transportation to sinks, and the lack of SuSy activity in phloem tissue of *sus1/sus4/sus5/sus6*, *sus1/sus4*, and *sus5/sus6* seedlings might affect this sucrose loading process. Consistently, the transcript level of *Arabidopsis* SuSy1 has been shown to be upregulated with sugar or osmotic feeding (Déjardin et al., 1999; Baud et al., 2004). No obvious growth alterations were observed when plants were treated with 3% mannitol, which suggested that growth inhibition of seedlings deficient in SuSy activity was specifically induced by sucrose instead of constant osmotic stress.

Chapter 5: Investigation of the effect of phosphorylation on SuSy4 subcellular localization and functional properties

5.1 Introduction

Reversible protein phosphorylation is characterized by the addition or removal of a phosphate group from a protein, which is catalyzed by a protein kinase and protein phosphatase respectively. This phenomenon is the most common posttranslational modification modulating diverse protein functions, including enzymatic activity, protein turnover, interaction, conformation and localization (Humphrey et al., 2015). Importantly, in higher plants, the signal transduction pathway can also be regulated by this mechanism, which in turn modulates plant growth, development and response to the environment (Ardito et al., 2017). For instance, light-dependent phosphorylation of a thylakoid membrane protein is believed to be implicated in signalling between photosynthesis and the regulation of gene expression (Pesaresi et al., 2009; Pesaresi et al., 2011; Schonberg and Baginsky, 2012). Phosphorylation of sucrose phosphate synthase has been reported to modulate protein activity in response to light/dark signals and end-product accumulation (Huber and Huber, 1996). The phosphorylation of several proteins involved in starch metabolism has been identified, including starch synthase, starch branching enzyme and ADP-glucose pyrophosphorylase (Tetlow et al., 2004; Reiland et al., 2009; Nakagami et al., 2010). In addition, it has been proposed that phosphorylation potentially regulates the activity of CesAs (Somerville, 2006). In *Arabidopsis*, plants lacking two protein kinases displayed severe growth defects, suggesting their essential role in cell expansion and seed development (Chaiwongsar et al., 2012). It has been reported that plants

with reduced activity of phytochrome kinase showed a hyposensitive response to far-red light (Shin et al., 2016). Furthermore, a calcium-dependent protein kinase has been proposed to negatively regulate the immune signaling process in *Arabidopsis* (Monaghan et al., 2014).

According to current literature, SuSy activity, its intracellular localization, and protein stability are believed to be modulated by its phosphorylation status. In maize leaves, phosphorylation of SuSy by a calcium-dependent protein kinase (CDPK) occurred at two conserved sites, located on Ser-15 and Ser-170 of SUS 1 protein (Huber et al., 1996; Hardin et al., 2003). In soybean, mung bean, and castor bean plants, SuSy has been shown to be phosphorylated at Ser-11 by CDPKs (Nakai et al., 1998; Zhang et al., 1999; Fedosejevs et al., 2014; Fedosejevs et al., 2016). Studies examining the protein structure of *Arabidopsis* sucrose synthase 1 (SuSy1) suggested that phosphorylation of Ser-13 would change the electrostatic environment in this region (Zheng et al., 2011).

Phosphorylation is a reversible regulatory process. Nakai et al. (1998) illustrated that when the Ser-11 residue of mung bean SuSy was replaced with an aspartic acid (S11D), the protein mimicked the phosphorylation status by exhibiting similar subunit mass, structure and kinetic properties, and showed dramatically increased activity by elevating the apparent affinity of the enzyme for sucrose and UDP. In addition, the S11E mutant, which introduced a glutamic acid at Ser-11, was superior to both the phosphorylated SuSy and S11D mutant enzyme in *in vitro* assays (Nakai et al., 1998). In maize leaves, Ser-15 has also been shown to be the major phosphorylation site of SuSy, and has been proposed to regulate enzyme activity and localization, while Ser-170 is a minor phosphorylation site which has been proposed to regulate proteolysis (Hardin et al., 2003;

Hardin et al., 2004). The presence of a negative charge at Ser-15 has been suggested to promote the binding of SuSy to defined membranes, and enhance the enzyme activity in the direction of sucrose cleavage (Hardin et al., 2004). In addition, suppression of a CDPK isoenzyme in rice seed has been shown to lead to reduced SuSy activity and significantly enhanced sucrose concentrations in a variety of tissues (Asano et al., 2002). SuSy phosphorylation of the cultured cells of sycamore did not affect its association with the membrane, but impacted its enzymatic activity (Pozueta-Romero et al., 2004). In contrast, in soybean nodules and maize plants, phosphorylation has been reported to have no effect on SuSy activity, but decreased the surface hydrophobicity of SuSy protein and therefore promoted a soluble phase of localization (Winter et al., 1997; Zhang et al., 1999). Furthermore, Persia et al. (2008) showed that in tobacco pollen tube cells, phosphorylated SuSy was more abundant in the cytoplasm and cell wall, while non-phosphorylated SuSy localized specifically to the plasma membrane. In addition, *in vivo* phosphorylation of a castor bean SuSy displayed no impact on its kinetic properties and subcellular localization, but protected the protein from proteolysis (Fedosejevs et al., 2014). Overall, conclusions drawn from studies of *in vitro* phosphorylation are difficult to extend to *in vivo* phosphorylation. At present, therefore, there is no consensus on the role of SuSy phosphorylation in higher plants.

Clearly, further studies are needed to elucidate the *in vivo* effect of SuSy phosphorylation. In this chapter, site-directed mutagenesis was employed to mutagenize the Ser-13 residue of *Arabidopsis* SuSy4. Ser-13 of *Arabidopsis* SuSy is the residue homologous to Ser-15 in maize and Ser-11 in soybean and mung bean. As mentioned above, both of these residues have been reported to be the major phosphorylation sites of SuSy in different plant species (Huber et al., 1996; Nakai et al.,

1998; Zhang et al., 1999). In addition, using Net phos 2.0 (http://www.cbs.dtu.dk/services/NetPhos/), the predicted possibility of phosphorylation at Ser-13 of *Arabidopsis* SuSy4 is 0.997/1. Since Ser-13 is positioned on the N-terminus of SuSy, the effect of phosphorylation is more likely to be disrupted by an N-terminal fusion to YFP protein and therefore I generated *YFP* reporter gene constructs that were C-terminus the CDS. To modify phosphorylation status of the SuSy4 proteins, Ser-13 was substituted with negatively charged aspartic acid (D) and glutamic acid (E) to mimic phosphorylation, or the neutral amino acid alanine (A) to inhibit phosphorylation. Transgenic lines were subsequently generated containing *SuSy4$_{pro}$::SuSy4(S13A)::YFP, SuSy4$_{pro}$::SuSy4(S13E)::YFP* or *At SuSy4$_{pro}$::SuSy4(S13D)::YFP*. To investigate the phosphorylation of SuSy4 in relation to its membrane association and activity, subcellular localization, soluble sugar and starch content were analyzed in all transgenic lines. The results showed that both phosphomimetic and phosphoresistant SuSy4 were largely localized to the cytoplasm of companion cells, similar to that of non-modified SuSy4. When subjected to flooding, transgenic lines carrying non-phosphorylatable SuSy4 displayed soluble sugar and starch content similar to that of SuSy-YFP complemented lines. In contrast, SuSy4 phosphomimetic transgenic lines exhibited obvious reductions in soluble sugar and starch content.

5.2 Methodologies

5.2.1 Site-directed mutagenesis and plasmid construction

QuickChanges II Site-Directed Mutagenesis kit (Agilent Technologies) was employed to mutagenize the Ser-13 residue of *Arabidopsis* SuSy4 according to the manufacturer's instructions. Specifically, pDONR/Zeo vector containing SuSy4 CDS served as the template for the synthesis

of mutant plasmid using *PfuUltra* high-fidelity DNA polymerase. Mutagenic primers were designed by the QiukChange Primer Design program (https://www.genomics.agilent.com/primerDesignProgram.jsp) and are shown in Table 5.1. The program conditions used to synthesize mutant strand were as follows: 95 °C for 30 seconds, followed by 16 cycles of 95 °C for 30 seconds, 55 °C for 1 minute, and 65 °C for 10 minutes. Once the reaction was completed, the parental template was digested with the *Dpn* I restriction enzyme after incubation at 37 °C for 30 minutes. Mutated molecules were subsequently transformed into XL1-Blue supercompetent cells and selected on plates containing the appropriate antibiotic. SuSy4 coding sequence with different point mutations was further confirmed by sequencing and then subcloned into a modified pBIN19 vector described in Chapter 2 using Gateway™ technology. The *35S* promoter region was replaced with the *SuSy4* native promoter, approximately 2000 kb upstream of the translational start codon, and the protein was fused to YFP at its C-terminus. All constructs were transformed independently into *sus1/sus4* double mutant plants. Positive lines were identified by growing them on half-strength MS medium supplemented with 5 mg/L sulfadiazine. Two or three transgenic lines with bright YFP signal were selected for further analyses of protein subcellular localization, and leaf soluble sugar and starch content.

Table 5.1 Primers employed for the site-directed mutagenesis of AtSuSy4 at Ser-13 residue

Point mutation	Forward primers (5′ to 3′)	Reverse primers (5′ to 3′)
Aspartic acid	TAATAACGCGAGTCCACGACCAGCG AGAGCGTTTGG	CCAAACGCTCTCGCTGGTCGTGGACTCGC GTTATTA
Glutamic acid	TATGATAACGCGCGTCCACGAGCAA CGTGAGCGTTTGAACG	CGTTCAAACGCTCACGTTGCTCGTGGACG CGCGTTATCATA
Alanine	CAAACGCTCTCGCTGGGCGTGGACT CGCGTTATT	AATAACGCGAGTCCACGCCCAGCGAGAG CGTTTG

5.2.2 Microscopy

Longitudinal sections of leaf petiole were employed to check the subcellular localization of SuSy4 with different phosphorylation status. A Leica DMI 6000 B inverted microscope fitted with a Perkin Elmer Ultraview VoX Spinning Disk scan head with excitation/emission wavelengths of 514 nm/540 nm was employed for visualization of all SuSy4-YFP fusions. At least 20 cells from each of three individual plants from two independent transgenic lines were examined. Images were captured on a Hamamatsu 9100-02 CCD camera using Volocity 6.3 software (Improvision) and processed using Image J software (National Institutes of Health; http://rsb.info.nih.gov/ij/).

5.2.3 Soluble carbohydrate analysis

After 5 days of flooding treatment, rosette leaves of 4-week-old WT, *sus1/sus4* double mutant, two YPF-complemented transgenic lines, and three individual SuSy4 phosphoresistant and phosphomimetic transgenic lines were harvested and immediately flash-frozen in liquid nitrogen (harvest consistently occurred 2-4 hours after the end of dark period). Isolated leaves were ground using a mortar and pestle and freeze-dried overnight. Soluble sucrose was extracted from 10-12

mg freeze-dried tissue using 1 mL methanol:chloroform:water (12:5:3) incubated at 4 °C overnight. On the following day, samples were centrifuged for 10 minutes at 6000 rpm and the supernatant was transferred to a new tube. The extraction was repeated two more times to obtain any residual sugar, and the supernatants were pooled. The pellet was dried at 55 °C overnight and used for starch analysis. To partition the solvents, 1 mL of deionized water was added to the supernatants prior to vortexing and centrifuging for 4 minutes at 4000 rpm. The top phase, containing soluble sugars, was subsequently collected and 2 mL was then dried in a vacuum centrifuge overnight, and the pellet re-suspended in 0.5 mL deionized water and filtered through a 0.45 μm syringe filter into an HPLC vial. The soluble sugar concentration was quantified by an anion-exchange high-performance liquid chromatography (ICS-5000; Dionex, Sunnyvale, CA) fit with a Dionex™ CarboPac™ PA1 column and a pulsed amperometric detector and a gold electrode. Sugars were eluted with 16 mM NaOH, 2 mM NaOAc at a flow rate of 0.8 mL/minute. The concentration of soluble sugar was determined using an external calibration standard curve generated with known sucrose concentrations.

5.2.4 Starch analysis

For starch measurement, the residue pellet from soluble sugar extraction was weighed and then hydrolyzed in 1 mL 4% H_2SO_4 at 121 °C for 5 minutes. After centrifuging at 500 rpm for 5 minutes, the supernatant containing liberated glucose was collected. A 760 μL sample and 40 μL fucose stock (5 mg/mL), used as internal standard, were weighed and passed through a 0.45 μm syringe filter into a HPLC vial. Glucose content was determined by HPLC fit with a CarboPac™ PA1 column and an electrochemical detector. Carbohydrate was eluted using water

at the flow rate of 1 mL/minute. The starch content was quantified using an external calibration standard curve generated with known glucose concentrations.

5.3 Results

Subcellular localization of phosphomimetic and phosphoresistant forms of SuSy4 was analyzed using a spinning disc confocal microscope, in comparison to the non-modified SuSy4. Live-cell imaging showed that the YFP signal of both phosphomimetic and phosphoresistant SuSy4 were all largely confined to the cytoplasm of companion cells, similar to that of SuSy4-YFP fusion (Figure 5.1). In previous chapters (Chapter 2 and Chapter 3), significantly increased soluble sugar and starch content was apparent only in the *sus1*/*sus4* mutant under hypoxic conditions (not under normal growth conditions). Moreover, the SuSy-YFP fusions were shown to partially rescue this phenotype. Therefore, to investigate the effect(s) of phosphorylation of SuSy, only the plants grown under hypoxic conditions were examined after a five-day-flooding treatment, including assessing leaf soluble sugar and starch content of 4-week-old WT, *sus1/sus4* double mutant, YPF-complemented transgenic lines, and SuSy4 phosphomimetic and phosphoresistant transgenic lines. Consistent with the data in Chapter 2, significantly elevated soluble sucrose and fructose content was observed in the rosette leaves of *sus1/sus4* mutant compared to WT plants when subjected to flooding (Figure 5.3 and Figure 5.4). However, soluble glucose and starch content of the *sus1/sus4* mutant was not significantly different from WT plants (Figure 5.2 and Figure 5.5). Transgenic lines containing SuSy4-YFP fusions displayed complete or partial recovery of elevated soluble sucrose and fructose content (Figure 5.3 and Figure 5.4). In addition, their soluble glucose and starch levels were indistinguishable from those of WT and *sus1/sus4* plants (Figure 5.2 and 5.5).

Similarly, all three transgenic lines containing phosphoresistant SuSy4 were not obviously different from YFP-complemented lines in soluble sugar and starch content in response to flooding (Figure 5.2 to Figure 5.5). In general, phosphomimetic SuSy4-YFP fusions completely rescued the accumulated soluble sucrose level apparent in *sus1/sus4* mutant when grown under hypoxic conditions (Figure 5.3). Moreover, most of SuSy4 phosphomimetic lines exhibited a partial recovery of the observed soluble fructose content (Figure 5.4). However, significantly reduced soluble glucose, sucrose and starch content was observed in one transgenic line containing *SuSy4$_{pro}$::SuSy4(S13D)::YFP* (Figure 5.2, Figure 5.3, and Figure 5.5). Average levels of soluble glucose, sucrose and starch content in line 3 were only 62%, 55%, and 37%, respectively, of those of WT plants. Introduction of glutamic acid (E) at the Ser-11 residue of mung bean SuSy has been proposed to yield an enzyme superior to both the phosphorylated SuSy and S11D mutant enzyme in catalytic efficiency of sucrose (Nakai et al., 1998). In our study, inhibited accumulation of soluble sugar and starch content was also apparent in transgenic plants carrying *SuSy4$_{pro}$::SuSy4(S13E)::YFP* (Figure 5.2, Figure 5.3, and Figure 5.5). Compared to WT plants, transgenic line 3 showed a reduction in soluble glucose, sucrose and starch content, by approximately 58%, 60% and 82%, respectively.

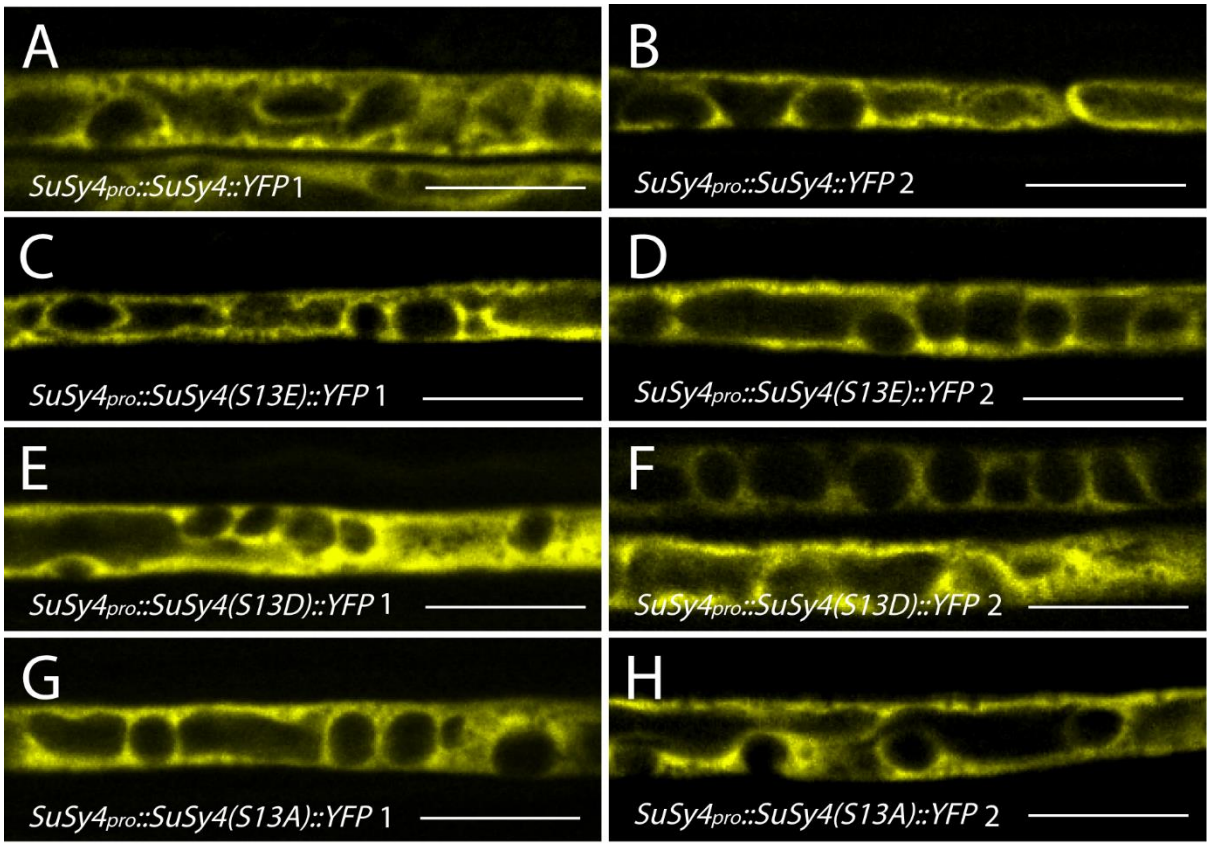

Figure 5.1 Subcellular localization of phosphomimetic and phosphoresistant AtSuSy4-YFP in the companion cells of leaf petioles. Analysis of subcellular localization was performed via a confocal microscope using 2 independent transgenic lines containing *SuSy4$_{pro}$::SuSy4::YFP*, *SuSy4$_{pro}$::SuSy4(S13A)::YFP*, *SuSy4$_{pro}$::SuSy4(S13E)::YFP* or *SuSy4$_{pro}$::SuSy4(S13D)::YFP*. Images showing that YFP signal of both phosphomimetic (C-F) and phosphoresistant (G and H) SuSy4 were still largely present in the cytoplasm, similar to that of non-modified SuSy4 (A and B). Bars=10 µm.

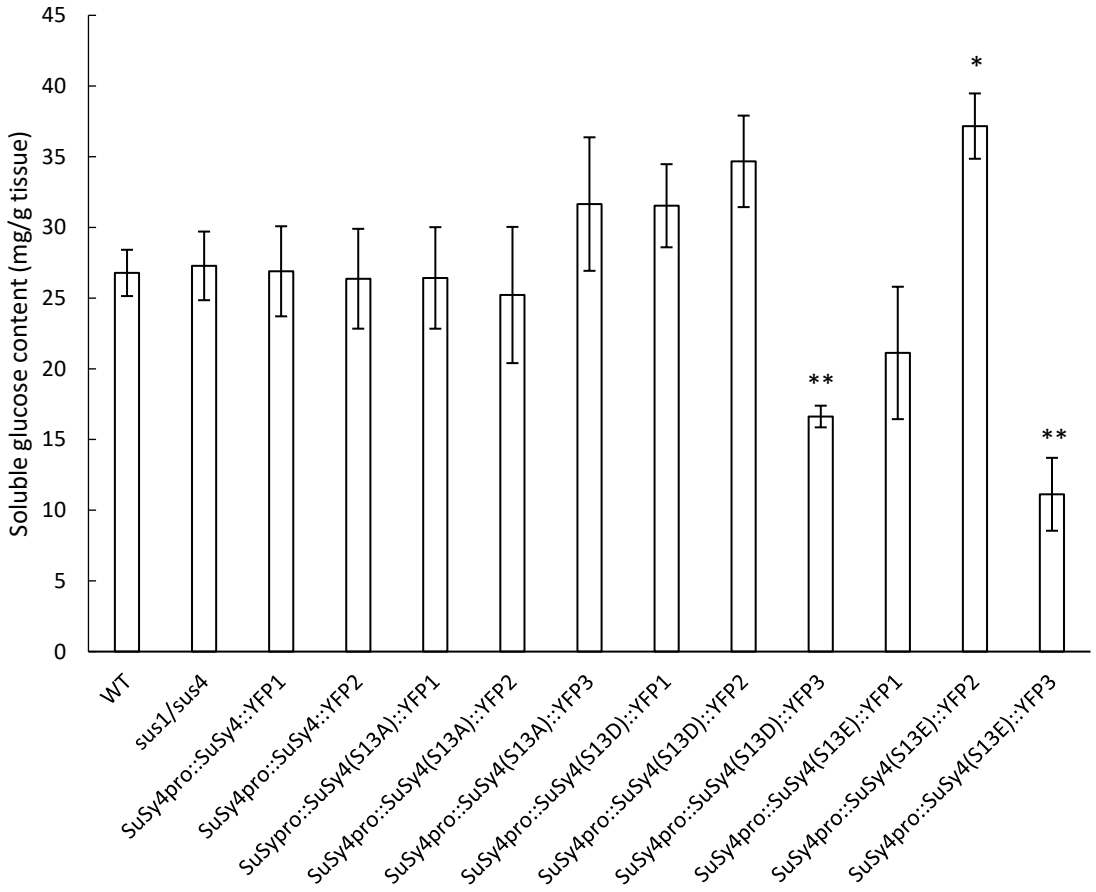

Figure 5.2 Leaf soluble glucose content of 4-week-old WT, *sus1/sus4*, , SuSy4-YPF transgenic lines (*SuSy4$_{pro}$::SuSy4::YFP)*, SuSy4 phosphoresistant (*SuSy4$_{pro}$::SuSy4(S13A)::YFP*) and phosphomimetic (*SuSy4$_{pro}$::SuSy4(S13E)::YFP* and *SuSy4$_{pro}$::SuSy4(S13D)::YFP*) transgenic lines after five days flooding. Data are means ± SE calculated from at least 4 individual plants per line. Asterisks indicate significant difference (* *p*-value < 0.1, ** *p*-value < 0.05) from WT plants using a Benjamini-Hachberg corrected Student *t*-test.

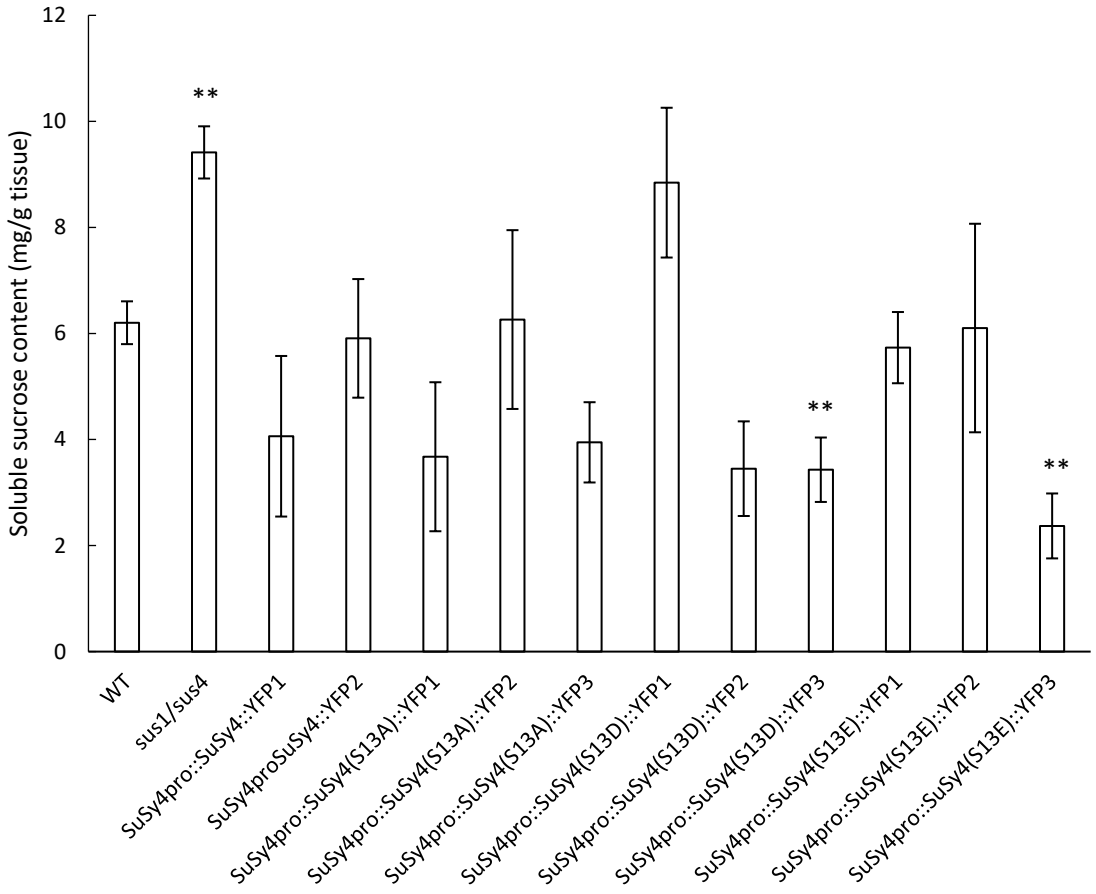

Figure 5.3 Leaf soluble sucrose content of 4-week-old WT, *sus1/sus4*, SuSy4-YPF complemented lines (*SuSy4$_{pro}$::SuSy4::YFP)*, SuSy4 phosphoresistant (*SuSy4$_{pro}$::SuSy4(S13A)::YFP*) and phosphomimetic (*SuSy4$_{pro}$::SuSy4(S13E)::YFP* and *SuSy4$_{pro}$::SuSy4(S13D)::YFP*) transgenic lines after five days flooding. Data are means ± SE calculated from at least 4 individual plants per line. Asterisks indicate significant difference (*p*-value < 0.05) from WT plants using a Benjamini-Hochberg corrected Student *t*-test.**

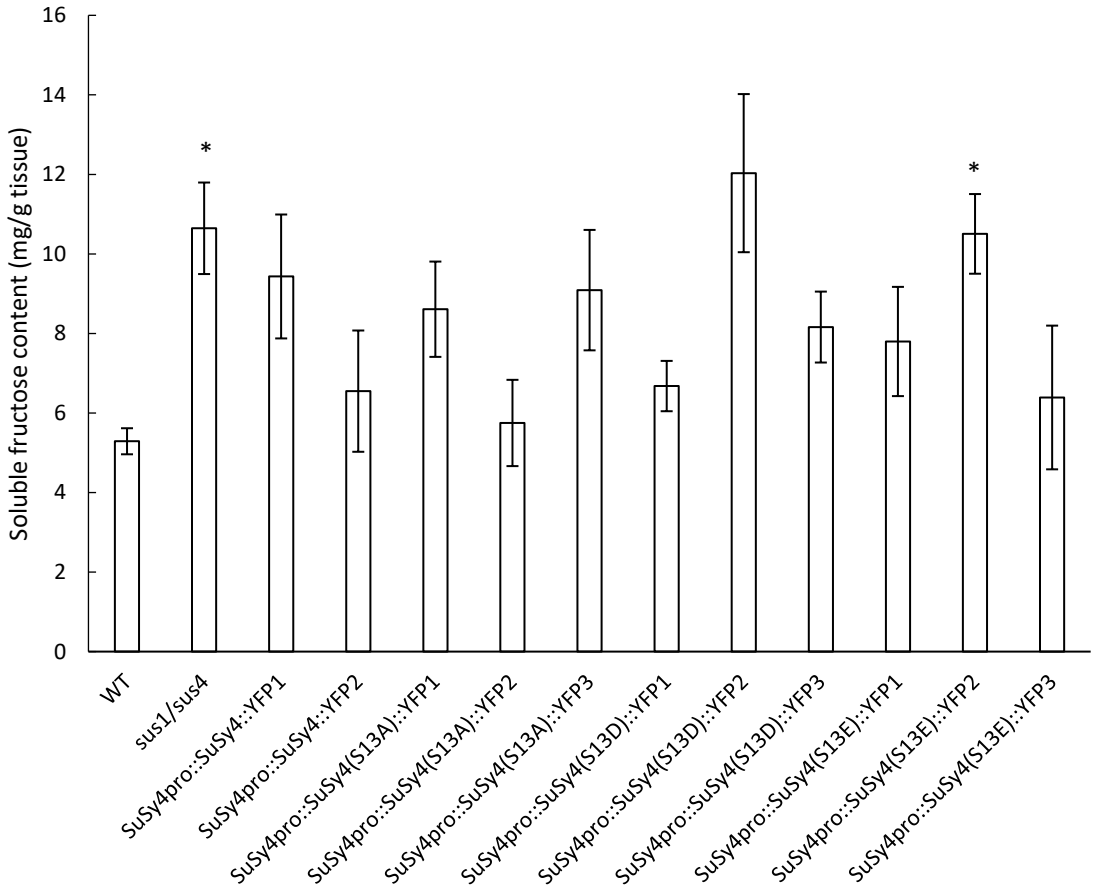

Figure 5.4 Leaf soluble fructose content of 4-week-old WT, *sus1/sus4*, SuSy4-YPF transgenic lines (*SuSy4$_{pro}$::SuSy4::YFP)*, SuSy4 phosphoresistant (*SuSy4$_{pro}$::SuSy4(S13A)::YFP*) and phosphomimetic (*SuSy4$_{pro}$::SuSy4(S13E)::YFP* and *SuSy4$_{pro}$::SuSy4(S13D)::YFP*) transgenic lines after five days flooding. Data are means ± SE calculated from at least 4 individual plants per line. Asterisks indicate significant difference (* *p*-value < 0.1) from WT plants using a Benjamini-Hochberg corrected Student *t*-test.

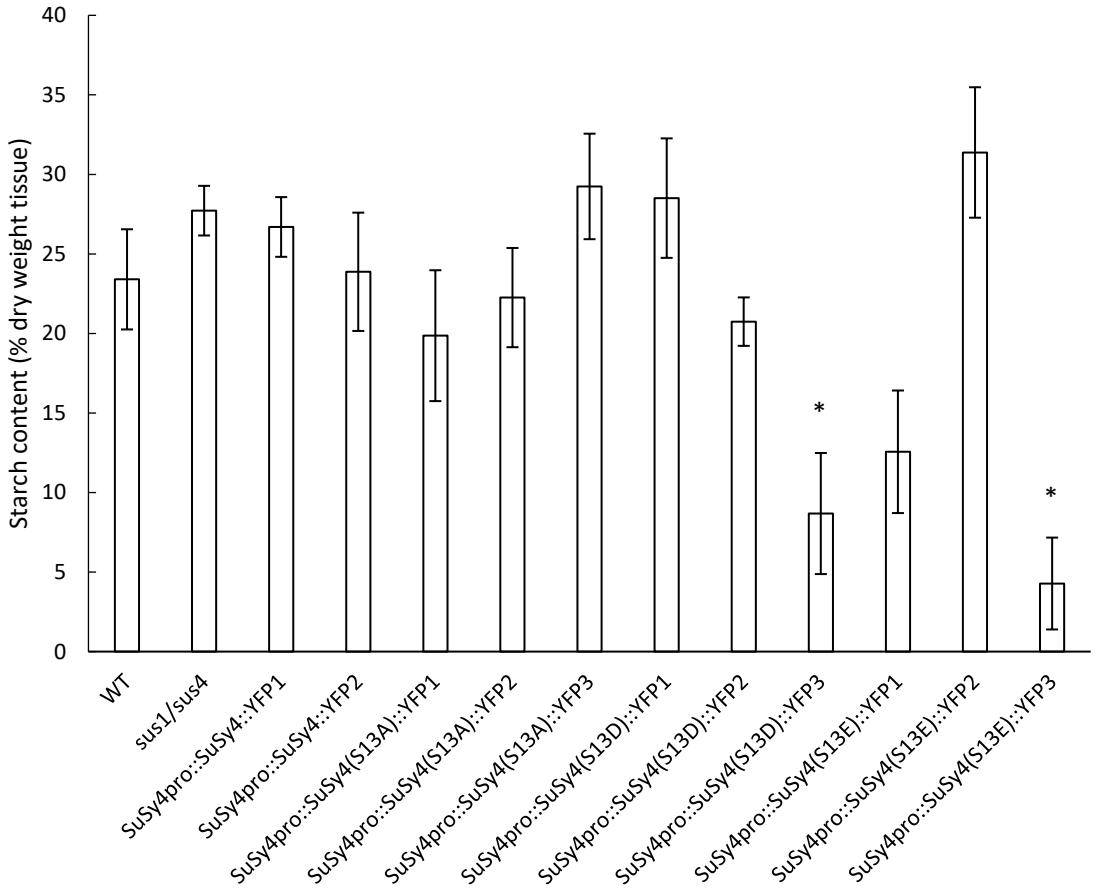

Figure 5.5 Leaf starch content of 4-week-old WT, *sus1/sus4*, , SuSy4-YPF transgenic lines (*SuSy4$_{pro}$::SuSy4::YFP)*, SuSy4 phosphoresistant (*SuSy4$_{pro}$::SuSy4(S13A)::YFP*) and phosphomimetic (*SuSy4$_{pro}$::SuSy4(S13E)::YFP* and *SuSy4$_{pro}$::SuSy4(S13D)::YFP*) transgenic lines after five days flooding. Data are means ± SE calculated from at least 4 individual plants per line. Asterisks indicate significant difference (* *p*-value < 0.1) from WT plants using a Benjamini-Hochberg corrected Student *t*-test.

5.4 Discussion

The results obtained in this study indicate that subcellular localization of the YFP fusions of phosphomimetic and phosphoresistant SuSy4 was not different from native SuSy4. Longitudinal sections of leaf petiole showed that SuSy4-YFP fusions were largely present in the cytoplasm of companion cells in all the transgenic lines including *SuSy4$_{pro}$::SuSy4::YFP*, *SuSy4$_{pro}$::SuSy4(S13A)::YFP*, *SuSy4$_{pro}$::SuSy4(S13E)::YFP* or *SuSy4$_{pro}$::SuSy4(S13D)::YFP*. Our observations suggest that phosphorylation of Ser-13 seems to have no effect on the membrane association of *Arabidopsis* SuSy4. These results are consistent with the study of Fedosejevs et al. (2014), who reported that *in planta* phosphorylation of castor oil seed SuSy did not influence its association with micromembrane. In addition, it has also been shown that SuSy subcellular localization and association to membrane were generally unrelated to phosphorylation status in cultured cells of sycamore maple (*Acer pseudoplatanus*; Pozueta-Romero et al., 2004). However, our results contrast previous reports from Winter et al. (1997) and Zhang et al. (1999), who proposed that reversible phosphorylation of SuSy may change its surface hydrophobicity and ultimately determine its membrane-binding capacity. This does not appear to be the case with AtSuSy4, but the other isoforms have not been tested.

Our data examining leaf soluble sugar and starch content after flooding indicate that transgenic lines carrying phosphoresistant SuSy4 were not obviously different from SuSy4-YFP complemented lines. In contrast, significantly reduced soluble glucose, sucrose and starch content were observed in the rosette leaves of transgenic lines containing phosphomimetic SuSy4. It remains possible that SuSy4 activity was stimulated by mimicking phosphorylation at the Ser-13

residue, which could promote the efficiency of sugar loading and transportation in leaf tissue under hypoxic conditions. Therefore, the accumulation of carbohydrate was reduced in both *SuSy4$_{pro}$::SuSy4(S13D)::YFP* and *SuSy4$_{pro}$::SuSy4(S13E)::YFP* mutant lines. Consistently, Hardin et al. (2004) showed that *in vitro* phosphorylation of maize SuSy protein promoted its catalytic activity. Similar results were shown by Nakai et al. (1998), who suggested that the introduction of an acid substitution at Ser-11 resulted in high catalytic efficiency of recombinant mung bean SuSy (S11E and S11D). In this study, I have only altered the phosphorylation status of Ser-13. There may be other phosphorylation sites that need to be investigated independently or together with Ser-13 to draw any firm conclusion regarding the role of phosphorylation and membrane association.

Chapter 6: Conclusion

6.1 Thesis summary

SuSy is one of two enzymes that catalytically cleaves sucrose. In higher plants, it has been proposed to serve different functional roles in metabolism, including modulating sink strength and phloem loading, and facilitating the biosynthesis of starch and cell-wall polymers. The underlying hypothesis is that plasma membrane-localized SuSy could tightly associate with cellulose synthase complex to channel UDP-glucose derived from sucrose directly to cellulose biosynthesis. Although many studies examining poplar wood and cotton fiber development support this model, direct evidence of a true interaction between SuSy and CesA is still lacking, and SuSy has been shown not to be necessary for cellulose production in *Arabidopsis* (Amor et al., 1995; Haigler et al., 2001; Song et al., 2010; Barratt et al., 2009). The primary goal of this project was to investigate the proposed model of cellulose biosynthesis using the model plant *Arabidopsis*. More specifically, this thesis attempts to examine the spatiotemporal localization of all six isoforms of *Arabidopsis* SuSy and their possible contribution to cellulose synthesis. To achieve this goal, my research was divided into three main studies:

In Chapter 2, I demonstrated that in *Arabidopsis* SuSy1 and SuSy4 were not directly involved in cellulose biosynthesis as the model suggested, and instead appear to be important for phloem loading and unloading. In *Arabidopsis*, six SuSy genes are grouped into three pairs of similar isoforms (Baud et al., 2004). Initially, real-time quantitative studies showed that *SuSy1* and *SuSy4* were most highly expressed in developing stems, which contain a large portion of fibers and are

therefore a useful model system to study cellulose synthesis. As such, I characterized *sus1/sus4* double knock out mutants and confirmed no obvious phenotype excepted for mild chlorosis under well-aerated conditions. However, after five days flooding, *sus1/sus4* mutant showed a reduced growth rate and elevated soluble sugar and starch content, consistent with the study of Bieniawask et al. (2007). I then proceeded to clone these two *SuSy* isoforms and generate YFP-fusions. With the VND7 inducible system developed by Yamaguchi et al. (2010), I was able to visualize the proteins participating in secondary cell wall thickening in protoxylem tracheary elements. Constructs containing SuSy-YFP fusions were transformed into both *sus1/sus4* double mutant and VND7 inducible plants. Here, I demonstrated that no YFP signal was detected in developing protoxylem tracheary elements during cellulose deposition, in contrast to what would be expected of proteins proposed to be involved in cellulose deposition. Additionally, visualization of SuSy1 and SuSy4 indicated that they were not present in xylem tissue in a series of plant organs, including stems, roots, petioles, and siliques. In contrast, live-cell imaging clearly showed that SuSy1 and SuSy4 were specifically localized to phloem companion cells, and SuSy-YFP fusions were observed to be streaming in the cytoplasm. To further confirm the identity of companion cells, I employed aniline blue staining to specifically label the callose-enriched sieve plates of sieve elements. Together, these results suggest that AtSuSy1 and AtSuSy4 are probably involved in phloem loading, not cellulose synthesis.

To examine the possibility that the other *Arabidopsis* SuSy isoforms are participating in cellulose synthesis, further studies (Chapter 3) to investigate the spatiotemporal localization and functional roles of AtSuSy2, AtSuSy3, AtSuSy5 and AtSuSy6 were conducted. To achieve this, I inserted

the coding sequence of these four SuSy into YFP fused constructs driven by their respective SuSy promoters. All constructs were independently transformed into WT plants and the spatiotemporal distributions of SuSy-YFP fusions were subsequently analyzed by confocal microscopy. Live-cell imaging clearly showed that none of the four SuSy-YFP proteins were detectable in the developing xylem tissue of organs examined, indicating that these isoforms are not directly involved in cellulose biosynthesis as the existing models imply. In contrast, *Arabidopsis* SuSy5 and SuSy6 were exclusively localized to phloem sieve elements, which is consistent with the results from the previous study of Barratt et al. (2009). This finding was confirmed by aniline blue staining that labels the callose-enriched sieve plate. By examining the subcellular localization, my studies illustrated that YFP fusions of SuSy5 and SuSy6 were parietally positioned along the entire sieve element and largely accumulated as immobile puncta. Employing the styryl dye FM4-64, which specifically labels the plasma membrane, SuSy5 and SuSy6 were shown to be restricted to the inner side of the plasma membrane, indicating a cytoplasmic localization. This observation could be explained by the ultrastructure of a sieve element reported by Froelich et al. (2011), who demonstrated that organelles in a sieve element are usually embedded in an amorphous ground matrix at the margin of the cells. Therefore, my results suggested that SuSy5 and SuSy6 were probably trapped in this parietal protein layer and likely to facilitate callose synthesis or osmotic adjustment specifically in sieve elements. In addition, a sucrose transporter, AtSUC3, has been identified in the phloem sieve elements and proposed to be responsible for the retrieval of sucrose during phloem transport (Meyer et al., 2004). Thus, I postulate that SuSy5 and SuSy6 are involved in providing energy for this described sucrose retrieval.

Though SuSy2 and SuSy3 were not detectable in the vasculature of every organ examined, they have been reported to be highly expressed in defined phases of seed development (Bieniawska et al., 2007; Fallahi et al., 2008; Nunez et al., 2008). To test this, the spatiotemporal localization of these two isoforms in seeds was investigated via live-cell imaging. I found that SuSy2 was localized to the endosperm and embryo at the early maturation stage, but not detected in the epidermal cells of the seed coat. Similarly, SuSy3 was highly expressed in the embryo in the late maturation phase. The YFP signal associated with SuSy3 was also identified in the phloem of seedling roots as well as the guard cells of leaf stomata. Further studies investigating the subcellular localization of these two isoforms showed that SuSy2 and SuSy3 were largely present in the cytoplasm. These results suggest that SuSy2 and SuSy3 are involved in seed development.

To confirm the results of live-cell imaging, I carried out immunofluorescent labelling on WT *Arabidopsis* using a SuSy-specific immune serum. First, I tested the cross-reactivity of this SuSy serum against total proteins extracted from *Arabidopsis* leaves and stems. Only a single band at the predicted size was apparent, indicating that this serum was not binding to other proteins. Immunolocalization on stem and leaf petiole cross-sections was subsequently performed and the results showed that SuSy was detected in phloem tissue, agreeing with live-cell imaging data. Given these results, I hypothesize that the putative model implicating SuSy in cellulose biosynthesis does not exist in *Arabidopsis*, but may in other species that have a sink-driven process and accumulate significant quantities of cellulose.

The data presented in the previous chapters indicated that four isoforms of *Arabidopsis* SuSy (SuSy1, SuSy4, SuSy5 and SuSy6) were confined to the phloem tissue where they may play a role in phloem loading or sucrose retrieval. Previous studies failed to find an obvious phenotype of double knock out mutants of *sus1/sus4* and *sus5/sus6* when grown under normal conditions (Bieniawska et al., 2007). This observation may be due to the fact that these four proteins are functionally redundant in *Arabidopsis*. Therefore, I hypothesized that a mutant lacking all these four SuSy isoforms might exhibit an obvious growth defect. To test this, in Chapter 4, I created *sus1/sus4/sus5/sus6* homozygous quadruple mutant plants and carried out a series of phenotypic characterizations. I generated the quadruple mutant of *sus1/sus4/sus5/sus6* by crossing T-DNA insertion homozygous lines of *sus1/sus4* with *sus5/sus6*. Employing specific primers, mutant plants were selected and confirmed by PCR genotyping. Subsequently, I characterized several aspects of growth and development of *sus1/sus4/sus5/sus6* mutant in comparison with WT, and the double mutant lines, *sus1/sus4* and *sus5/sus6* plants. Surprisingly, results showed that the *sus1/sus4/sus5/sus6* mutant was not significantly different from WT plants when examining rosette leaf size, inflorescence stem height, dry seed weight, and cell wall morphology and thickness. In addition, no obvious difference in soluble sugar content was observed between *sus1/sus4/sus5/sus6* and WT plants with or without flooding. These results suggest that when SuSy activity is lacking in phloem tissue, induced INV activity in the quadruple mutant may compensate for the loss of SuSy activity. Therefore, further investigations were carried out to examine the response of *sus1/sus4/sus5/sus6* seedlings to sugar availability and osmotic stress. Our results showed that *sus1/sus4/sus5/sus6*, *sus1/sus4*, and *sus5/sus6* mutants exhibited reduced seedling growth compared to WT plants when treated with high concentration of sucrose. Quadruple

seedlings displayed the smallest seedling size. In addition, no growth difference of seedlings was observed in plates supplied with 3% mannitol. These data together suggested that the reduced seedling growth of *sus1/sus4/sus5/sus6*, *sus1/sus4*, and *sus5/sus6* may possibly be due to the inhibited phloem function in mutants lacking SuSy activity.

Phosphorylation has been proposed to be a determining factor influencing SuSy subcellular localization and activity (Winter et al., 1997; Nakai et al., 1998; Zhang et al., 1999; Hardin et al., 2004; Pozueta-Romero et al., 2004). To test this, site-directed mutagenesis was employed to modify the phosphorylation status of AtSuSy4. Specifically, the Ser-13 residue of SuSy4 was substituted with negatively charged aspartic acid (D) and glutamic acid (E) to mimic phosphorylation, or the neutral amino acid alanine (A) to inhibit phosphorylation. Modified SuSy-YFP fusion constructs were subsequently generated and transformed into *sus1/sus4* double mutant plants. Subcellular localization of phosphomimetic and phosphoresistant SuSy4 was then investigated using a confocal microscope and live-cell imaging indicated that YFP signal of both phosphomimetic and phosphoresistant SuSy4 was still largely confined to the cytoplasm of companion cells. In addition, analysis of soluble sugar and starch content of the rosette leaves after five days flooding treatment showed that the transgenic lines containing phosphoresistant SuSy4 were not obviously different from SuSy4-YFP complemented lines. In contrast, significantly reduced soluble glucose, sucrose and starch content was observed in transgenic lines carrying phosphomimetic SuSy when compared to WT plants. Therefore, I postulate that phosphorylation probably does not affect the membrane-association of AtSuSy4, but may stimulate its functional properties.

6.2 Future work

Fundamentally, results from this thesis contribute to our understanding of the functionality of the six *Arabidopsis* SuSy isoforms. This work suggests that the predominant role of SuSy in *Arabidopsis* is to supply energy for phloem loading, not directly contribute UDP-glucose for cellulose synthesis. Several additional questions have been generated based on the findings of this work and future research prospects are listed below:

6.2.1 Using a soybean-SuSy immune serum to investigate the spatial localization of sucrose synthase in poplar

Although my research could not detect any SuSy protein in xylem tissue of *Arabidopsis*, previous findings have indicated that there is not only SuSy protein in the xylem but also it can be plasma-membrane-localized, where it could provide substrate precursors to support a high rate of cellulose biosynthesis, such as in developing cotton fiber and poplar xylem (Amor et al., 1995; Song et al., 2010). Therefore, there is a possibility that *Arabidopsis* is different from some of the other plant species. As such, an investigation of the spatial localization of SuSy in species like poplar should be a natural progression. Immunofluorescent experiments with *Arabidopsis* stems and leaves in Chapter 3 showed strong fluorescence in xylem tissue because of non-specific binding to the secondary cell wall. Thus, a tissue printing technique could be employed as it is simple and could avoid this artifact (McClure and Guilfoyle, 1989; Taylor et al., 1993).

6.2.2 Examining the expression level of secondary CesAs in the tissues used for SuSy live-cell imaging

Data presented in this thesis (Chapter 2 and Chapter 3) showed a lack of SuSy signal in xylem tissue. This could be due to the slowing of cellulose synthesis when xylem is mature. This discrepancy could be resolved by examining if the CesA proteins are still being expressed. To achieve this, future work should analyze the transcript level or protein abundance of secondary CesAs and SuSy in the same tissues used for live-cell imaging. Real-time quantitative PCR with gene-specific primers could be used to check transcript abundance while western blotting using specific SuSy and CesA antibodies could be employed to check the protein abundance in the tissues.

6.2.3 Using poplar SuSy promoter to drive the expression of *Arabidopsis* SuSy

Recent studies have identified isoforms of poplar SuSy in developing xylem and mature xylem tissues (Zhang et al., 2011; Sundell et al., 2017). For instance, PtSuSy1 and PtSuSy2, the homologs of AtSuSy1 and AtSuSy4, have been shown to be abundantly present in developing xylem tissues according to the RNA sequencing data. This distinct expression pattern of poplar SuSy is likely driven by the native promoters. Thus, future work could perform some analyses of sequences comparing AtSuSy and PtSuSy promoters. In addition, a promoter swap study could be conducted where the PtSuSy1 or PtSuSy2 could be used to direct the expression of *Arabidopsis* SuSy genes and analyze their spatial localization in *Arabidopsis*. Specifically, AtSuSy promoters in the YFP fusion constructs (Chapter 2 and Chapter 3) could be replaced by the poplar SuSy promoters and the YFP signal are subsequently investigated via the same live-cell imaging used in this thesis.

6.2.4 Analysis of *Arabidopsis* mutants lacking invertase activity

Sucrose synthase has generally been considered to be more important than invertases in catalyzing the entry of carbon into plant carbohydrate metabolism. However, previous studies and the results shown in Chapter 4 have clearly demonstrated that SuSy does not impact the normal growth and development of *Arabidopsis*. In contrast, invertases would therefore have to be the dominant route for sucrose catabolism. In *Arabidopsis*, the functionality of neutral and alkaline invertases is not well known yet despite a relatively mild phenotype has been observed in *CINV1* mutants (Lou et al., 2007; Qi et al., 2007). Plants lacking two (*CINV1* and *CINV2*) of the nine neutral and alkaline invertase isoforms, however, exhibited severe growth defects, such as dramatic growth retardation, and abnormal extension and expansion of root growth (Barratt et al., 2009). Therefore, future work could include phenotypic analysis of *Arabidopsis* mutant lines missing other isoforms of the neutral and alkaline invertase family. Single mutant lines of neutral and alkaline invertases could be obtained from *Arabidopsis* stock banks and double knock mutants could be generated by crossing individual single mutant lines. Understanding the functional roles of INVs in carbon allocation and metabolism of *Arabidopsis* may help to explain the lack of obvious phenotype in the SuSy quadruple mutant.

References

Albrecht, G., and Mustroph, A. (2003). Localization of sucrose synthase in wheat roots: increased in situ activity of sucrose synthase correlates with cell wall thickening by cellulose deposition under hypoxia. Planta **217,** 252-260.

Amor, Y., Haigler, C.H., Johnson, S., Wainscott, M., and Delmer, D.P. (1995). A membrane-associated form of sucrose synthase and its potential role in synthesis of cellulose and callose in plants. Proceedings of the National Academy of Sciences of the United States of America **92,** 9353-9357.

Angeles-Nunez, J.G., and Tiessen, A. (2010). Arabidopsis sucrose synthase 2 and 3 modulate metabolic homeostasis and direct carbon towards starch synthesis in developing seeds. Planta **232,** 701-718.

Ardito, F., Giuliani, M., Perrone, D., Troiano, G., and Lo Muzio, L. (2017). The crucial role of protein phosphorylation in cell signaling and its use as targeted therapy. International Journal of Molecular Medicine **40,** 271-280.

Asano, T., Kunieda, N., Omura, Y., Ibe, H., Kawasaki, T., Takano, M., Sato, M., Furuhashi, H., Mujin, T., Takaiwa, F., Wu, C.Y., Tada, Y., Satozawa, T., Sakamoto, M., and Shimada, H. (2002). Rice SPK, a calmodulin-like domain protein kinase, is required for storage product accumulation during seed development: phosphorylation of sucrose synthase is a possible factor. The Plant Cell **14,** 619-628.

Azama, K., Abe, S., Sugimoto, H., and Davis, E. (2003). Lysine-containing proteins in maize endosperm: a major contribution from cytoskeleton-associated carbohydrate-metabolizing enzymes. Planta **217,** 628-638.

Bai, W.Q., Xiao, Y.H., Zhao, J., Song, S.Q., Hu, L., Zeng, J.Y., Li, X.B., Hou, L., Luo, M., Li, D.M., and Pei, Y. (2014). Gibberellin overproduction promotes sucrose synthase expression and secondary cell wall deposition in cotton fibers. PloS ONE **9,** e96537.

Barnes, W.J., and Anderson, C.T. (2018). Cytosolic invertases contribute to cellulose biosynthesis and influence carbon partitioning in seedlings of Arabidopsis thaliana. The Plant Journal **94,** 956-974.

Barnett, J.R., and Bonham, V.A. (2004). Cellulose microfibril angle in the cell wall of wood fibres. Biological Reviews of the Cambridge Philosophical Society **79,** 461-472.

Baroja-Fernandez, E., Munoz, F.J., Montero, M., Etxeberria, E., Sesma, M.T., Ovecka, M., Bahaji, A., Ezquer, I., Li, J., Prat, S., and Pozueta-Romero, J. (2009). Enhancing sucrose synthase activity in transgenic potato (Solanum tuberosum L.) tubers results in increased levels of starch, ADPglucose and UDPglucose and total yield. Plant and Cell Physiology **50,** 1651-1662.

Barratt, D.H., Derbyshire, P., Findlay, K., Pike, M., Wellner, N., Lunn, J., Feil, R., Simpson, C., Maule, A.J., and Smith, A.M. (2009). Normal growth of Arabidopsis requires cytosolic invertase but not sucrose synthase. Proceedings of the National Academy of Sciences of the United States of America **106,** 13124-13129.

Barratt, D.H.P., Kolling, K., Graf, A., Pike, M., Calder, G., Findlay, K., Zeeman, S.C., and Smith, A.M. (2011). Callose synthase GSL7 Is necessary for normal phloem transport and inflorescence growth in Arabidopsis. Plant Physiology **155,** 328-341.

Barrero-Sicilia, C., Hernando-Amado, S., Gonzalez-Melendi, P., and Carbonero, P. (2011). Structure, expression profile and subcellular localisation of four different sucrose synthase genes from barley. Planta **234,** 391-403.

Baud, S., Vaultier, M.N., and Rochat, C. (2004). Structure and expression profile of the sucrose synthase multigene family in Arabidopsis. Journal of Experimental Botany **55,** 397-409.

Baud, S., Boutin, J.P., Miquel, M., Lepiniec, L., and Rochat, C. (2002). An integrated overview of seed development in Arabidopsis thaliana ecotype WS. Plant Physiology and Biochemistry **40,** 151-160.

Baud, S., Wuilleme, S., Lemoine, R., Kronenberger, J., Caboche, M., Lepiniec, L., and Rochat, C. (2005). The AtSUC5 sucrose transporter specifically expressed in the endosperm is involved in early seed development in Arabidopsis. The Plant Journal **43,** 824-836.

Benjamini, Y., and Hochberg, Y. (1995). Controlling the false discovery rate: a practical and powerful approach to multiple testing. Journal of the Royal Statistical Society. Series B (Methodological), 289-300.

Berger, S., Papadopoulos, M., Schreiber, U., Kaiser, W., and Roitsch, T. (2004). Complex regulation of gene expression, photosynthesis and sugar levels by pathogen infection in tomato. Physiologia Plantarum **122,** 419-428.

Biemelt, S., Hajirezaei, M.R., Melzer, M., Albrecht, G., and Sonnewald, U. (1999). Sucrose synthase activity does not restrict glycolysis in roots of transgenic potato plants under hypoxic conditions. Planta **210,** 41-49.

Bieniawska, Z., Paul Barratt, D.H., Garlick, A.P., Thole, V., Kruger, N.J., Martin, C., Zrenner, R., and Smith, A.M. (2007). Analysis of the sucrose synthase gene family in Arabidopsis. The Plant Journal **49,** 810-828.

Bologa, K.L., Fernie, A.R., Leisse, A., Loureiro, M.E., and Geigenberger, P. (2003). A bypass of sucrose synthase leads to low internal oxygen and impaired metabolic performance in growing potato tubers. Plant Physiology **132,** 2058-2072.

Bolte, S., Talbot, C., Boutte, Y., Catrice, O., Read, N.D., and Satiat-Jeunemaitre, B. (2004). FM-dyes as experimental probes for dissecting vesicle trafficking in living plant cells. Journal of Microscopy-Oxford **214,** 159-173.

Braun, D.M., Wang, L., and Ruan, Y.L. (2014). Understanding and manipulating sucrose phloem loading, unloading, metabolism, and signalling to enhance crop yield and food security. Journal of Experimental Botany **65,** 1713-1735.

Brill, E., van Thournout, M., White, R.G., Llewellyn, D., Campbell, P.M., Engelen, S., Ruan, Y.L., Arioli, T., and Furbank, R.T. (2011). A novel isoform of sucrose synthase is targeted to the cell wall during secondary cell wall synthesis in cotton fiber. Plant Physiology **157,** 40-54.

Cai, G., Faleri, C., Del Casino, C., Emons, A.M., and Cresti, M. (2011). Distribution of callose synthase, cellulose synthase, and sucrose synthase in tobacco pollen tube is controlled in dissimilar ways by actin filaments and microtubules. Plant Physiology **155,** 1169-1190.

Canam, T., Park, J.-Y., Yu, K.Y., Campbell, M.M., Ellis, D.D., and Mansfield, S.D. (2006). Varied growth, biomass and cellulose content in tobacco expressing yeast-derived invertases. Planta **224,** 1315-1327.

Carlson, S.J., and Chourey, P.S. (1996). Evidence for plasma membrane-associated forms of sucrose synthase in maize. Molecular Genetics and Genomics **252,** 303-310.

Carlson, S.J., Chourey, P.S., Helentjaris, T., and Datta, R. (2002). Gene expression studies on developing kernels of maize sucrose synthase (SuSy) mutants show evidence for a third SuSy gene. Plant Molecular Biology **49,** 15-29.

Carpaneto, A., Geiger, D., Bamberg, E., Sauer, N., Fromm, J., and Hedrich, R. (2005). Phloem-localized, proton-coupled sucrose carrier ZmSUT1 mediates sucrose efflux under the control of the sucrose gradient and the proton motive force. The Journal of Biological Chemistry **280,** 21437-21443.

Carpita, N.C. (2011). Update on mechanisms of plant cell wall biosynthesis: how plants make cellulose and other (1->4)-beta-D-glycans. Plant Physiology **155,** 171-184.

Cayla, T., Batailler, B., Le Hir, R., Revers, F., Anstead, J.A., Thompson, G.A., Grandjean, O., and Dinant, S. (2015). Live imaging of companion cells and sieve elements in Arabidopsis leaves. PloS ONE **10,** e0118122.

Chaiwongsar, S., Strohm, A.K., Su, S.H., and Krysan, P.J. (2012). Genetic analysis of the Arabidopsis protein kinases MAP3K epsilon 1 and MAP3K epsilon 2 indicates roles in cell expansion and embryo development. Frontiers in Plant Science **3**.

Chen, A.Q., He, S., Li, F.F., Li, Z., Ding, M.Q., Liu, Q.P., and Rong, J.K. (2012). Analyses of the sucrose synthase gene family in cotton: structure, phylogeny and expression patterns. BMC Plant Biology **12**.

Cheng, W.H., Taliercio, E.W., and Chourey, P.S. (1996). The Miniature1 seed locus of maize encodes a cell wall invertase required for normal development of endosperm and maternal cells in the pedicel. The Plant Cell **8,** 971-983.

Chopra, J., Kaur, N., and Gupta, A. (2005). Role of enzymes of sucrose-starch conversion in seed sink strength in mung bean. Biologia Plantarum **49,** 561-566.

Chourey, P.S., Taliercio, E.W., Carlson, S.J., and Ruan, Y.L. (1998). Genetic evidence that the two isozymes of sucrose synthase present in developing maize endosperm are critical, one for cell wall integrity and the other for starch biosynthesis. Molecular Genetics and Genomics **259,** 88-96.

Coleman, H.D., Yan, J., and Mansfield, S.D. (2009). Sucrose synthase affects carbon partitioning to increase cellulose production and altered cell wall ultrastructure. Proceedings of the National Academy of Sciences of the United States of America **106,** 13118-13123.

Cosgrove, D.J. (2005). Growth of the plant cell wall. Nature Reviews. Molecular Cell Biology **6,** 850-861.

Cosgrove, D.J., and Jarvis, M.C. (2012). Comparative structure and biomechanics of plant primary and secondary cell walls. Frontiers in Plant Science **3,** 204.

Craig, J., Barratt, P., Tatge, H., Dejardin, A., Handley, L., Gardner, C.D., Barber, L., Wang, T., Hedley, C., Martin, C., and Smith, A.M. (1999). Mutations at the rug4 locus alter the carbon and nitrogen metabolism of pea plants through an effect on sucrose synthase. Plant Journal **17,** 353-362.

Cronshaw, J. (1981). Phloem structure and function. Annual Review of Plant Physiology **32,** 465-484.

D'Aoust, M.A., Yelle, S., and Nguyen-Quoc, B. (1999). Antisense inhibition of tomato fruit sucrose synthase decreases fruit setting and the sucrose unloading capacity of young fruit. The Plant Cell **11,** 2407-2418.

Daloso, D.M., Williams, T.C.R., Antunes, W.C., Pinheiro, D.P., Muller, C., Loureiro, M.E., and Fernie, A.R. (2016). Guard cell-specific upregulation of sucrose synthase 3 reveals that the role of sucrose in stomatal function is primarily energetic. New Phytologist **209,** 1470-1483.

da Silva, P.M.F.R., Eastmond, P.J., Hill, L.M., Smith, A.M., and Rawsthorne, S. (1997). Starch metabolism in developing embryos of oilseed rape. Planta **203,** 480-487.

Davies, C., and Robinson, S.P. (1996). Sugar accumulation in grape berries. Cloning of two putative vacuolar invertase cDNAs and their expression in grapevine tissues. Plant Physiology **111,** 275-283.

Déjardin , A., Sokolov, L.N., and Kleczkowski, L.A. (1999). Sugar/osmoticum levels modulate differential abscisic acid-independent expression of two stress-responsive sucrose synthase genes in Arabidopsis. Biochemical Journal **344,** 503-509.

Delmer, D.P. (1999). Cellulose biosynthesis: exciting times for a difficult field of study. Annual Review of Plant Biology **50,** 245-276.

Desprez, T., Juraniec, M., Crowell, E.F., Jouy, H., Pochylova, Z., Parcy, F., Hofte, H., Gonneau, M., and Vernhettes, S. (2007). Organization of cellulose synthase complexes involved in primary cell wall synthesis in Arabidopsis thaliana. Proceedings of the National Academy of Sciences of the United States of America **104,** 15572-15577.

Duncan, K.A., and Huber, S.C. (2007). Sucrose synthase oligomerization and F-actin association are regulated by sucrose concentration and phosphorylation. Plant and Cell Physiology **48,** 1612-1623.

Duncan, K.A., Hardin, S.C., and Huber, S.C. (2006). The three maize sucrose synthase Isoforms differ in distribution, localization, and phosphorylation. Plant and Cell Physiology **47,** 959-971.

Edwards, K., Johnstone, C., and Thompson, C. (1991). A simple and rapid method for the preparation of plant genomic DNA for PCR analysis. Nucleic Acids Research **19,** 1349.

Eklof, J.M., and Brumer, H. (2010). The XTH gene family: an update on enzyme structure, function, and phylogeny in xyloglucan remodeling. Plant Physiology **153,** 456-466.

Endler, A., and Persson, S. (2011). Cellulose synthases and synthesis in Arabidopsis. Molecular Plant **4,** 199-211.

Esau, K. (1969). The phloem.

Eschrich, W. (1975). Sealing systems in phloem. Transport in Plants I (Springer), pp. 39-56.

Eschrich, W. (1980). Free space invertase, its possible role in phloem unloading. Berichte Der Deutschen Botanischen Gesellschaft **93,** 363-378.

Etxeberria, E., and Gonzalez, P. (2003). Evidence for a tonoplast-associated form of sucrose synthase and its potential involvement in sucrose mobilization from the vacuole. Journal of Experimental Botany **54,** 1407-1414.

Evert, R.F., and Derr, W.F. (1964). Callose substance in sieve elements. American Journal of Botany **51,** 552-559.

Fait, A., Angelovici, R., Less, H., Ohad, I., Urbanczyk-Wochniak, E., Fernie, A.R., and Galili, G. (2006). Arabidopsis seed development and germination is associated with temporally distinct metabolic switches. Plant Physiology **142,** 839-854.

Fallahi, H., Scofield, G.N., Badger, M.R., Chow, W.S., Furbank, R.T., and Ruan, Y.L. (2008). Localization of sucrose synthase in developing seed and siliques of Arabidopsis thaliana reveals diverse roles for SUS during development. Journal of Experimental Botany **59,** 3283-3295.

Fedosejevs, E.T., Ying, S., Park, J., Anderson, E.M., Mullen, R.T., She, Y.M., and Plaxton, W.C. (2014). Biochemical and molecular characterization of RcSUS1, a cytosolic sucrose synthase phosphorylated in vivo at serine 11 in developing castor oil seeds. The Journal of Biological Chemistry **289,** 33412-33424.

Fedosejevs, E.T., Gerdis, S.A., Ying, S., Pyc, M., Anderson, E.M., Snedden, W.A., Mullen, R.T., She, Y.M., and Plaxton, W.C. (2016). The calcium-dependent protein kinase RcCDPK2 phosphorylates sucrose synthase at Ser11 in developing castor oil seeds. The Biochemical Journal **473,** 3667-3682.

Fernandes, A.N., Thomas, L.H., Altaner, C.M., Callow, P., Forsyth, V.T., Apperley, D.C., Kennedy, C.J., and Jarvis, M.C. (2011). Nanostructure of cellulose microfibrils in spruce wood. Proceedings of the National Academy of Sciences of the United States of America **108,** E1195-1203.

Fowler, S., and Thomashow, M.F. (2002). Arabidopsis transcriptome profiling indicates that multiple regulatory pathways are activated during cold acclimation in addition to the CBF cold response pathway. The Plant Cell **14,** 1675-1690.

Frankova, L., and Fry, S.C. (2013). Biochemistry and physiological roles of enzymes that cut and paste plant cell-wall polysaccharides. Journal of Experimental Botany **64,** 3519-3550.

Froelich, D.R., Mullendore, D.L., Jensen, K.H., Ross-Elliott, T.J., Anstead, J.A., Thompson, G.A., Pelissier, H.C., and Knoblauch, M. (2011). Phloem ultrastructure and pressure flow: Sieve-Element-Occlusion-Related agglomerations do not affect translocation. The Plant Cell **23,** 4428-4445.

Fry, S.C. (2011). Plant cell walls. From chemistry to biology (Oxford University Press).

Fujii, S., Hayashi, T., and Mizuno, K. (2010). Sucrose synthase is an integral component of the cellulose synthesis machinery. Plant and Cell Physiology **51,** 294-301.

Gerber, L., Zhang, B., Roach, M., Rende, U., Gorzsas, A., Kumar, M., Burgert, I., Niittyla, T., and Sundberg, B. (2014). Deficient sucrose synthase activity in developing wood does not specifically affect cellulose biosynthesis, but causes an overall decrease in cell wall polymers. New Phytologist **203,** 1220-1230.

Goetz, M., Godt, D.E., Guivarc'h, A., Kahmann, U., Chriqui, D., and Roitsch, T. (2001). Induction of male sterility in plants by metabolic engineering of the carbohydrate supply. Proceedings of the National Academy of Sciences of the United States of America **98,** 6522-6527.

Gottwald, J.R., Krysan, P.J., Young, J.C., Evert, R.F., and Sussman, M.R. (2000). Genetic evidence for the in planta role of phloem-specific plasma membrane sucrose transporters. Proceedings of the National Academy of Sciences of the United States of America **97,** 13979-13984.

Greiner, S., Rausch, T., Sonnewald, U., and Herbers, K. (1999). Ectopic expression of a tobacco invertase inhibitor homolog prevents cold-induced sweetening of potato tubers. Nature Biotechnology **17,** 708-711.

Guglielminetti, L., Perata, P., and Alpi, A. (1995). Effect of anoxia on carbohydrate-metabolism in rice seedlings. Plant Physiology **108,** 735-741.

Haigler, C., and Brown, R. (1986). Transport of rosettes from the Golgi apparatus to the plasma membrane in isolated mesophyll cells of Zinnia elegans during differentiation to tracheary elements in suspension culture. Protoplasma **134,** 111-120.

Haigler, C.H., Ivanova-Datcheva, M., Hogan, P.S., Salnikov, V.V., Hwang, S., Martin, K., and Delmer, D.P. (2001). Carbon partitioning to cellulose synthesis. Plant Molecular Biology **47,** 29-51.

Hamant, O., and Traas, J. (2010). The mechanics behind plant development. The New Phytologist **185,** 369-385.

Hannah, M.A., Heyer, A.G., and Hincha, D.K. (2005). A global survey of gene regulation during cold acclimation in Arabidopsis thaliana. PLoS Genetics **1,** e26.

Hardin, S.C., Winter, H., and Huber, S.C. (2004). Phosphorylation of the amino terminus of maize sucrose synthase in relation to membrane association and enzyme activity. Plant Physiology **134,** 1427-1438.

Hardin, S.C., Tang, G.Q., Scholz, A., Holtgraewe, D., Winter, H., and Huber, S.C. (2003). Phosphorylation of sucrose synthase at serine 170: occurrence and possible role as a signal for proteolysis. Plant Journal **35,** 588-603.

Haritatos, E., Ayre, B.G., and Turgeon, R. (2000). Identification of phloem involved in assimilate loading in leaves by the activity of the galactinol synthase promoter. Plant Physiology **123,** 929-937.

Haughn, G., and Chaudhury, A. (2005). Genetic analysis of seed coat development in Arabidopsis. Trends in Plant Science **10,** 472-477.

Hayes, M.A., Davies, C., and Dry, I.B. (2007). Isolation, functional characterization, and expression analysis of grapevine (Vitis vinifera L.) hexose transporters: differential roles in sink and source tissues. Journal of Experimental Botany **58,** 1985-1997.

Hirose, T., Scofield, G.N., and Terao, T. (2008). An expression analysis profile for the entire sucrose synthase gene family in rice. Plant Science **174,** 534-543.

Huber, S.C., and Huber, J.L. (1996). Role and regulation of sucrose-phosphate synthase in higher plants. Annual Review of Plant Physiology and Plant Molecular Biology **47,** 431-444.

Huber, S.C., Huber, J.L., Liao, P.C., Gage, D.A., McMichael, R.W., Jr., Chourey, P.S., Hannah, L.C., and Koch, K. (1996). Phosphorylation of serine-15 of maize leaf sucrose synthase. Occurrence in vivo and possible regulatory significance. Plant Physiology **112,** 793-802.

Humphrey, S.J., James, D.E., and Mann, M. (2015). Protein phosphorylation: a major switch mechanism for metabolic regulation. Trends in Endocrinology and Metabolism: TEM **26,** 676-687.

Imlau, A., Truernit, E., and Sauer, N. (1999). Cell-to-cell and long-distance trafficking of the green fluorescent protein in the phloem and symplastic unloading of the protein into sink tissues. The Plant Cell **11,** 309-322.

Jia, L., Zhang, B., Mao, C., Li, J., Wu, Y., Wu, P., and Wu, Z. (2008). OsCYT-INV1 for alkaline/neutral invertase is involved in root cell development and reproductivity in rice (Oryza sativa L.). Planta **228,** 51-59.

Kang, I.H., Steffen, J.G., Portereiko, M.F., Lloyd, A., and Drews, G.N. (2008). The AGL62 MADS domain protein regulates cellularization during endosperm development in Arabidopsis. The Plant Cell **20,** 635-647.

Keegstra, K. (2010). Plant cell walls. Plant Physiology **154,** 483-486.

Kerepesi, I., and Galiba, G. (2000). Osmotic and salt stress-induced alteration in soluble carbohydrate content in wheat seedlings. Crop Science **40,** 482-487.

Kermode, A.R., Gifford, D.J., and Bewley, J.D. (1985). The role of maturation drying in the transition from seed development to germination: III. Insoluble protein synthetic pattern changes within the endosperm of Ricinus communis L. seeds. Journal of Experimental Botany **36,** 1928-1936.

Klann, E.M., Hall, B., and Bennett, A.B. (1996). Antisense acid invertase (TIV1) gene alters soluble sugar composition and size in transgenic tomato fruit. Plant Physiology **112,** 1321-1330.

Kleczkowski, L.A., Kunz, S., and Wilczynska, M. (2010). Mechanisms of UDP-glucose synthesis in plants. Critical Reviews in Plant Sciences **29,** 191-203.

Kleczkowski, L.A., Geisler, M., Ciereszko, I., and Johansson, H. (2004). UDP-glucose pyrophosphorylase. An old protein with new tricks. Plant Physiology **134,** 912-918.

Klok, E.J., Wilson, I.W., Wilson, D., Chapman, S.C., Ewing, R.M., Somerville, S.C., Peacock, W.J., Dolferus, R., and Dennis, E.S. (2002). Expression profile analysis of the low-oxygen response in Arabidopsis root cultures. The Plant Cell **14,** 2481-2494.

Knoblauch, M., and van Bel, A.J. (1998). Sieve tubes in action. The Plant Cell **10,** 35-50.

Koch, K. (1996). Carbohydrate-modulated gene expression in plants. Annual Review of Plant Biology **47,** 509-540.

Koch, K. (2004). Sucrose metabolism: regulatory mechanisms and pivotal roles in sugar sensing and plant development. Current Opinion in Plant Biology **7,** 235-246.

Komina, O., Zhou, Y., Sarath, G., and Chollet, R. (2002). In vivo and in vitro phosphorylation of membrane and soluble forms of soybean nodule sucrose synthase. Plant Physiology **129,** 1664-1673.

Konishi, T., Ohmiya, Y., and Hayashi, T. (2004). Evidence that sucrose loaded into the phloem of a poplar leaf is used directly by sucrose synthase associated with various beta-glucan synthases in the stem. Plant Physiology **134,** 1146-1152.

Krook, J., van't Slot, K.A., Vreugdenhil, D., Dijkema, C., and van der Plas, L.H. (2000). The triose-hexose phosphate cycle and the sucrose cycle in carrot (Daucus carota L.) cell suspensions are controlled by respiration and PPi: fructose-6-phosphate phosphotransferase. Journal of Plant Physiology **156,** 595-604.

Kubo, M., Udagawa, M., Nishikubo, N., Horiguchi, G., Yamaguchi, M., Ito, J., Mimura, T., Fukuda, H., and Demura, T. (2005). Transcription switches for protoxylem and metaxylem vessel formation. Genes & Development **19,** 1855-1860.

Kuhn, C., Barker, L., Burkle, L., and Frommer, W.B. (1999). Update on sucrose transport in higher plants. Journal of Experimental Botany **50,** 935-953.

Kumar, S., Stecher, G., and Tamura, K. (2016). MEGA7: molecular evolutionary genetics analysis version 7.0 for bigger datasets. Molecular Biology and Evolution **33,** 1870-1874.

Lammens, W., Le Roy, K., Schroeven, L., Van Laere, A., Rabijns, A., and Van den Ende, W. (2009). Structural insights into glycoside hydrolase family 32 and 68 enzymes: functional implications. Journal of Experimental Botany **60,** 727-740.

Lee, K.J.D., Dekkers, B.J.W., Steinbrecher, T., Walsh, C.T., Bacic, A., Bentsink, L., Leubner-Metzger, G., and Knox, J.P. (2012). Distinct cell wall architectures in seed endosperms in representatives of the brassicaceae and solanaceae. Plant Physiology **160,** 1551-1566.

Lei, L., Li, S.D., and Gu, Y. (2012). Cellulose synthase complexes: composition and regulation. Frontiers in Plant Science **3**.

Lei, L., Li, S.D., Du, J., Bashline, L., and Gu, Y. (2013). CELLULOSE SYNTHASE INTERACTIVE3 regulates cellulose biosynthesis in both a microtubule-dependent and microtubule-Independent manner in Arabidopsis. The Plant Cell **25,** 4912-4923.

Levy, M., Edelbaum, O., and Sela, I. (2004). Tobacco mosaic virus regulates the expression of its own resistance gene N. Plant Physiology **135,** 2392-2397.

Li, J., Baroja-Fernandez, E., Bahaji, A., Munoz, F.J., Ovecka, M., Montero, M., Sesma, M.T., Alonso-Casajus, N., Almagro, G., Sanchez-Lopez, A.M., Hidalgo, M., Zamarbide, M., and Pozueta-Romero, J. (2013). Enhancing sucrose synthase activity results in increased levels of starch and ADP-Glucose in maize (Zea mays L.) seed endosperms. Plant and Cell Physiology **54,** 282-294.

Lin, Y., Ulanov, A.V., Lozovaya, V., Widholm, J., Zhang, G.R., Guo, J.H., and Goodman, H.M. (2006). Genetic and transgenic perturbations of carbon reserve production in Arabidopsis seeds reveal metabolic interactions of biochemical pathways. Planta **225,** 153-164.

Liu, Y.H., Offler, C.E., and Ruan, Y.L. (2016). Cell wall invertase promotes fruit set under heat stress by suppressing ROS-independent cell death. Plant Physiology **172,** 163-180.

Lou, Y., Gou, J.Y., and Xue, H.W. (2007). PIP5K9, an Arabidopsis phosphatidylinositol monophosphate kinase, interacts with a cytosolic invertase to negatively regulate sugar-mediated root growth. The Plant Cell **19,** 163-181.

Lunn, J.E. (2016). Sucrose metabolism. In Encyclopedia of Life Science (ELS) (Chichester: John Wiley & Sons, Ltd) https://doi.org/10.1002/9780470015902.a0021259.pub2.

Marana, C., Garcia-Olmedo, F., and Carbonero, P. (1990). Differential expression of two types of sucrose synthase-encoding genes in wheat in response to anaerobiosis, cold shock and light. Gene **88,** 167-172.

Martin, T., Frommer, W.B., Salanoubat, M., and Willmitzer, L. (1993). Expression of an Arabidopsis sucrose synthase gene indicates a role in metabolization of sucrose both during phloem loading and in sink organs. Plant Journal **4,** 367-377.

Mayer, U., Ruiz, R.A.T., Berleth, T., Miséra, S., and Jürgens, G. (1991). Mutations affecting body organization in the Arabidopsis embryo. Nature **353,** 402.

McClure, B.A., and Guilfoyle, T.J. (1989). Tissue print hybridization. A simple technique for detecting organ-and tissue-specific gene expression. Plant Molecular Biology **12,** 517-524.

Meyer, S., Lauterbach, C., Niedermeier, M., Barth, I., Sjolund, R.D., and Sauer, N. (2004). Wounding enhances expression of AtSUC3, a sucrose transporter from Arabidopsis sieve elements and sink tissues. Plant Physiology **134,** 684-693.

Monaghan, J., Matschi, S., Shorinola, O., Rovenich, H., Matei, A., Segonzac, C., Malinovsky, F.G., Rathjen, J.P., MacLean, D., Romeis, T., and Zipfel, C. (2014). The calcium-dependent protein kinase CPK28 buffers plant immunity and regulates BIK1 turnover. Cell Host & Microbe **16,** 605-615.

Morey, S.R., Hirose, T., Hashida, Y., Miyao, A., Hirochika, H., Ohsugi, R., Yamagishi, J., and Aoki, N. (2018). Genetic evidence for the role of a rice vacuolar invertase as a molecular sink strength determinant. Rice **11,** 6.

Muller, K., Tintelnot, S., and Leubner-Metzger, G. (2006). Endosperm-limited Brassicaceae seed germination: abscisic acid inhibits embryo-induced endosperm weakening of Lepidium sativum (cress) and endosperm rupture of cress and Arabidopsis thaliana. Plant and Cell Physiology **47,** 864-877.

Munoz, F.J., Baroja-Fernandez, E., Moran-Zorzano, M.T., Viale, A.M., Etxeberria, E., Alonso-Casajus, N., and Pozueta-Romero, J. (2005). Sucrose synthase controls both intracellular ADP glucose levels and transitory starch biosynthesis in source leaves. Plant and Cell Physiology **46,** 1366-1376.

Murayama, S., and Handa, H. (2007). Genes for alkaline/neutral invertase in rice: alkaline/neutral invertases are located in plant mitochondria and also in plastids. Planta **225,** 1193-1203.

Nakagami, H., Sugiyama, N., Mochida, K., Daudi, A., Yoshida, Y., Toyoda, T., Tomita, M., Ishihama, Y., and Shirasu, K. (2010). Large-scale comparative phosphoproteomics identifies conserved phosphorylation sites in plants. Plant Physiology **153,** 1161-1174.

Nakai, T., Konishi, T., Zhang, X.Q., Chollet, R., Tonouchi, N., Tsuchida, T., Yoshinaga, F., Mori, H., Sakai, F., and Hayashi, T. (1998). An increase in apparent affinity for sucrose of mung bean sucrose synthase is caused by in vitro phosphorylation or directed mutagenesis of Ser11. Plant and Cell Physiology **39,** 1337-1341.

Nolte, K.D., and Koch, K.E. (1993). Companion-cell specific localization of sucrose synthase in zones of phloem loading and unloading. Plant Physiology **101,** 899-905.

Nunez, J.G.A., Kronenberger, J., Wuilleme, S., Lepiniec, L., and Rochat, C. (2008). Study of AtSUS2 localization in seeds reveals a strong association with plastids. Plant and Cell Physiology **49,** 1621-1626.

Oparka, K.J., and Turgeon, R. (1999). Sieve elements and companion cells-traffic control centers of the phloem. The Plant Cell **11,** 739-750.

Pagant, S., Bichet, A., Sugimoto, K., Lerouxel, O., Desprez, T., McCann, M., Lerouge, P., Vernhettes, S., and Hofte, H. (2002). KOBITO1 encodes a novel plasma membrane protein necessary for normal synthesis of cellulose during cell expansion in Arabidopsis. The Plant Cell **14,** 2001-2013.

Paredez, A.R., Somerville, C.R., and Ehrhardt, D.W. (2006). Visualization of cellulose synthase demonstrates functional association with microtubules. Science **312,** 1491-1495.

Persia, D., Cai, G., Del Casino, C., Faleri, C., Willemse, M.T.M., and Cresti, M. (2008). Sucrose synthase is associated with the cell wall of tobacco pollen tubes. Plant Physiology **147,** 1603-1618.

Persson, S., Paredez, A., Carroll, A., Palsdottir, H., Doblin, M., Poindexter, P., Khitrov, N., Auer, M., and Somerville, C.R. (2007). Genetic evidence for three unique components in primary cell-wall cellulose synthase complexes in Arabidopsis. Proceedings of the National Academy of Sciences of the United States of America **104,** 15566-15571.

Pesaresi, P., Pribil, M., Wunder, T., and Leister, D. (2011). Dynamics of reversible protein phosphorylation in thylakoids of flowering plants: the roles of STN7, STN8 and TAP38. Biochimica Et Biophysica Acta-Bioenergetics **1807,** 887-896.

Pesaresi, P., Hertle, A., Pribil, M., Kleine, T., Wagner, R., Strissel, H., Ihnatowicz, A., Bonardi, V., Scharfenberg, M., Schneider, A., Pfannschmidt, T., and Leister, D. (2009). Arabidopsis STN7 kinase provides a link between short- and long-term photosynthetic acclimation. The Plant Cell **21,** 2402-2423.

Pozueta-Romero, J., Pozueta-Romero, D., Gonzalez, P., and Etxeberria, E. (2004). Activity of membrane-associated sucrose synthase is regulated by its phosphorylation status in cultured cells of sycamore (Acer pseudoplatanus). Physiologia Plantarum **122,** 275-280.

Preston, R.D. (1974). Physical biology of plant cell walls (Chapman and Hall, London).

Qi, X., Wu, Z., Li, J., Mo, X., Wu, S., Chu, J., and Wu, P. (2007). AtCYT-INV1, a neutral invertase, is involved in osmotic stress-induced inhibition on lateral root growth in Arabidopsis. Plant Molecular Biology **64,** 575-587.

Regmi, K.C., Zhang, S., and Gaxiola, R.A. (2016). Apoplasmic loading in the rice phloem supported by the presence of sucrose synthase and plasma membrane-localized proton pyrophosphatase. Annals of Botany **117,** 257-268.

Reiland, S., Messerli, G., Baerenfaller, K., Gerrits, B., Endler, A., Grossmann, J., Gruissem, W., and Baginsky, S. (2009). Large-scale Arabidopsis phosphoproteome profiling reveals novel chloroplast kinase substrates and phosphorylation networks. Plant Physiology **150,** 889-903.

Rende, U., Wang, W., Gandla, M.L., Jonsson, L.J., and Niittyla, T. (2017). Cytosolic invertase contributes to the supply of substrate for cellulose biosynthesis in developing wood. The New Phytologist **214,** 796-807.

Ricard, B., Rivoal, J., Spiteri, A., and Pradet, A. (1991). Anaerobic stress induces the transcription and translation of sucrose synthase in rice. Plant Physiology **95,** 669-674.

Ricard, B., VanToai, T., Chourey, P., and Saglio, P. (1998). Evidence for the critical role of sucrose synthase for anoxic tolerance of maize roots using a double mutant. Plant Physiology **116,** 1323-1331.

Roitsch, T., and Gonzalez, M.C. (2004). Function and regulation of plant invertases: sweet sensations. Trends in Plant Science **9,** 606-613.

Rolletschek, H., Borisjuk, L., Koschorreck, M., Wobus, U., and Weber, H. (2002). Legume embryos develop in a hypoxic environment. Journal of Experimental Botany **53,** 1099-1107.

Ross, P., Mayer, R., and Benziman, M. (1991). Cellulose biosynthesis and function in bacteria. Microbiological Reviews **55,** 35-58.

Ruan, Y.L. (2014). Sucrose Metabolism: Gateway to diverse carbon use and sugar signaling. Annual Review of Plant Biology, Vol 65 **65,** 33-67.

Ruan, Y.L., Llewellyn, D.J., and Furbank, R.T. (2003). Suppression of sucrose synthase gene expression represses cotton fiber cell initiation, elongation, and seed development. The Plant Cell **15,** 952-964.

Ruan, Y.L., Jin, Y., Yang, Y.J., Li, G.J., and Boyer, J.S. (2010). Sugar input, metabolism, and signaling mediated by invertase: roles in development, yield potential, and response to drought and heat. Molecular Plant **3,** 942-955.

Saitou, N., and Nei, M. (1987). The neighbor-joining method: a new method for reconstructing phylogenetic trees. Molecular Biology and Evolution **4,** 406-425.

Salmen, L. (2004). Micromechanical understanding of the cell-wall structure. Comptes Rendus Biologies **327,** 873-880.

Salnikov, V.V., Grimson, M.J., Delmer, D.P., and Haigler, C.H. (2001). Sucrose synthase localizes to cellulose synthesis sites in tracheary elements. Phytochemistry **57,** 823-833.

Salnikov, V.V., Grimson, M.J., Seagull, R.W., and Haigler, C.H. (2003). Localization of sucrose synthase and callose in freeze-substituted secondary-wall-stage cotton fibers. Protoplasma **221,** 175-184.

Samac, D.A., Bucciarelli, B., Miller, S.S., Yang, S.S., O'Rourke, J.A., Shin, S., and Vance, C.P. (2015). Transgene silencing of sucrose synthase in alfalfa (Medicago sativa L.) stem vascular tissue suggests a role for invertase in cell wall cellulose synthesis. BMC Plant Biology **15**.

Schonberg, A., and Baginsky, S. (2012). Signal integration by chloroplast phosphorylation networks: an update. Frontiers in Plant Science **3**.

Schuetz, M., Smith, R., and Ellis, B. (2013). Xylem tissue specification, patterning, and differentiation mechanisms. Journal of Experimental Botany **64,** 11-31.

Sergeeva, L.I., Keurentjes, J.J., Bentsink, L., Vonk, J., van der Plas, L.H., Koornneef, M., and Vreugdenhil, D. (2006). Vacuolar invertase regulates elongation of Arabidopsis thaliana roots as revealed by QTL and mutant analysis. Proceedings of the National Academy of Sciences of the United States of America **103,** 2994-2999.

Sherson, S.M., Alford, H.L., Forbes, S.M., Wallace, G., and Smith, S.M. (2003). Roles of cell-wall invertases and monosaccharide transporters in the growth and development of Arabidopsis. Journal of Experimental Botany **54,** 525-531.

Shin, A.Y., Han, Y.J., Baek, A., Ahn, T., Kim, S.Y., Nguyen, T.S., Son, M., Lee, K.W., Shen, Y., Song, P.S., and Kim, J.I. (2016). Evidence that phytochrome functions as a protein kinase in plant light signalling. Nature Communications **7,** 11545.

Sivitz, A.B., Reinders, A., Johnson, M.E., Krentz, A.D., Grof, C.P., Perroux, J.M., and Ward, J.M. (2007). Arabidopsis sucrose transporter AtSUC9. High-affinity transport activity, intragenic control of expression, and early flowering mutant phenotype. Plant Physiology **143,** 188-198.

Somerville, C. (2006). Cellulose synthesis in higher plants. Annual Review of Cell and Developmental Biology **22,** 53-78.

Song, D., Shen, J., and Li, L. (2010). Characterization of cellulose synthase complexes in Populus xylem differentiation. The New Phytologist **187,** 777-790.

Sorek, N., Sorek, H., Kijac, A., Szemenyei, H.J., Bauer, S., Hematy, K., Wemmer, D.E., and Somerville, C.R. (2014). The Arabidopsis COBRA protein facilitates cellulose crystallization at the plasma membrane. Journal of Biological Chemistry **289,** 34911-34920.

Stadler, R., and Sauer, N. (1996). The Arabidopsis thaliana AtSUC2 gene is specifically expressed in companion cells. Botanica Acta **109,** 299-306.

Stadler, R., Lauterbach, C., and Sauer, N. (2005a). Cell-to-cell movement of green fluorescent protein reveals post-phloem transport in the outer integument and identifies symplastic domains in Arabidopsis seeds and embryos. Plant Physiology **139,** 701-712.

Stadler, R., Truernit, E., Gahrtz, M., and Sauer, N. (1999). The AtSUC1 sucrose carrier may represent the osmotic driving force for anther dehiscence and pollen tube growth in Arabidopsis. The Plant Journal **19,** 269-278.

Stadler, R., Wright, K.M., Lauterbach, C., Amon, G., Gahrtz, M., Feuerstein, A., Oparka, K.J., and Sauer, N. (2005b). Expression of GFP-fusions in Arabidopsis companion cells reveals non-specific protein trafficking into sieve elements and identifies a novel post-phloem domain in roots. Plant Journal **41,** 319-331.

Sturm, A. (1999). Invertases. Primary structures, functions, and roles in plant development and sucrose partitioning. Plant Physiology **121,** 1-8.

Sturm, A., and Chrispeels, M.J. (1990). cDNA cloning of carrot extracellular beta-fructosidase and its expression in response to wounding and bacterial-infection. The Plant Cell **2,** 1107-1119.

Subbaiah, C.C., and Sachs, M.M. (2001). Altered patterns of sucrose synthase phosphorylation and localization precede callose induction and root tip death in anoxic maize seedling. Plant Physiology **125,** 585-594.

Subbaiah, C.C., Palaniappan, A., Duncan, K., Rhoads, D.M., Huber, S.C., and Sachs, M.M. (2006). Mitochondrial localization and putative signaling function of sucrose synthase in maize. Journal of Biological Chemistry **281,** 15625-15635.

Sundell, D., Street, N.R., Kumar, M., Mellerowicz, E.J., Kucukoglu, M., Johnsson, C., Kumar, V., Mannapperuma, C., Delhomme, N., Nilsson, O., Tuominen, H., Pesquet, E., Fischer, U., Niittyla, T., Sundberg, B., and Hvidsten, T.R. (2017). AspWood: high-spatial-resolution transcriptome profiles reveal uncharacterized modularity of wood formation in Populus tremula. The Plant Cell, tpc. 00153.02017.

Swarbrick, P.J., Schulze-Lefert, P., and Scholes, J.D. (2006). Metabolic consequences of susceptibility and resistance (race-specific and broad-spectrum) in barley leaves challenged with powdery mildew. Plant Cell and Environment **29,** 1061-1076.

Taiz, L., and Zeiger, E. (2010). Plant physiology 5th Ed. Sunderland, MA: Sinauer Associates.

Takahashi, J., Rudsander, U.J., Hedenstrom, M., Banasiak, A., Harholt, J., Amelot, N., Immerzeel, P., Ryden, P., Endo, S., Ibatullin, F.M., Brumer, H., del Campillo, E., Master, E.R., Scheller, H.V., Sundberg, B., Teeri, T.T., and Mellerowicz, E.J. (2009). KORRIGAN1 and its aspen homolog PttCel9A1 decrease cellulose crystallinity in Arabidopsis stems. Plant and Cell Physiology **50,** 1099-1115.

Tang, G.Q., and Sturm, A. (1999). Antisense repression of sucrose synthase in carrot (Daucus carota L.) affects growth rather than sucrose partitioning. Plant Molecular Biology **41,** 465-479.

Tang, G.Q., Luscher, M., and Sturm, A. (1999). Antisense repression of vacuolar and cell wall invertase in transgenic carrot alters early plant development and sucrose partitioning. The Plant Cell **11,** 177-189.

Taylor, N.G. (2008). Cellulose biosynthesis and deposition in higher plants. New Phytologist **178,** 239-252.

Taylor, N.G., Laurie, S., and Turner, S.R. (2000). Multiple cellulose synthase catalytic subunits are required for cellulose synthesis in Arabidopsis. The Plant Cell **12,** 2529-2539.

Taylor, N.G., Howells, R.M., Huttly, A.K., Vickers, K., and Turner, S.R. (2003). Interactions among three distinct CesA proteins essential for cellulose synthesis. Proceedings of the National Academy of Sciences of the United States of America **100,** 1450-1455.

Taylor, R., Inamine, G., and Anderson, J.D. (1993). Tissue printing as a tool for observing immunological and protein profiles in young and mature celery petioles. Plant Physiology **102,** 1027-1031.

Tetlow, I.J., Wait, R., Lu, Z., Akkasaeng, R., Bowsher, C.G., Esposito, S., Kosar-Hashemi, B., Morell, M.K., and Emes, M.J. (2004). Protein phosphorylation in amyloplasts regulates starch branching enzyme activity and protein-protein interactions. The Plant Cell **16,** 694-708.

Thompson, M.V., and Wolniak, S.M. (2008). A plasma membrane-anchored fluorescent protein fusion illuminates sieve element plasma membranes in Arabidopsis and tobacco. Plant Physiology **146,** 1599-1610.

Truernit, E., and Sauer, N. (1995). The promoter of the Arabidopsis-thaliana SUC2 sucrose-H^+ symporter gene directs expression of beta-glucuronidase to the phloem: evidence for phloem loading and unloading by SUC2. Planta **196,** 564-570.

Turgeon, R., and Medville, R. (2004). Phloem loading. A reevaluation of the relationship between plasmodesmatal frequencies and loading strategies. Plant Physiology **136,** 3795-3803.

Valentovic, P., Luxova, M., Kolarovic, L., and Gasparikova, O. (2006). Effect of osmotic stress on compatible solutes content, membrane stability and water relations in two maize cultivars. Plant Soil and Environment **52,** 184.

van Bel, A.J., Ehlers, K., and Knoblauch, M. (2002). Sieve elements caught in the act. Trends in Plant Science **7,** 126-132.

Vargas, W.A., Pontis, H.G., and Salerno, G.L. (2008). New insights on sucrose metabolism: evidence for an active A/N-Inv in chloroplasts uncovers a novel component of the intracellular carbon trafficking. Planta **227,** 795-807.

Verbancic, J., Lunn, J.E., Stitt, M., and Persson, S. (2018). Carbon supply and the regulation of cell wall synthesis. Molecular Plant **11,** 75-94.

Wächter, R., Langhans, M., Aloni, R., Götz, S., Weilmünster, A., Koops, A., Temguia, L., Mistrik, I., Pavlovkin, J., and Rascher, U. (2003). Vascularization, high-volume solution flow, and localized roles for enzymes of sucrose metabolism during tumorigenesis by Agrobacterium tumefaciens. Plant Physiology **133,** 1024-1037.

Wan, H., Wu, L., Yang, Y., Zhou, G., and Ruan, Y.L. (2018). Evolution of sucrose metabolism: the dichotomy of invertases and beyond. Trends in Plant Science **23,** 163-177.

Wang, E., Wang, J., Zhu, X.D., Hao, W., Wang, L.Y., Li, Q., Zhang, L.X., He, W., Lu, B.R., Lin, H.X., Ma, H., Zhang, G.Q., and He, Z.H. (2008). Control of rice grain-filling and yield by a gene with a potential signature of domestication. Nature Genetics **40,** 1370-1374.

Wang, F., Sanz, A., Brenner, M.L., and Smith, A. (1993). Sucrose synthase, starch accumulation, and tomato fruit sink strength. Plant Physiology **101,** 321-327.

Wang, W., Vignani, R., Scali, M., and Cresti, M. (2006). A universal and rapid protocol for protein extraction from recalcitrant plant tissues for proteomic analysis. Electrophoresis **27,** 2782-2786.

Wang, Z., Wei, P., Wu, M.Z., Xu, Y.L., Li, F., Luo, Z.P., Zhang, J.F., Chen, A., Xie, X.D., Cao, P.J., Lin, F.C., and Yang, J. (2015). Analysis of the sucrose synthase gene family in tobacco: structure, phylogeny, and expression patterns. Planta **242,** 153-166.

Watanabe, Y., Meents, M.J., McDonnell, L.M., Barkwill, S., Sampathkumar, A., Cartwright, H.N., Demura, T., Ehrhardt, D.W., Samuels, A.L., and Mansfield, S.D. (2015). Visualization of cellulose synthases in Arabidopsis secondary cell walls. Science **350,** 198-203.

Weber, H., Borisjuk, L., Heim, U., Buchner, P., and Wobus, U. (1995). Seed coat-associated invertases of fava bean control both unloading and storage functions: cloning of cDNAs and cell type-specific expression. The Plant Cell **7,** 1835-1846.

Wei, Z., Qu, Z., Zhang, L., Zhao, S., Bi, Z., Ji, X., Wang, X., and Wei, H. (2015). Overexpression of poplar xylem sucrose synthase in tobacco leads to a thickened cell wall and increased height. PloS ONE **10,** e0120669.

Welham, T., Pike, J., Horst, I., Flemetakis, E., Katinakis, P., Kaneko, T., Sato, S., Tabata, S., Perry, J., and Parniske, M. (2009). A cytosolic invertase is required for normal growth and cell development in the model legume, Lotus japonicus. Journal of Experimental Botany **60,** 3353-3365.

Western, T.L., Skinner, D.J., and Haughn, G.W. (2000). Differentiation of mucilage secretory cells of the Arabidopsis seed coat. Plant Physiology **122,** 345-355.

Williams, L.E., Lemoine, R., and Sauer, N. (2000a). Sugar transporters in higher plants-a diversity of roles and complex regulation. Trends in Plant Science **5,** 283-290.

Winter, H., and Huber, S.C. (2000). Regulation of sucrose metabolism in higher plants: localization and regulation of activity of key enzymes. Critical Reviews in Biochemistry and Molecular Biology **35,** 253-289.

Winter, H., Huber, J.L., and Huber, S.C. (1997). Membrane association of sucrose synthase: changes during the graviresponse and possible control by protein phosphorylation. FEBS Letters **420,** 151-155.

Winter, H., Huber, J.L., and Huber, S.C. (1998). Identification of sucrose synthase as an actin-binding protein. FEBS letters **430,** 205-208.

Xiang, L., Li, Y., Rolland, F., and Van den Ende, W. (2011a). Neutral invertase, hexokinase and mitochondrial ROS homeostasis: emerging links between sugar metabolism, sugar signaling and ascorbate synthesis. Plant Signaling & Behavior **6,** 1567-1573.

Xiang, L., Le Roy, K., Bolouri-Moghaddam, M.R., Vanhaecke, M., Lammens, W., Rolland, F., and Van den Ende, W. (2011b). Exploring the neutral invertase-oxidative stress defence connection in Arabidopsis thaliana. Journal of Experimental Botany **62,** 3849-3862.

Xu, S.M., Brill, E., Llewellyn, D.J., Furbank, R.T., and Ruan, Y.L. (2012). Overexpression of a potato sucrose synthase gene in cotton accelerates leaf expansion, reduces seed abortion, and enhances fiber production. Molecular Plant **5,** 430-441.

Yamaguchi, M., Goue, N., Igarashi, H., Ohtani, M., Nakano, Y., Mortimer, J.C., Nishikubo, N., Kubo, M., Katayama, Y., Kakegawa, K., Dupree, P., and Demura, T. (2010). VASCULAR-RELATED NAC-DOMAIN6 and VASCULAR-RELATED NAC-DOMAIN7 effectively induce transdifferentiation into xylem vessel elements under control of an induction system. Plant Physiology **153,** 906-914.

Yan, D., Duermeyer, L., Leoveanu, C., and Nambara, E. (2014). The functions of the endosperm during seed germination. Plant and Cell Physiology **55,** 1521-1533.

Yang, N.S., and Russell, D. (1990). Maize sucrose synthase-1 promoter directs phloem cell-specific expression of Gus gene in transgenic tobacco plants. Proceedings of the National Academy of Sciences of the United States of America **87,** 4144-4148.

Yau, Y.Y., and Simon, P.W. (2003). A 2.5-kb insert eliminates acid soluble invertase isozyme II transcript in carrot (Daucus carota L.) roots, causing high sucrose accumulation. Plant Molecular Biology **53,** 151-162.

Zanor, M.I., Osorio, S., Nunes-Nesi, A., Carrari, F., Lohse, M., Usadel, B., Kuhn, C., Bleiss, W., Giavalisco, P., Willmitzer, L., Sulpice, R., Zhou, Y.H., and Fernie, A.R. (2009). RNA interference of LIN5 in tomato confirms its role in controlling brix content, uncovers the influence of sugars on the levels of fruit hormones, and demonstrates the importance of sucrose cleavage for normal fruit development and fertility. Plant Physiology **150,** 1204-1218.

Zeeman, S.C., Kossmann, J., and Smith, A.M. (2010). Starch: its metabolism, evolution, and biotechnological modification in plants. Annual Review of Plant Biology **61,** 209-234.

Zeng, Y., Wu, Y., Avigne, W.T., and Koch, K.E. (1999). Rapid repression of maize invertases by low oxygen. Invertase/sucrose synthase balance, sugar signaling potential, and seedling survival. Plant Physiology **121,** 599-608.

Zeng, Y., Zhao, S., Yang, S., and Ding, S.Y. (2014). Lignin plays a negative role in the biochemical process for producing lignocellulosic biofuels. Current Opinion in Biotechnology **27,** 38-45.

Zhang, C.K., Han, L., Slewinski, T.L., Sun, J.L., Zhang, J., Wang, Z.Y., and Turgeon, R. (2014). Symplastic phloem loading in poplar. Plant Physiology **166,** 306-U443.

Zhang, D.Q., Xu, B.H., Yang, X.H., Zhang, Z.Y., and Li, B.L. (2011). The sucrose synthase gene family in Populus: structure, expression, and evolution. Tree Genetics & Genomes **7,** 443-456.

Zhang, L., Cohn, N.S., and Mitchell, J.P. (1996). Induction of a pea cell-wall invertase gene by wounding and its localized expression in phloem. Plant Physiology **112,** 1111-1117.

Zhang, X.Q., Lund, A.A., Sarath, G., Cerny, R.L., Roberts, D.M., and Chollet, R. (1999). Soybean nodule sucrose synthase (Nodulin-100): further analysis of its phosphorylation using recombinant and authentic root-nodule enzymes. Archives of Biochemistry and Biophysics **371,** 70-82.

Zheng, Y., Anderson, S., Zhang, Y., and Garavito, R.M. (2011). The structure of sucrose synthase-1 from Arabidopsis thaliana and its functional implications. The Journal of Biological Chemistry **286,** 36108-36118.

Zhong, R., and Ye, Z.H. (2015). Secondary cell walls: biosynthesis, patterned deposition and transcriptional regulation. Plant and Cell Physiology **56,** 195-214.

Zhong, R.Q., Kays, S.J., Schroeder, B.P., and Ye, Z.H. (2002). Mutation of a chitinase-like gene causes ectopic deposition of lignin, aberrant cell shapes, and overproduction of ethylene. The Plant Cell **14,** 165-179.

Zrenner, R., Salanoubat, M., Willmitzer, L., and Sonnewald, U. (1995). Evidence of the crucial role of sucrose synthase for sink strength using transgenic potato plants (Solanum-tuberosum L.). Plant Journal **7,** 97-107.

Appendices

Appendix A Supplemental data for Chapter 2

Movie S1

Motility of SuSy4-YFP in the companion cells of longitudinal sections of leaf petioles. Time-lapse video showing that SuSy-YFP was streaming in the cytoplasm of companion cells. Movie acquired at 5-second interval for total 1:35 minutes. Bar=10 μm.

Appendix B Supplemental data for Chapter 3

Movie S2

SuSy5-YFP was immobile in the sieve elements of petiole longitudinal sections. Time-lapse video showing that SuSy5-YFP was parietally localized in sieve elements and YFP signal was immobile as indicated by arrowheads. Movie acquired at 5-second interval for total 1:35 minutes. Bar=10 μm.